



**POLITECNICO
DI TORINO**

Politecnico di Torino

Department of Electronics and Telecommunications

Master of Science in Mechatronic Engineering

Master Degree Thesis

Hardware design of a motors control module in sensorless approach for memory seats application



Bitron Industrie S.p.A.

Grugliasco, Italy

Academic Tutor

Prof. Michele Angelo Pastorelli

Company Tutor

Ing. Giuseppe Frasca

Candidate

Gorkem Uygur

Academic Year 2019-2020

Abstract

In the last two decades, many applications of automotive are become varied to correspond driver and passengers comfort and ergonomy. Some applications are become standard specifications not additional one. Therefore, the car manufacturers take in consideration based on requirements of humans, then automotives are designed and developed. Memory seats, power windows, lift gate, power trunk and side mirrors are some applications of automotive that are improved and constructed. These type of applications before are only controlled by mechanically and but also from some years on the electronic control is used and become popular for many car manufacturers. Especially, the vehicle seats have different movement capabilities and ergonomic calibrations and each seat is controlled by an individual motor, hence the configuration and comfort settings can be adjusted by driver and passenger thanks to position memory.

The purpose of thesis is to implement electronic design of memory seats control module to drive brushed DC motor in sensorless approach as a research project of Electronic Division of Bitron Industrie S.p.A. in Grugliasco(TO). This division is specialized in the design of electronic systems and devices for the automotive applications. The idea is to developpe and design new sensorless approach model that can have same or similar capability as a sensed approach hence, the new model is an alternative for sensed one. The project is focused on hardware design that are comprised of circuit simulation, testing developed hardware, electrical schematics, characterization of seat motor.

Existing model, sensed approach is used multiple magnetic sensors mounted on the body of the motor to cause a feedback loop to motor control module. In contrast to sensed solution, sensorless approach reduces the number of sensors and the number of wirings that are required and also it decreases the cost of labour to assembly of sensors. For these reason, the aim of sensorless solution is to get convinient results with a cheaper and easily configurable way. A sensorless method could be applied with brushed DC motor in order to benefit from back-electromagnetic force(BEMF) has on the current enters the motor.

Position measurement is important and very precise for sensorless method of memory seats that is why position of the motor is followed current ripples that are counted by comparator in sensorless method. By using simulation program and by acquiring experimental acquisitions, these kind of works are performed only focused on the developement of measuring accuracy. For simulation of the system on the computer, TINA(TI) program has been used and for experimental approaches all testing equipments and electronic components are provided by Bitron Industrie S.p.A.

Acknowledgements

Regarding for all informations and helps, I would like to thank my academic supervisor, professor Michele Pastorelli. I informed him all updates of project and He really helped me so much along all the process of project.

Providing all equipments and supporting facilities by Bitron Industrie S.p.A. I appreciated the company. For me, it was great experience to do my thesis in Bitron. Also, I would like to thank my company tutor, hardware engineer Giuseppe Frasca. I and he worked along testing and simulation procedures. He helped me for whole project duration.

Table of Content

1. Introduction.....	1
1.1 Motivations.....	1
1.2 Outline.....	2
2. Adjustment with Brushed DC Motor.....	3
2.1 Manual Seat Adjustment.....	4
2.2 Memory Seat Adjustment.....	6
2.3 Brushed DC Motor	7
2.3.1 Working Principle.....	7
2.3.2 Stator.....	10
2.3.3 Rotor.....	11
2.3.4 Brushes and Commutator.....	11
2.3.5 Types of Brushed DC Motor	12
2.4 Complete System.....	14
3. Position Control Measurement	15
3.1 Sensored Approach	15
3.1.1 Hall-Effect Sensor.....	15
3.1.2 Optical Encoder	16
3.2 Sensorless Approach.....	17
3.2.1 Brushed DC Motor Current Ripple.....	19
3.2.2 PWM Effects on the Ripple.....	22
4. System Stages	23
4.1 Current-Sense Amplifier Stage.....	24
4.2 Band-Pass Filter Stage	25
4.3 Differential Amplifier Stage.....	26
4.4 Comparator Stage.....	27
4.5 Updated System Stages	29
4.5.1 Updated Current-Sense Amplifier Stage	29
4.5.2 Updated Band-Pass Filter Stage	31
4.5.3 Updated Comparator Stage.....	32
5. Circuit Analysis	33
5.1 Electrical Schematics	33
5.1.1 Current Sense Amplifier Stage	33
5.1.2 Band Pass Filter Stage.....	33
5.1.3 Differential Amplifier Stage	35

5.1.4 Comparator Stage	36
5.2 Updated Electrical Schematic	38
5.2.1 Updated Current Sense Amplifier Stage.....	38
5.2.2 Updated Band Pass Filter Stage	39
5.2.3 Updated Comparator Stage.....	40
5.3 Test & Simulation Result.....	41
5.3.1 9 V Backward	41
5.3.2 9 V Forward	43
5.3.3 12 V Backward	45
5.3.4 12 V Forward	47
5.3.5 16 V Backward	49
5.3.6 16 V Forward	51
5.4 Downward-Upward Motion	53
5.4.1 9 V Downward	56
5.4.2 9 V Upward.....	58
5.4.3 12 V Downward	60
5.4.4 12 V Upward.....	62
5.4.5 16 V Downward	64
5.4.6 16 V Upward.....	66
5.5 Updated System Test.....	68
5.5.1 9 V Downward Updated.....	68
5.5.2 9 V Upward Updated	70
5.5.3 12 V Downward Updated.....	72
5.5.4 12 V Upward Updated	74
5.5.5 16 V Downward Updated.....	76
5.5.6 16 V Upward Updated	78
6. Conclusion & Future Work.....	80
7. Appendix.....	82
7.1 Datasheets.....	82
7.2 Final Schematics.....	86
References	87

List of Figures

Figure 1: Electric Seat Adjustment	3
Figure 2: Electric Mirror Adjustment.....	3
Figure 3: Power Liftgate Adjustment.....	3
Figure 4: Power Windows Adjustment	3
Figure 5: Seat Adjust Functions.....	4
Figure 6: Electric Adjustment Buttons(Tesla).....	5
Figure 7: Memory Seat Adjustment (Mercedes-Benz).....	6
Figure 8: Scheme of Brushed DC Motor.....	7
Figure 9: Phase 1 of Brushed DC Motor.....	8
Figure 10: Phase 2 of Brushed DC Motor.....	8
Figure 11: Phase 3 of Brushed DC Motor.....	9
Figure 12: Phase 4 of Brushed DC Motor.....	9
Figure 13: The Overview of the Brushed DC Motor	10
Figure 14: Stator.....	10
Figure 15: Rotor.....	11
Figure 16: Brushes&Commutator	12
Figure 17: Permanent Magnet Brushed DC Motor	12
Figure 18: Shunt-Wound Brushed DC Motor	13
Figure 19: Series-Wound Brushed DC Motor	13
Figure 20: Compound-Wound Brushed DC Motor	14
Figure 21: Complete System Block Diagram	15
Figure 22: Hall-Effect Sensor.....	16
Figure 23: Optical Encoder	16
Figure 24: Periodic Changes in the Current Feedback	17
Figure 25: Current Sense Configuration	18
Figure 26: Ripple Production from a Rotating Motor.....	19
Figure 27: Rotation Process	20
Figure 28: Generated Ripple in Different PWM Duty Cycles	22
Figure 29: Back EMF Voltage Measurement	23
Figure 30: Schematic of Current Sense Amplifier.....	25
Figure 31: Schematic of Band-Pass Filter Stage	25
Figure 32: The Graph of Initial Current Spike	26
Figure 33: Schematic of Differential Amplifier Stage	27
Figure 34: Schematic of Comparator Stage.....	28
Figure 35: Single Opamp Difference Amplifier.....	29
Figure 36: Schematic of Updated Current Sense Amplifier	30
Figure 37: Updated Band-Pass Filter Stage	31
Figure 38: Updated Comparator Stage.....	32
Figure 39: Current Sense Amplifier Circuit	33
Figure 40: Band Pass Filter Circuit	34
Figure 41: Electrical Schematic of Differential Amplifier	36
Figure 42: Electrical Schematic of Comparator	37
Figure 43: Updated Electrical Schematic of Current Sense Amplifier	38
Figure 44: Updated Electrical Schematic of Band Pass Filter.....	39

Figure 45: Updated Electrical Schematic of Comparator Stage.....	40
Figure 46: Transient Analysis of 9 V Backward	41
Figure 47: 9 V Backward Each Stage Analysis.....	42
Figure 48: Test Sample for 9 V.....	42
Figure 49: 9 V Backward Steady State Region Details.....	43
Figure 50: Trasient Analysis of 9 V Forward	44
Figure 51: 9 V Forward Each Stage Analysis	44
Figure 52: 9 V Forward Steady State Region Details	45
Figure 53: Transient Analysis of 12 V Backward	46
Figure 54: 12 V Backward Each Stage Analysis.....	46
Figure 55: 12 V Backward Steady State Region Details.....	47
Figure 56: Transient Analysis of 12 V Forward	48
Figure 57: 12 V Forward Each Stage Analysis	48
Figure 58: 12 V Forward Steady State Region Details	49
Figure 59: Transient Analysis of 16 V Backward	50
Figure 60: 16 V Backward Each Stage Analysis.....	50
Figure 61: 16 V Backward Steady State Region Details.....	51
Figure 62: Transient Analysis of 16 V Forward	52
Figure 63: 16 V Forward Each Stage Analysis	52
Figure 64: 16 V Forward Steady State Region Details	53
Figure 65: Band Pass Filter Electrical Schematic for Upward-Downward Motion.....	54
Figure 66: Differential Amplifier Electrical Schematic for Upward-Downward Motion	55
Figure 67: Transient Analysis of 9 V Downward	56
Figure 68: 9 V Downward Each Stage Analysis	57
Figure 69: 9 V Downward Steady State Region Details	57
Figure 70: Transient Analysis of 9 V Upward.....	58
Figure 71: 9 V Upward Each Stage Analysis	59
Figure 72: 9 V Upward Steady State Region Details	59
Figure 73: Transient Analysis of 12 V Downward	60
Figure 74: 12 V Downward Each Stage Analysis	61
Figure 75: 12 V Downward Steady State Region Details.....	61
Figure 76: Transient Analysis of 12 V Upward.....	62
Figure 77: 12 V Upward Each Stage Analysis	63
Figure 78: 12 V Upward Steady State Region Details	63
Figure 79: Transient Analysis of 16 V Downward	64
Figure 80: 16 V Downward Each Stage Analysis	65
Figure 81: 16 V Downward Steady State Region Details.....	65
Figure 82: Transient Analysis of 16 V Upward.....	66
Figure 83: 16 V Upward Each Stage Analysis	67
Figure 84: 16 V Upward Steady State Region Details	67
Figure 85: Transient Analysis of 9 V Downward Updated.....	68
Figure 86: 9 V Downward Updated Each Stage Analysis	69
Figure 87: 9 V Downward Updated Steady State Region Details	70
Figure 88: Transient Analysis of 9 V Upward Updated	70
Figure 89: 9 V Upward Updated Each Stage Analysis	71
Figure 90: 9 V Upward Updated Steady State Region Details.....	72
Figure 91: Transient Analysis of 12 V Downward Updated.....	72

Figure 92: 12 V Downward Updated Each Stage Analysis	73
Figure 93: 12 V Downward Updated Steady State Region Details	74
Figure 94: Transient Analysis of 12 V Upward Updated	74
Figure 95: 12 V Upward Updated Each Stage Analysis.....	75
Figure 96: 12 V Upward Updated Steady State Region Details.....	76
Figure 97: Transient Analysis of 16 V Downward Updated.....	76
Figure 98: 16 V Downward Updated Each Stage Analysis.....	77
Figure 99: 16 V Downward Updated Steady State Region Details	78
Figure 100: Transient Analysis of 16 V Upward Test.....	78
Figure 101: 16 V Upward Updated Each Stage Analysis.....	79
Figure 102: 16 V Upward Updated Steady State Region Details.....	80
Figure 103: Final Electrical Schematic of System.....	86

1. Introduction

1.1 Motivations

The invention of car is one of the most important of invention that makes human life easy. From the first day, there has been many different developements in automotive industry. In shortly, these improvements have been come true for each sections of automobile such as engine, interior and exterior design, aerodynamic, comfort and ergonomy, fuel consumption, safety, control systems, propulsion systems, braking systems, tractions systems and electronic systems so on. Especially, since the beginning of 2000s thanks to technological growing, transformation from mechanical system to electrical system has been gained speed.

By the virtue of technological developements, ergonomy, configuration and comfort settings have been enhanced and provided ease of use for human. Particularly, adjustment of vehicle seats, windows, side mirrors, trunk gate, fuel tank cover have been become to use easily.

The dissertation is based on electrical adjustment of vehicle seats. Before, there was only mechanical adjustment of vehicle seats then electrical adjustment was discovered so some car models have this control but generally the mechanical method is still widely used because it is cheaper than electrical method. Also electrical control could have the additional property that is a memory for vehicle seats, that is saved position of seats. The feature of vehicle seats have capability of different axes of movement and ergonomic adjustment that are controlled by an individual motor hence position memory required for configuration and comfort settings for different driver and passengers to control motor more efficient and smarter. The electrical adjustment is branched into two which are sensed and sensorless approach. The thesis is focused on sensorless approach of electrical adjustment of vehicle memory seats. In contrast to sensed method, sensorless method is a new technic for control of vehicle seats. The sensed method needs to have hall-effect sensors on the motor to follow the movement of the motor. The sensorless method ensures to remove redundant wirings and hall-effect sensors that are required for the sensed method. For these reasons, the sensorless method can be described as cost efficient and easily configurable solutions. By means of impact of back electromagnetic force, brushed DC motors could be good solution for sensorless approach. The objectives of thesis are followings:

Analysis of the sensorless approach

Simulating and testing of sensorless approach circuit

Implementing hardware design of sensorless approach

This thesis is a research project of Bitron which is an Italian company. It works on research, development and manufacturing of mechatronic devices and systems for automotive, appliance, HVAC, medical and energy industries. The project is performed

at Bitron Electronic Division that is Business Unit of Bitron Group concentrated in the design of electronic systems and devices for automotive applications.

1.2 Outline

The thesis is consisted of seven chapters that are detailed as followings.

Chapter 1 is the introduction section that describes motivations, objectives and organization of dissertation.

Chapter 2 introduces adjustment with brushed DC motor then seat adjustment technics, working principle of brushed DC motor, sections of BDC motor, different types of BDC motor and complete system are explained.

Chapter 3 presents position control measurement technics for BDC motor that are comprised of sensed and sensorless approach. Also, sensed method which is comprised of hall-effect sensors and optical encoders, are clarified as subheadings. Sensorless method that is consisted of brushed DC motor current ripple and PWM effects on ripple, are represented in details.

In chapter 4, system stages of sensorless approach are described stage by stage in theory. Additionally, after evaluating system stages and complete system, to reduce cost updated system stages are expressed.

In chapter 5, electrical schematics and computations are performed for each system stage. Besides, required circuit analysis, transient analysis, are simulated for complete system by TINA software tool. Also, some comparisons between tests and comments for each test are accomplished.

Chapter 6 evaluates consequences of thesis and possible future work is suggested.

Chapter 7 is appendix part that demonstrates datasheets of electronic components and BDC motor and final schematic of complete system.

2. Adjustment with Brushed DC Motor

In the last two decades, safety, efficiency and comfort become more significant role in mobility. Car and component manufacturers focus on making the driving experience more satisfying, eco-friendly and secure. To accomplish this, motor control systems act essential role in the automotive industry. The usage of electrical motor become widespread in automotive applications such as windows, sliding doors, memory seats, lift gates, side mirrors, power trunk. For these kind of applications are preferred brushed DC motor. It is shown some automotive applications in the following figures.



Figure 1: Electric Seat Adjustment



Figure 2: Electric Mirror Adjustment



Figure 3: Power Liftgate Adjustment



Figure 4: Power Windows Adjustment

Electric seat adjustment is provided to regulate vehicle seat that driver and passenger sit in comfort position. The vehicle seats can have various movement capabilities such as backward, forward, upward, downward and changing seat back angle. Generally, the electric seat adjustment is separated into two branches that are manual seat adjustment and memory seat adjustment.

2.1 Manual Seat Adjustment

The electric seat adjustment axes are simple requirement to apply the user with the complete comfort and safety. Generally, it has competence to adjust usual fore and aft, seat height, backrest angle and headrest height, additionally it could be possible to regulate seat angle, seat length, backrest width, upper backrest angle and even footrest with electric adjustment. People can manage seat to their desired position by pressing corresponding operating controls both conventional switches or a modern human-machine interface. In the following figures, the possible vehicle adjustments are shown.

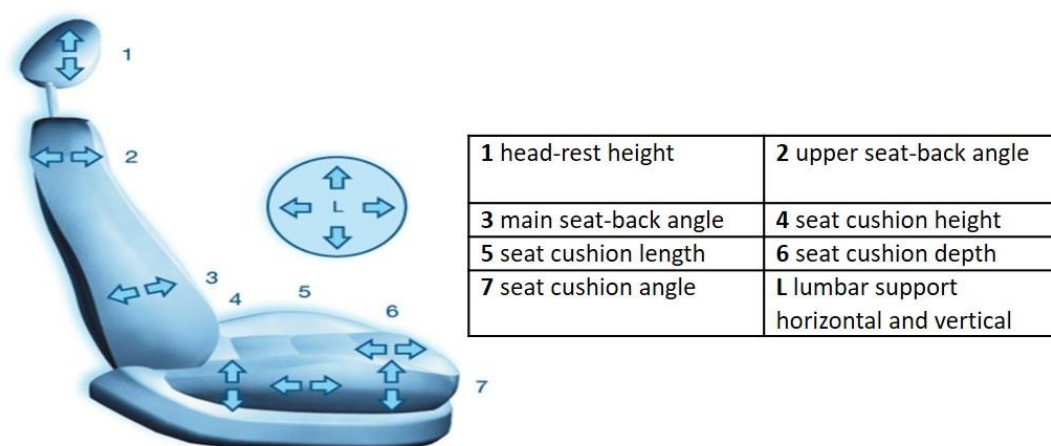


Figure 5: Seat Adjust Functions



Figure 6: Electric Adjustment Buttons(Tesla)

1. It has ability to move forward/backward and regulate the seat's height and tilt angle up/down
2. It has competence to adjust backrest
3. It has adjust lumbar support

2.2 Memory Seat Adjustment

By means of assistance of specially produced positioning logic, it could be possible to store seat positions are defined by user, they can be recall by pressing button. This logic can be applied both ways that are electrically by sensors or algorithmically by Sensorless Positioning(SLP). Beside of basic position saving, it is also possible to save to key memory. After saving driver's seat position, when the driver unlocks the vehicle with remote key or when the driver opens the door, position of driver seat is automatically set. It is limited place in the interior for coupe car models, the vehicle seats have special aspect that is used for entering vehicle and exiting from the vehicle easily. Thus the front seats are temporarily acted forward to make room for passengers. In order to this action, high speed motor is required for fore and aft adjustment.



Figure 7: Memory Seat Adjustment (Mercedes-Benz)

2.3 Brushed DC Motor

More than a century, brushed DC motors have been around as an advanced technology. The name of brushed DC (BDC) motors derives from the "brushes" used for commutation. Household appliances and automobiles are the main utilization areas for brushed DC motors. They are also cheaper and easy to drive and can be found in all sizes and shapes. The ability to alter the torque to speed ratio makes the brushed DC motors a strong industrial niche. Also, the features like speed and torque which are proportional to the applied voltage / current provides brushed DC motors an easy control.

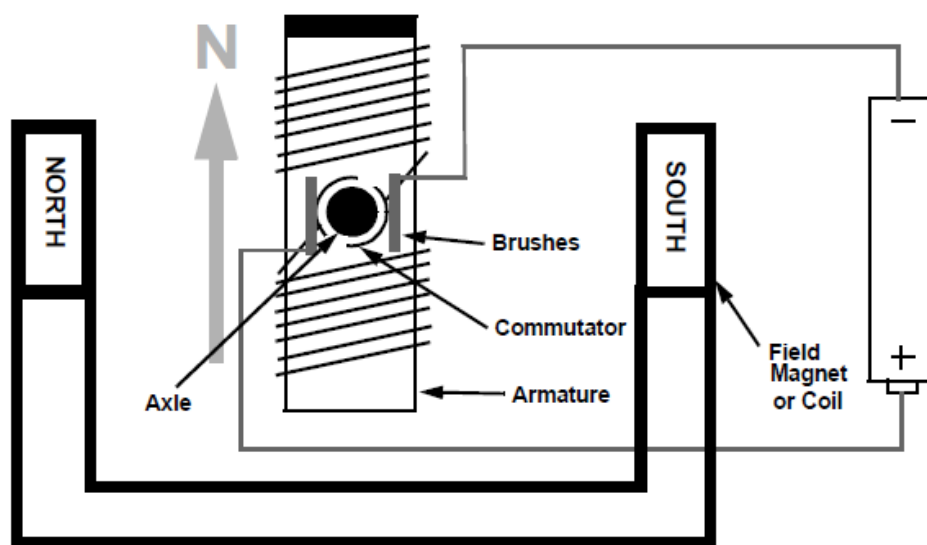
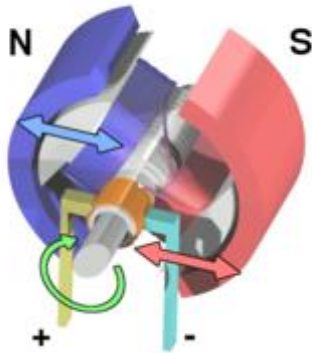


Figure 8: Scheme of Brushed DC Motor

2.3.1 Working Principle

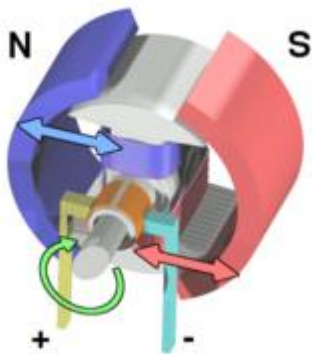
The brushed DC motor consists two magnets fronting the same direction, which envelops two coils of wire that settle in the middle of the brushed DC motor, around a rotor. To face the magnets, the coils are placed, providing electricity to flow to them. This operates a magnetic field, that thrusts the coils away from the magnets they are facing, and causes rotor to turn. When rotor turns a 180 degree, the current switches off at rotor. As the current switches on again, the flowing of electricity is adversely, forwarding another pulsation that provides the rotor to turn one time again. The brushed are placed within the brushed DC motor switch it off and on when assigned, by flowing electricity from the motor.

The following figures demonstrate a movement of brushed DC motor phase by phase.



When the power supply is applied to the coil, around the armature windings the magnetic field is generated. The left side of the armature winding is thrust from the left side of magnet and it causes to start rotation of motor.

Figure 9: Phase 1 of Brushed DC Motor



The armature windings maintain to rotate.

Figure 10: Phase 2 of Brushed DC Motor

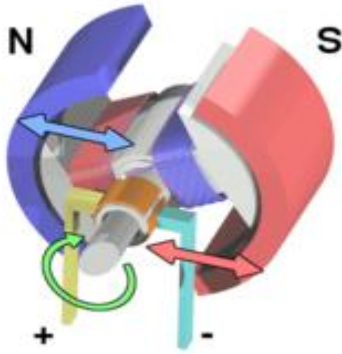


Figure 11: Phase 3 of Brushed DC Motor.

When the armature windings align horizontally, the torque of motor becomes zero. At this step, the direction of current is reversed by commutator, overturn the magnetic field.

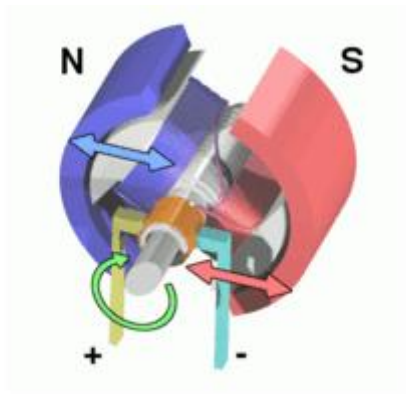


Figure 12: Phase 4 of Brushed DC Motor

The process of motor iterates, generating continuous rotation.

The brushed DC motor consists of 4 main components that are, the stator, the rotor, brushes and commutator.

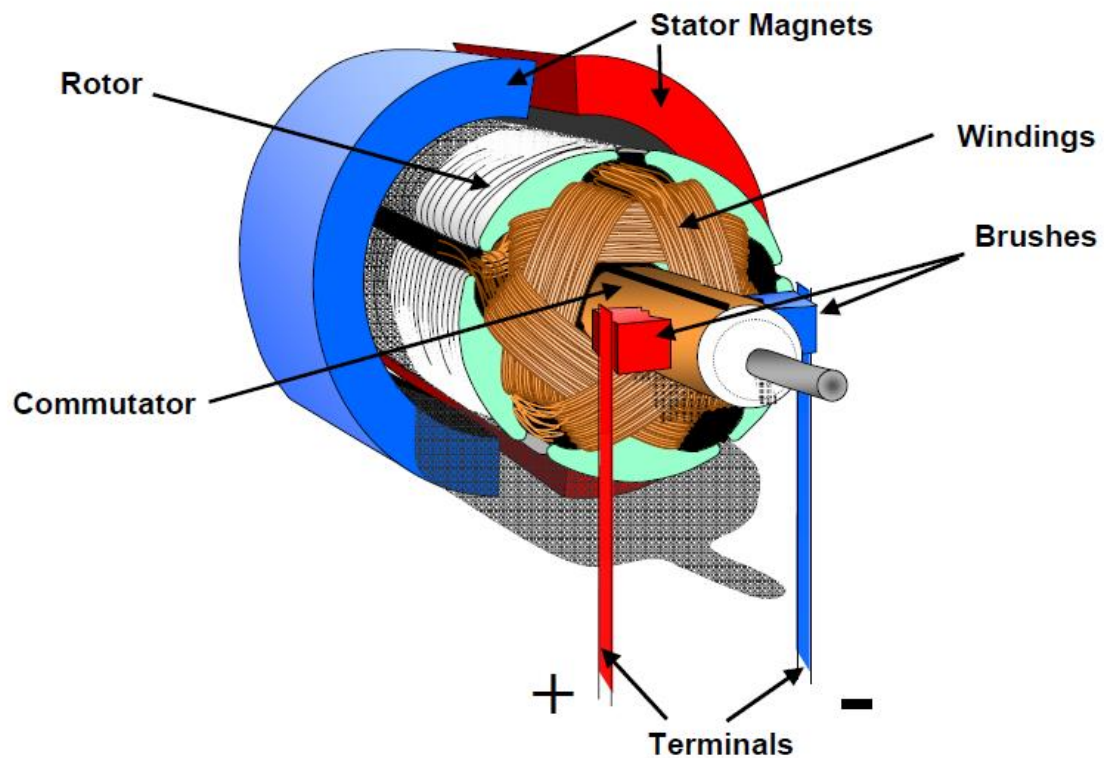


Figure 13: The Overview of the Brushed DC Motor

2.3.2 Stator

The stationary magnetic field, which is generated by the stator, envelops the rotor. The permanent magnets or the electromagnetic windings create this field. The assembly of the stator or the route the electromagnetic windings are bonded to the power supply.

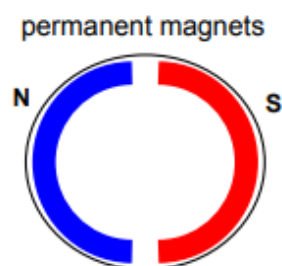


Figure 14: Stator

2.3.3 Rotor

The rotor which is also called the armature, is consist of one or more windings. The magnetic field is occured when these windings are energized. The magnetic poles of the stator interacts with the opposite poles of the rotor and causes rotor to turn. When the motor rotates, the windings are always being energized in a various sequence because of that the magnetic poles produced by the rotor do not exceed the poles produced in the stator. The diverting of the field in the armature windings is called commutation.

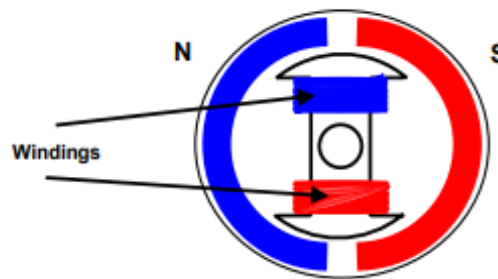


Figure 15: Rotor

2.3.4 Brushes and Commutator

Brushed DC motor windings do not need to have any additional controller to switch current. Instead of electronic controller, a segmented copper sleeve which is called commutator, provides exchange of windings mechanically. While motor is running, carbon brushes get contact with different segments of commutator by sliding over. These segments are connected with various rotor windings, when a voltage is supplied across the brushes of the the motor, a dynamic magnetic field is produced inside the motor. It is significant that the brushes and commutator are components of brushed DC motor that are tended friction as they are slipping each other. While rotor is rotating inside the stator, the brushes in contact with the different commutator segments providing a charge that matching winding and segment. The supplied electrical charge change commutator segments, when the brushes pass around the commutator gaps hence, exchanging electrical polarity of the rotor windings. It is generated an allure of different polarities and retain the rotor turning within stator field. Since the motor is supplied this action advances.

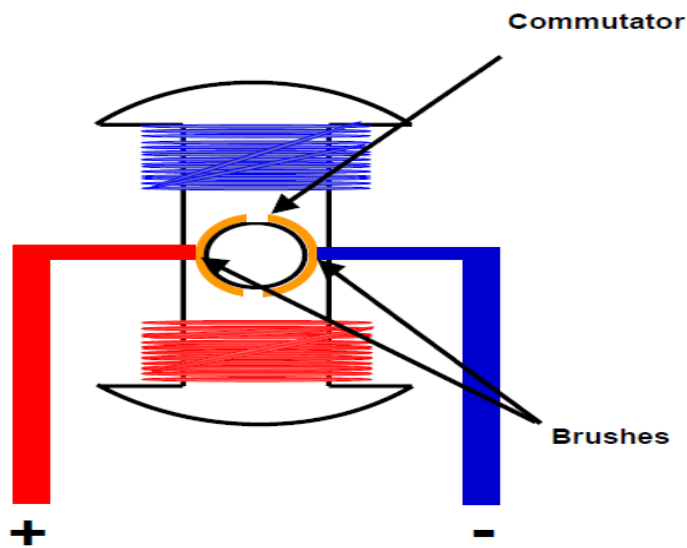


Figure 16: Brushes&Commutator

2.3.5 Types of Brushed DC Motor

The variety of the magnetic field is generated in the stator that cause the various types of brushed DC motor.

2.3.5.1 Permanent Magnet

Permanent Magnet Brushed DC(PMDC) motors the most prevailing BDC motors that are found in the world. This type of motor wields permanent magnets to generates the stator field. Generally, PMDC motors are used for fractional horsepower as to be more cost effectiveness it is used permanent magnets than wound stators. The disadvantage of PMDC, these magnets lose their magnetic properties over time. In order to prevent losing magnetic properties, some PMDC motors contain windings built into them. The relation between voltage and speed is linear also current changes linearly with the torque. The response of these motor for changes is very quickly as the stator field is always constant.

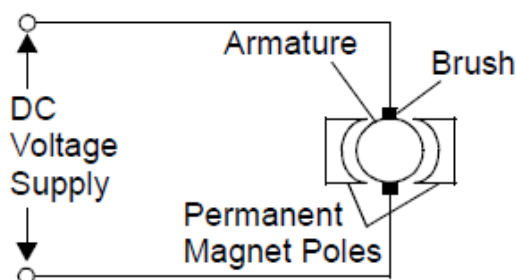


Figure 17: Permanent Magnet Brushed DC Motor

2.3.5.2 Shunt Wound

Shunt-Wound Brushed DC (SWBDC) motors are connected in parallel to shunt field coil with armature. The current in the coil and the armature do not depend on each other. Consequently, SWBDC motors have perfect speed control. General applications that are needed five or more horsepower. Losing magnetic properties is not a problem for SHWDC hence they are more safe than PMDC motors.

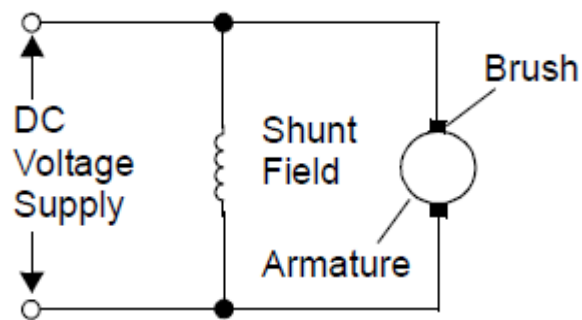


Figure 18: Shunt-Wound Brushed DC Motor

2.3.5.3 Series-Wound

Series-Wound Brushed DC (SWDC) motors are connected in series to field coil with the armature. These motors are used for high-torque applications because of increasing current in both stator and armature under the load. In contrast to PMDC and SHWDC motors, SWDC motors do not possess accurate speed control.

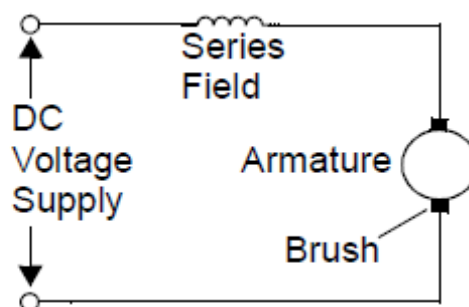


Figure 19: Series-Wound Brushed DC Motor

2.3.5.4 Compound-Wound

Compound-Wound(CWDC) motors comprise of merging of Shunt-Wound and Series-Wound motors. CWDC motors have both series and shunt field. Therefore, the specification of CWDC motors are between SWDC and SHWDC motors. Thereby, CWDC motors have better speed control than SWDC motors and they have higher torque than SHWDC motors.

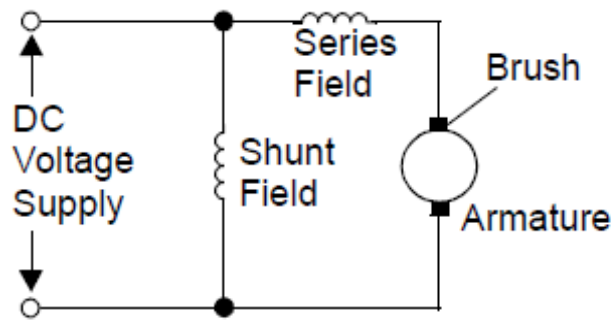


Figure 20: Compound-Wound Brushed DC Motor

2.4 Complete System

Motor position memory is used in many areas of the automotive applications that consist configuration and comfort settings according to different driver requirements for diagnostics to be more efficient and smarter control of the motor. More cost-efficient and easily-configurable applications have been become widespread for various motor types. For instance, the vehicle seats can have characteristics that are for many axes of movement and ergonomic adjustment controlled by individual motors. Sensored approach for vehicle seats consist of motor with hall-effect sensors plus the additional extra wiring for each sensors. Whereas sensorless approach decreases many sensors and wirings by sensing the in-line motor current at the seat control module itself. It is possible to provide sensorless solution with brushed DC motors thanks to impact of the back-electromagnetic force(BEMF) has on the motor current. When the motor rotates, regularly changing of the BEMF through the property of the DC motor brushes causes contact with multiple poles of the motor and significantly shorting some of motor windings. The alteration of impedance provides the measured current at fixed intervals proportional to the actual speed of motor. The variable in-line motor current is measured by the system, filtering and conditioning the resultant signal, then ensure digital logic level series of rising and falling edges to examine and count up for precision and feedback to main motor controller. The changing in current sense resistor values and filter bandwidths, it can adapt easily to use with several small motor systems.

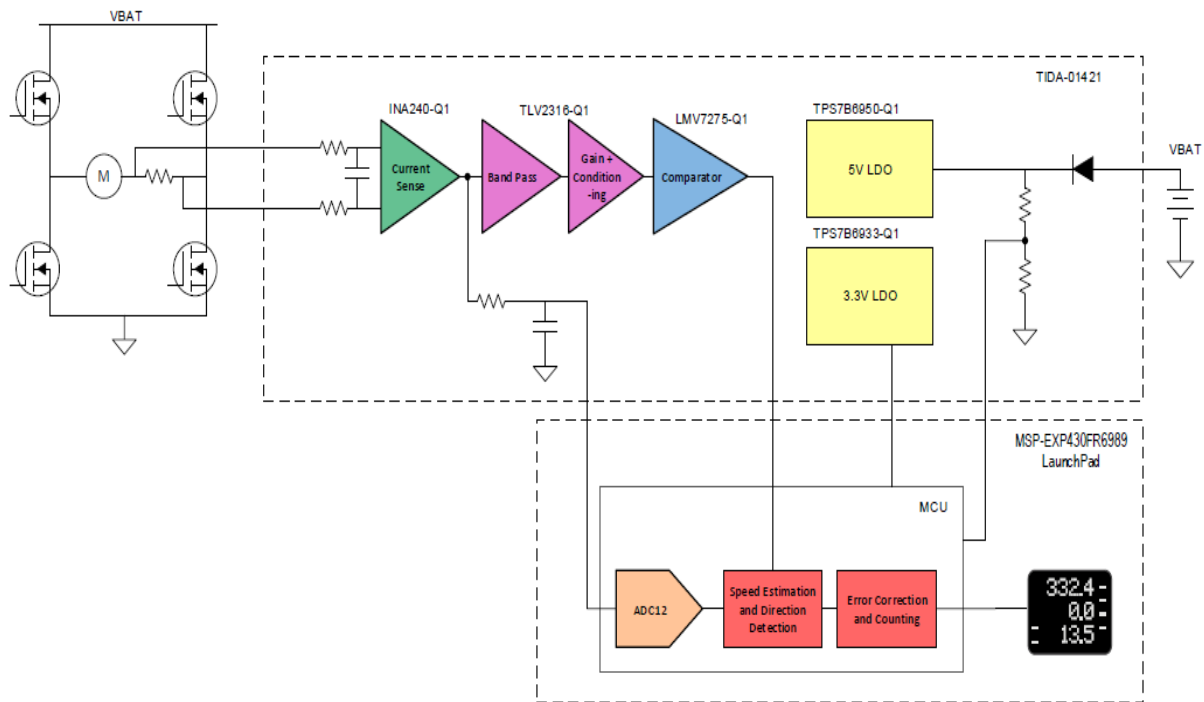


Figure 21: Complete System Block Diagram

3. Position Control Measurement

The stator and rotor magnetic fields always should be perpendicular to each other to operate the motor synchronously at maximum torque. The motor position should be known to achieve for this movement. The motor position is directly related to the rotor position. There are two main techniques to understand rotor position, the first technique is position measurement with sensors and the second technique is the one without sensors. The sensed approach for brushed DC motors is branched into 2 ways, that are used Hall-Effect Sensors and Optical Encoders. In the following sections these branches are going to be mentioned in a detailed way.

3.1 Sensored Approach

3.1.1 Hall-Effect Sensor

As there is no electric contact between stator and rotor, the relative rotor position requires thanks to help of hall-effect sensors to determine position. It is used to provide position feedback. It is needed a rotary element mounted on the motor and a stationary component. The rotary element is wheel with one or more magnets that are assembled on outer rim. While rotor is turning, the stationary magnets sensors check the magnets for every passes it generates transistor-transistor logic(TTL) pulse. Therefore, it counts every movement of rotor.

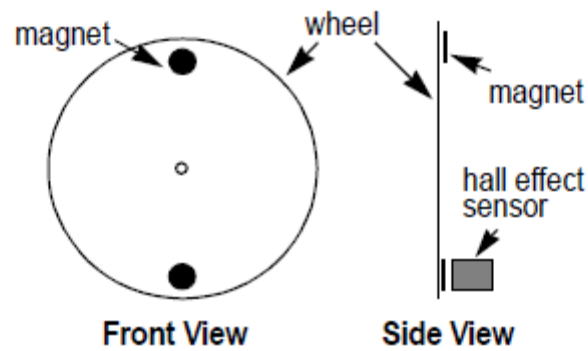


Figure 22: Hall-Effect Sensor

3.1.2 Optical Encoder

Optical Encoders consist of several components. On the shaft a slotted wheel is assembled at the non-driving end of the motor. One side of the wheel there is an infrared LED supplies a light source and on the other side of the light is detected by photo transistor. While the rotor is turning, infrared LED generates a light that are passing through the slots of the wheel that cause to switch on and switch off photo transistor. The frequency that depends on the transistor toggles is an indication of motor speed. For position measurement, the optical encoder ensures feedback for the position of the motor.

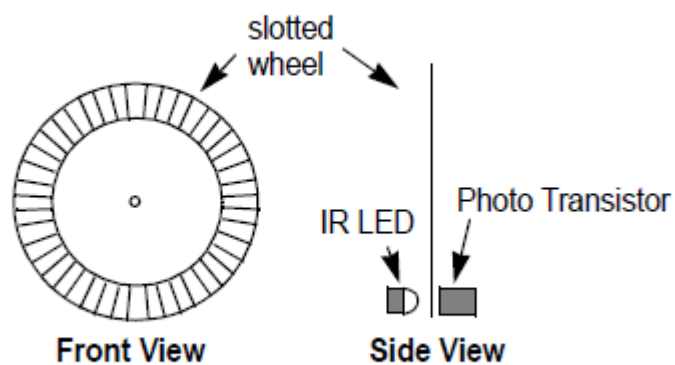


Figure 23: Optical Encoder

3.2 Sensorless Approach

The sensorless approach is motor control technique that does not require sensors to specify the actual motor speed or position. The position of the motor is specified depending electrical parameters as Back-EMF or motor current feedback that is existing during the motor operating time.

The aim of current feedback usage is for position control, circuit protection or motor speed estimation. To pursue the motor current, the current sense resistor is connected in series with the motor. The determined current is transformed to a measurable voltage which behaves as a speed or position feedback signal to a closed loop motor control by using current sense amplifier touched on the resistor terminals. Depending BDC motor electromechanical structure, the periodic changes in current feedback are sighted.

While motor is rotating, the displacement can be determined by counting number of these periodic changes. To specify motor position and speed, the technic of using motor current feedback is called as ripple counting. In the following figure the periodic changes in the current feedback are demonstrated.

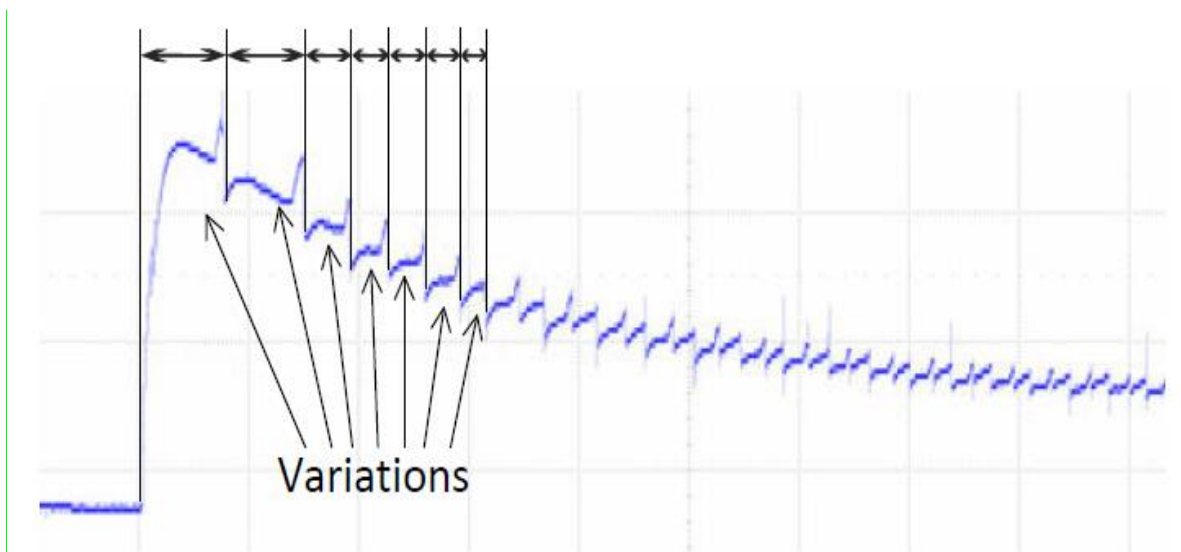


Figure 24: Periodic Changes in the Current Feedback

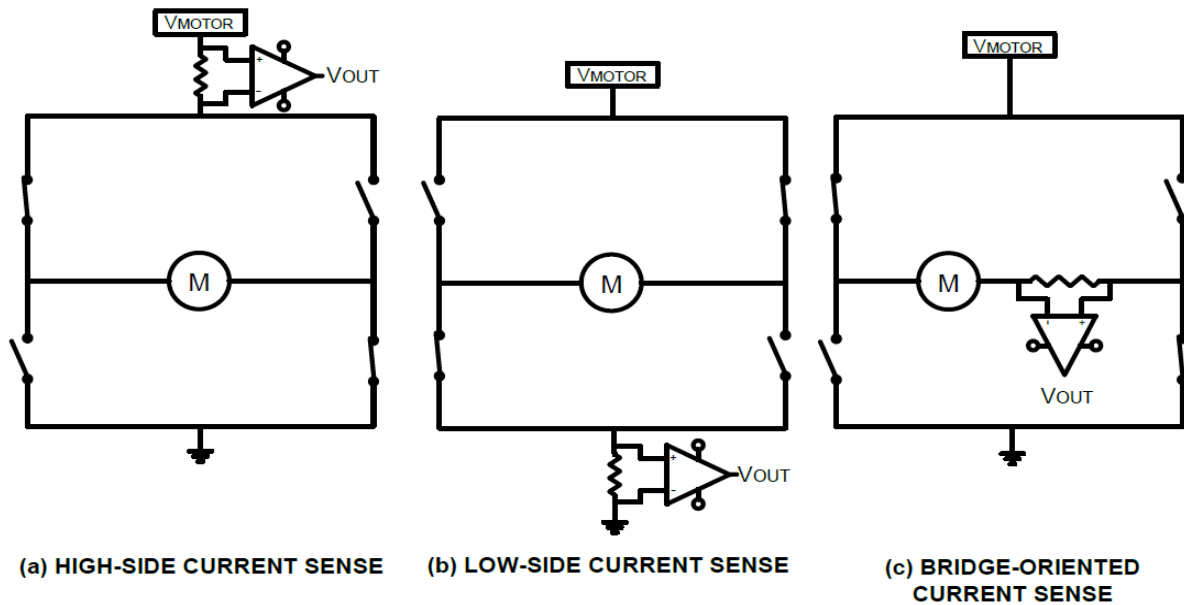


Figure 25: Current Sense Configuration

Firstly, to apply a sensorless drive the ripple counting technic relies on the motor current feedback. Shown in the previous figure, various current sense configuration depending on sensing resistance installment can be utilized to follow current feedback.

The bridge oriented current sensing and high side current sensing are generally applied for functional safety. Even if it is proven efficiently, these kind of configurations need to have high end current sense amplifier with high common mode voltage and more complicated circuits.

When the current sense resistance is fixed between the ground and the motor, the current sense configuration is called as low side current sensing. Depending on choosing amplifier and complexity of electronic circuit are the simplest and most cost effective applying of sensing configurations. The average voltage of current sensing resistance that is nearly zero because it is referenced to ground. It is not difficult to choose devices for its design and applying since high input common mode voltage is not needed. It is also used for high voltage motor applications as it has resistant against voltage spikes or surges.

Low side current sensing has special restrictions. The installment of the current sense resistance generates the load that does not reference ground. The resistance that is brought by sensing, the low side of load is higher several millivolts than ground. It can not determine the short circuit between ground and load without ground reference. Although there is a disadvantage, it is an acceptable selection for ripple counting application since it does not require to have ground reference thanks to its simplicity and load.

3.2.1 Brushed DC Motor Current Ripple

For a spinning motor, there are different kind of ripples which are categorized according to torque ripple, speed ripple and current ripple. By undesirable variation of torque production during shaft revolution and preventing smooth motor rotation the torque ripples are distinguished and they are observed by in low frequency mode. The speed ripples are activated by parasitic torque pulsations which differ as a periodic with respect to rotor position.

While motor is rotating the current ripple is generated and it is known as low amplitude current interchange, driving on the DC voltage supply. This current ripple is a recurrent alternation in generated current by rotor motion when rotor coils connects and disconnects power supply by the brushes. The generated current ripple suggest an idea about commutation action in a BDC motor. In the following figures, it is shown that motor rotation of three commutator segment and how the current ripples or commutation spikes are generated by rotation.

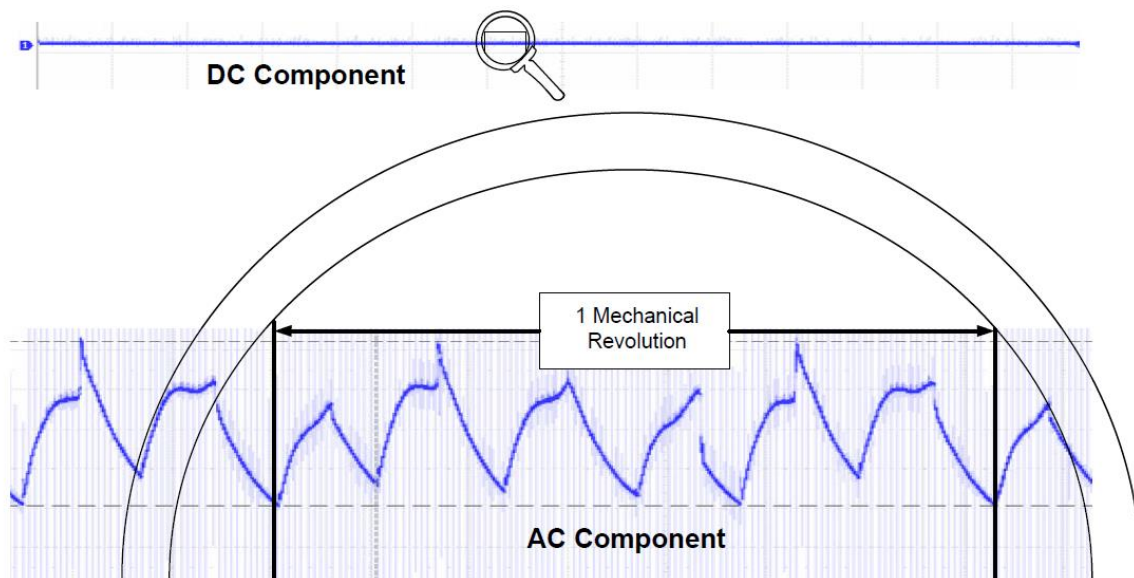


Figure 26: Ripple Production from a Rotating Motor

When the signal which comes from a rotating motor, is analyzed the DC component is easily monitored on a measuring instrument. To examine the AC component or current ripple, the DC component should be analyzed closely.

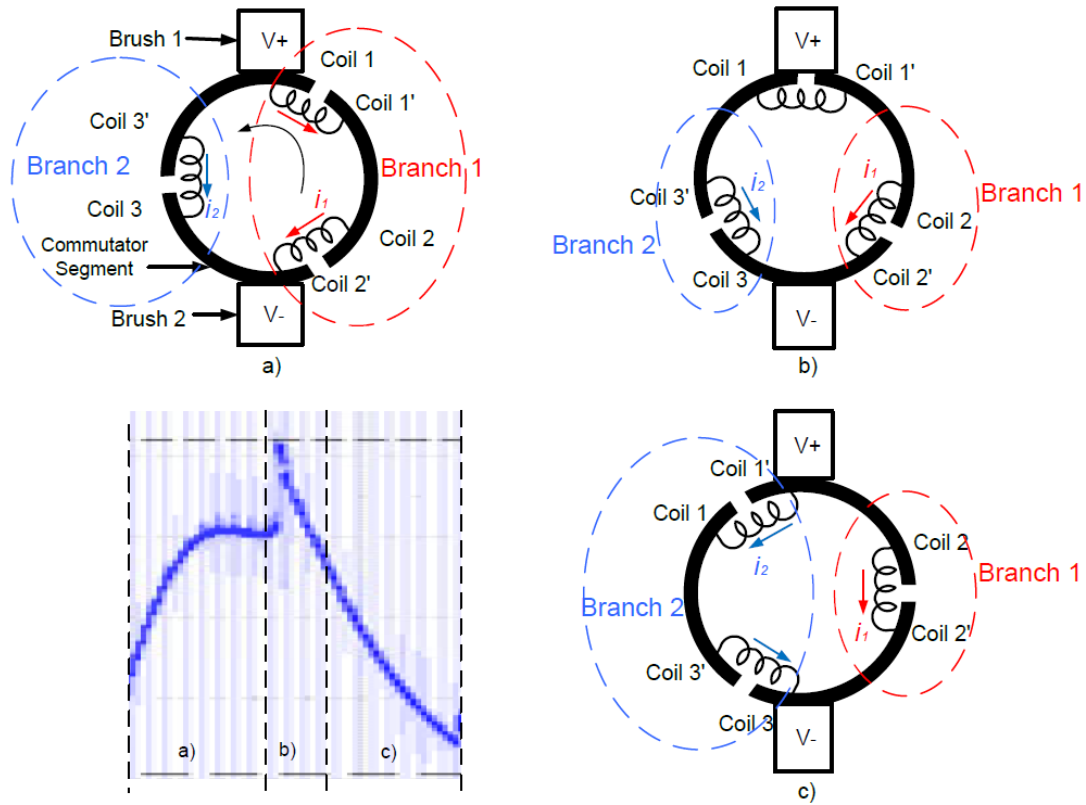


Figure 27: Rotation Process

While the BDC motor is rotating, the brushes short circuit with adjacent commutator segments which causes current circulation with other segments. It induces the Back-EMF of commutator segments as a short circuit, so it generates high voltage pulses on the motor terminal in a short time. The impedance of armature is decreased by the high voltage pulses, hence it causes that the overall current increases and current ripple produces. The brush moves periodically from one coil to another so it generates a periodic current ripple. Further, each ripple waveform can be various each other.

The direction of rotation of DC motor is supposed as counterclockwise as represented by black arrow in the Figure 27(a). Positive supply is connected Brush 1 and negative supply is connected to Brush 2. The Branch circuit 1 that is consisted of Coil 1 and Coil 2 and its current direction is clockwise from Brush 1 to Brush 2 represented by red arrow. The opposite side the branch circuit 2 that is comprised of Coil 3 and its current direction is counterclockwise from Brush 1 to Brush 2. The current flow of Branch 1 is called i_1 and the current flow of Branch 2 is identified as i_2 . According to the Kirchhoff's current law the total current of DC motor equal to sum of both currents as shown following equation.

$$i = i_1 + i_2$$

When Coil 1 coincides on the Brush 1 as in the Figure 27(b), it reduces voltage across Branch 1 since this branch is comprised of only Coil 2. The applied voltage across Brush 1 and Brush 2 always remains constant, the current of Branch 1 immediately increases thanks to short circuit of Coil 1, in the mean time the current of Branch 2 remains the same. The total current that flows into DC motor, increases quickly.

After immediate short circuit, the following stage is demonstrated in Figure 27(c). The Branch 1 is comprised of only Coil 2 whereas Branch 2 is comprised of Coil 1 and Coil 3. The direction of current in Coil 2 remains same as the voltage direction. By the way current value of Branch 2 suddenly reduces when commutation finishes. In this way, the generated current ripple is represented in the graph of previous figure, it was divided subsections to show the commutation process from (a) to (c).

The subsequent ripples are generated through same operation of contact between coil and brush. For complete rotation each coil should contact the two brushes. Moreover, every contact between coil and brush generates a different ripple waveform. The reason is that each brush of motor is particular and the coils are designed variously.

In a particular motor the number of commutator poles and brushes are fastened up. For this reason the number of ripples does not change in a complete rotation. For each rotation, the ripple is repeating and the number of ripples per revolution is computed in the following equation.

Equation 1: Number of ripples per revolution

$$\text{Number of ripples per revolution} = \text{Brush} \times \text{Commutator Segment}$$

For geared motor, the equation changes a little bit to compute number of ripples per revolution multiply by gear ratio as shown in the following equation.

Equation 2: Number of ripples per revolution using geared motor

$$\text{Number of ripples per revolution} = \text{Brush} \times \text{Commutator Segment} \times \text{Gear Ratio}$$

In this project, BDC motor have two brushes and four commutator poles.

Number of ripples per revolution = $2 \times 4 = 8$ ripples per revolution

In order to know total number of ripples for one turn, it is enough to know number of ripples that demands to turn exact degree of an angle. To count current ripples by microcontroller, it should be filtered, conditioned and converted rising and falling edges of logic level series.

3.2.2 PWM Effects on the Ripple

The other method of controlling speed of BDC motor is to control its supply voltage which is the easiest method. The higher voltage provides to rotate motor in higher speed. For many DC motor speed control applications the Pulse Width Modulation method is utilized on the low-side of the full bridge driver. The motor speed is specified according to the ratio of 'ON' and 'OFF' time.

As a low amplitude, high frequency signal qualifies the current ripple, any modulating alters as a periodic the driving voltage give rise to the system which does not identify the ripple or lower its signal completeness. In the following figure demonstrates the various PWM speed modulations generate the ripple. Relying on the degree of modulation, the visibility of ripple is influenced by the PWM speed modulation. The PWM method concentrates on precision control application so the speed modulation is adjusted 100% modulation.

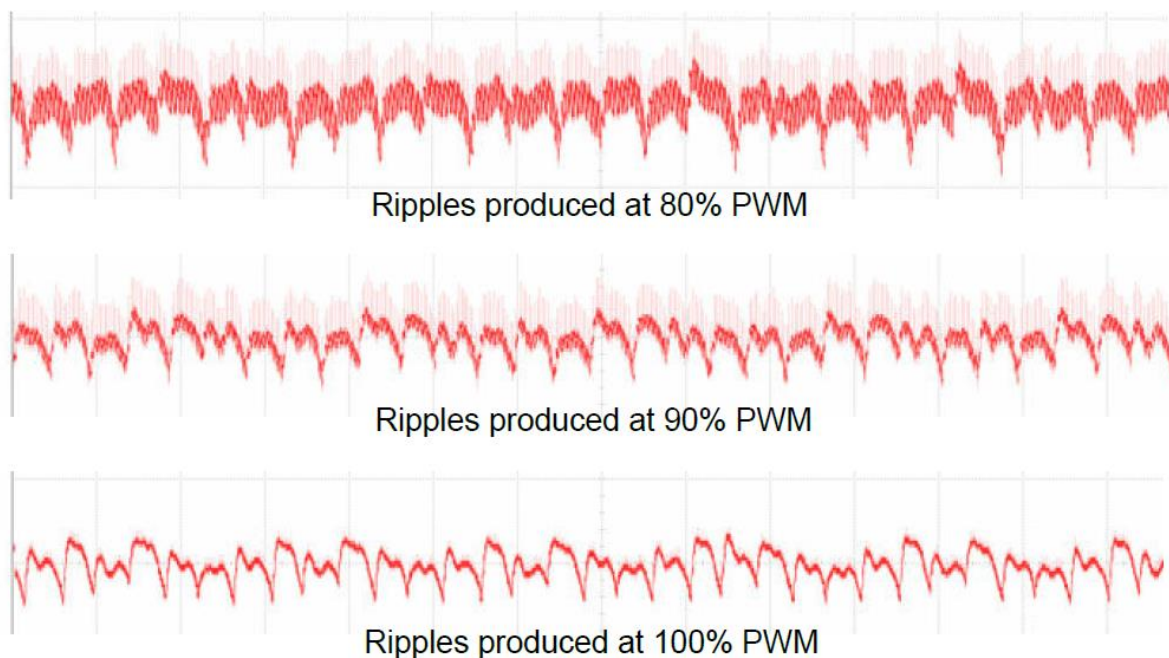


Figure 28: Generated Ripple in Different PWM Duty Cycles

3.2.2.1 Back Electro Magnetic Flux

The electromotive force voltage can be predicted based on the machine electric model that are included voltage and current signal for sensorless approach. Whereas, EMF voltage depends on speed. When the speed reduces, the signal-to-noise(SNR) ratio of EMF voltage reduces. For low speed operation, change of resistance and voltage errors by reason of the inverter PWM modulation influence the EMF prediction. The first concern of EMF predictions at low speed is the inverter voltage error. This kind of error consists of semiconductor voltage drop and inverter resistance voltage and switch dead-time. In order to balance nonlinear behaviour of voltage error, an off-line voltage measurement is applied to base a look-up table for the balance. Nonetheless, prediction error can not be solved by look-up tables, as the deadtime error may not be depended by phase currents. Additionally, look-up tables for balance count on various machine feature.

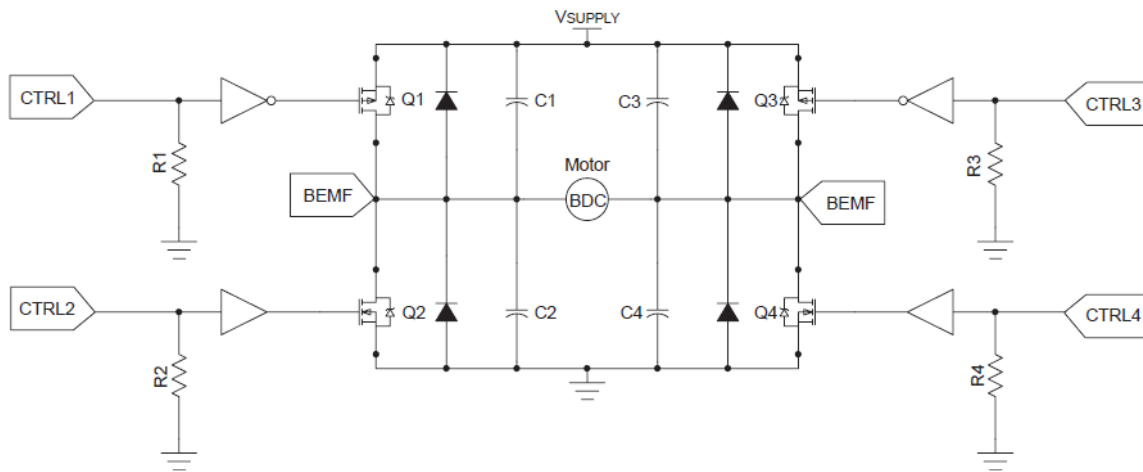


Figure 29: Back EMF Voltage Measurement

Due to voltage divider, BEMF voltage decreases 0-5 V range thereby, it is read by an analog-to-digital converter. The BEMF voltage measurement is provided by PWM Pulses, while one side of motor is behaved as supply, the other side is behaved as ground. At the same time, motor is running like a generator and generates BEMF voltage that is proportional to speed. Each BDC motors may vary because it has different efficiency values and material properties. The best way of determination of the BEMF voltage is testing to find motor speed.

4. System Stages

Firstly, complete system consists of 4 stages. After doing theoretical computation and test and simulation number of stages can be changed. Also, cost efficient is the

important issue for this project hence, some electronic components can be removed or changed due to cost reduction.

4.1 Current-Sense Amplifier Stage

The first stage is current-sense amplifier that brushed DC motor current converts to voltage. Entering the current the current-sense amplifier and stemming voltage as an output. Measuring the total BDC Motor current is provided by detection on the low side of the driver bridge, or in-line with BDC Motor. To maintain precision of the ripple signal, detection current on the low side presents impedance and layout issues. In addition to this, measuring ripples in both side, detection of low side needs a sensing amplifier for both sides of the full bridge that enhances the total component count. Measuring in-line with BDC Motor is possible that bidirectional measurement with a single device. Nonetheless, some design issues should be solved to provide a precise output for the next stage. The automotive battery supplies power to the MOSFET bridge driving the BDC Motor in an automotive application. The general supply range of the battery is between 9 V and 14 V but operating voltages can be changed between 6 V and 40 V for some automotive conditions. When selecting a current sense amplifier, common mode voltages are important to block functional damage from the device.

The current sense amplifier component is called as INA240-Q1 that has common mode voltage range between -4 V to 80 V, is compatible for all the possible common mode condition that requires for the design. The INA240-Q1 is also capable to supply a bidirectional output measuring both motor rotational directions. There are two reference pins, REF1 and REF2 that supplies to output of the INA240-Q1. REF1 is connected 5 V and REF2 is connected to ground. The INA240-Q1 is supplied with 5 V so the output range is 0 V to 2,5 V or 2,5 V to 5 V and it depends on the BDC Motor rotation direction. The following equation is demonstrated calculation of the output voltage.

$$V_{OUT} = I_{MOTOR} \times R_{SENSE} \times GAIN + 2.5V$$

The shunt resistor is adjusted according to the maximum current and 16 A has been selected for this stage. The gain of INA240-Q1 is 20 V/V and the maximum output voltage is 4,9 V. This resistor value is chosen 3 mΩ.

The shunt resistor is selected to use very high amount of power and it's size 2512 resistor has 3 W power. In order to decrease the noise is generated by high frequency motor brush and potential PWM switching noise, common mode RC input filter is used to connect to INA240-Q1 as an input.

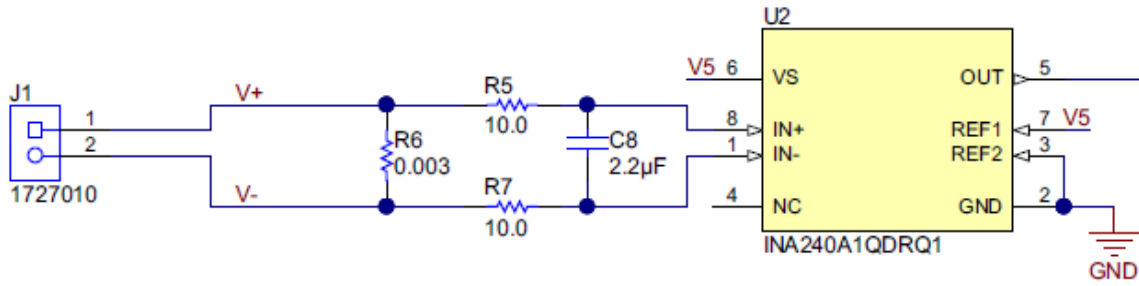


Figure 30: Schematic of Current Sense Amplifier

4.2 Band-Pass Filter Stage

The second stage is band-pass filter which adjusts interval of frequency of system. The output of current sense amplifier enters to this stage as an input that is filtered by band-pass filter to manage motor current ripple and to remove unwanted current ripples. The measuring of ripple frequency is dependent on rotations per minute(RPM) of the motor and the total number of commutator poles. For this system, bandwidth of band-pass filter is between 333 Hz to 669 Hz. To allow biasing, an inverting band-pass filter is used. The TLV316-Q1 was selected and it is convenient low voltage operation and rail to rail input. The following figure demonstrates schematic of band-pass filter stage.

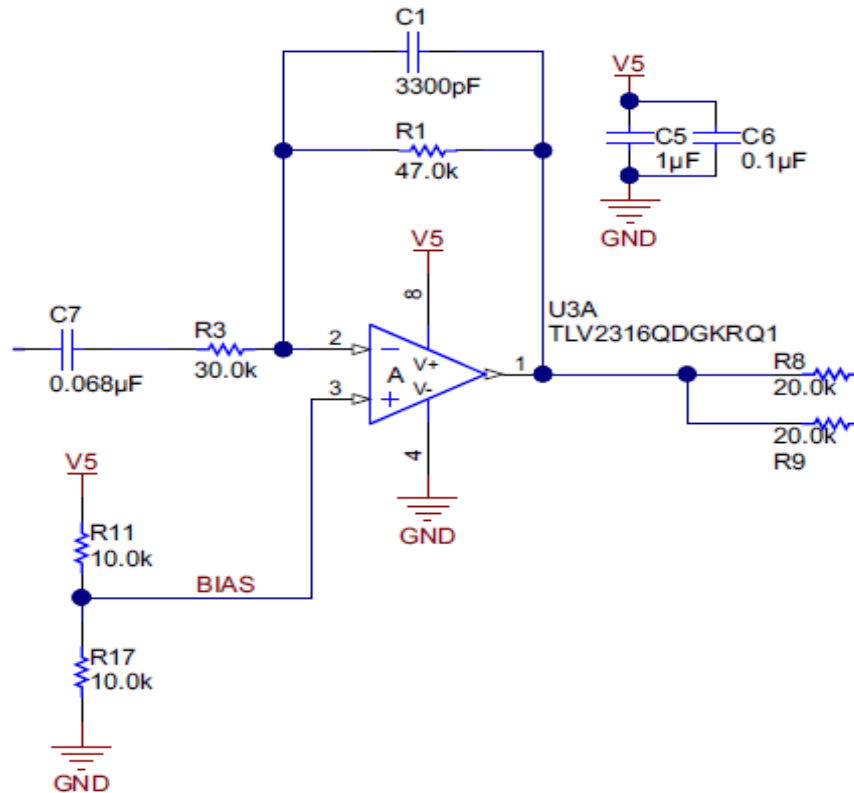


Figure 31: Schematic of Band-Pass Filter Stage

4.3 Differential Amplifier Stage

The third stage is differential amplifier aims to produce clean, low noise AC signal which is measured between 0 V to 5 V square wave by comparator with changing frequency equal to brushed DC motor ripple frequency. To generate square wave, the sinusoidal ripple waveform about comparator reference point is used. The previous stage initiates this operation though there is additional stage required for specific filter requirements and operating frequency range to provide appropriate biasing for the next stage.

The frequency of high-pass filter of previous stage is adjusted 333 Hz that needs to success by large RC filter. This filter produces extremely large time constant which demonstrates its impact on the signal at the start up motor current as a large initial spike. By the reason of this current spike being huge enough and sluggish enough, it can not be filtered by high pass filter of previous stage and the RC time constant value signifies the low frequency DC component of the signal can not indweel a resting point rapidly. While brushed DC motor is rotating, this current spike and current ripples are produced. Some multiple ripples for counting can be missed by the comparator, if the alteration is remained same in the effective DC-bias point of the signal. The following graph displays resultant signal after the differential amplifier(green waveform) and the initial spike in current(yellow waveform).

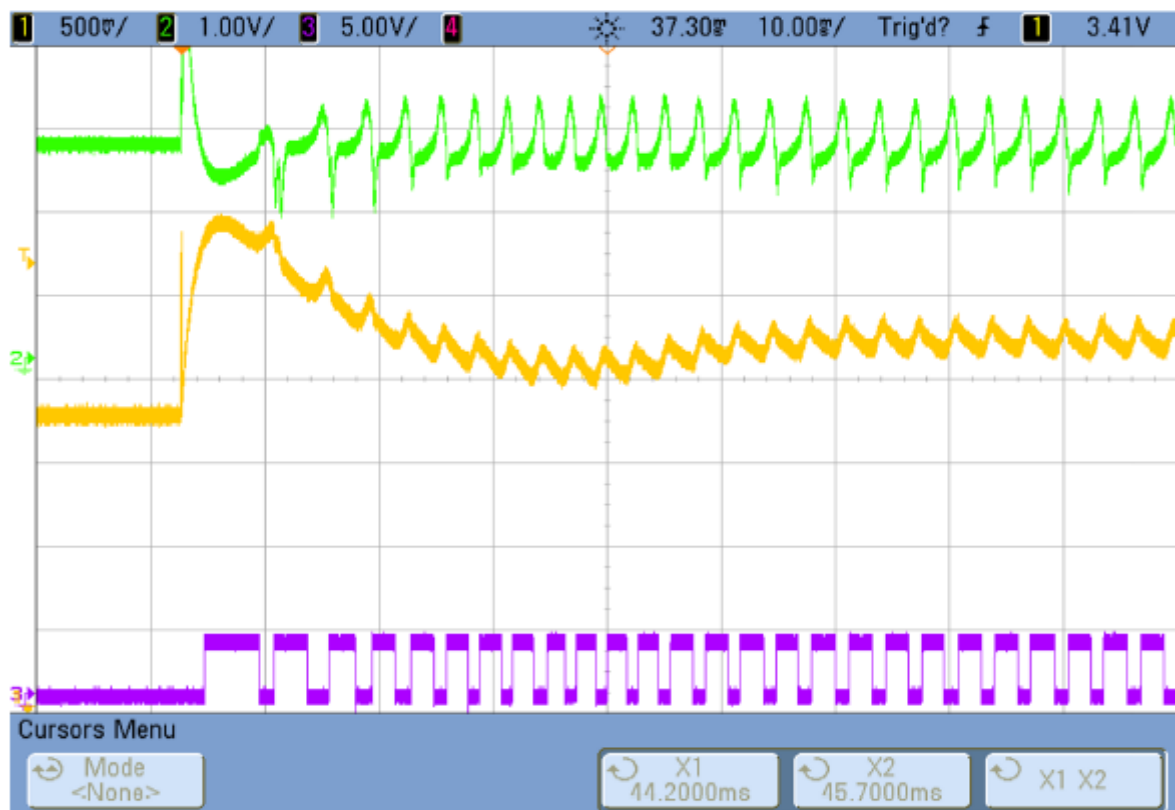


Figure 32: The Graph of Initial Current Spike

Thanks to usage of differential amplifier, the low speed current ripples and the high amplitude current spike are expelled from the signal. The non-inverting and the inverting ports of differential amplifier are connected to the output of band pass filter, nevertheless one side of the differential amplifier is filtered by low pass RC filter. A small phase shift and attenuation of the ripple signal are generated by small RC filter, though there is very insufficient effect on the large DC bias spike. The common mode remains same for both inputs and it is rejected by the differential amplifier. To maintain ripple frequency component, output of the differential amplifier is led by the phase and amplitude difference between the AC signals on the both inputs. The differential gain is 55 V/V causes huge fluctuation of signal difference and DC re-biasing about 2,5 V approves the output of differential amplifier to possess a very clean and stable bias point for the signal that is gauged by the comparator. The schematic of the differential amplifier stage is illustrated in the following figure. The BIAS signal refers to resistor divider that is used in the band pass filter stage.

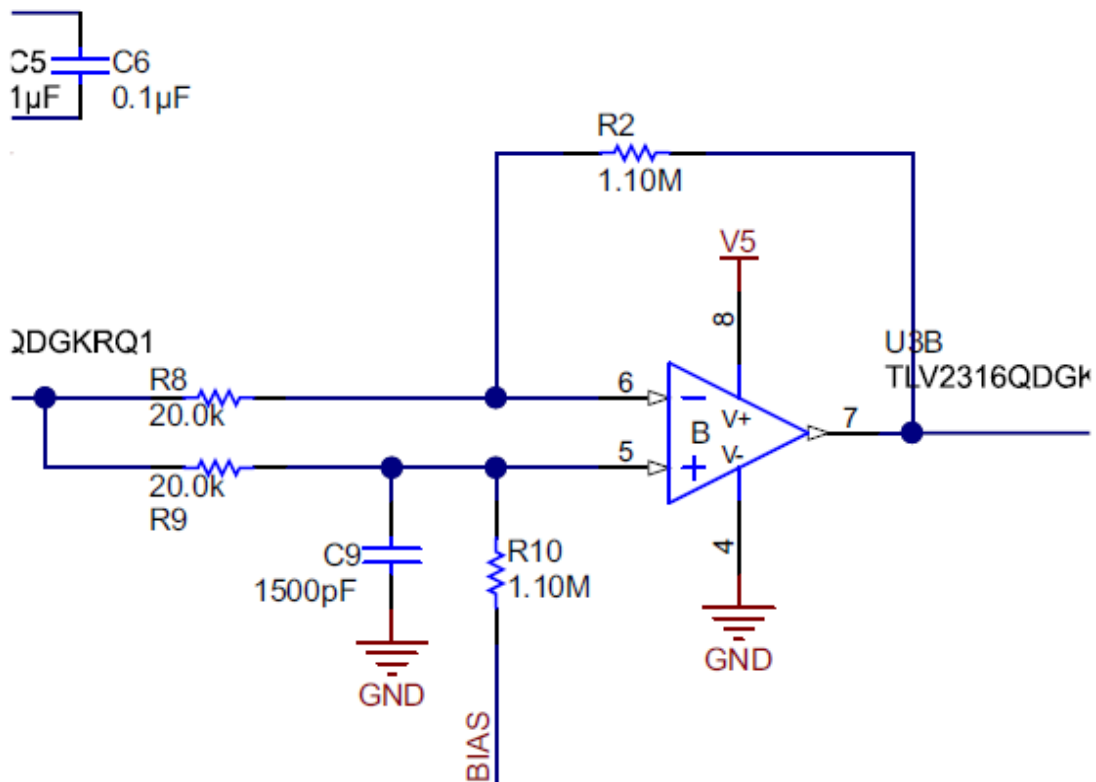


Figure 33: Schematic of Differential Amplifier Stage

4.4 Comparator Stage

The goal of comparator stage is to produce 0 to 5 V signal supplied for microcontroller to count movement of brushed DC motor. To generate proper 5 V for input into a typical

microcontroller, an open drain output device is selected. For reducing impact of noise on the input of comparator, an inverting hysteresis topology is adopted. In the follow page, the schematic of comparator stage is demonstrated.

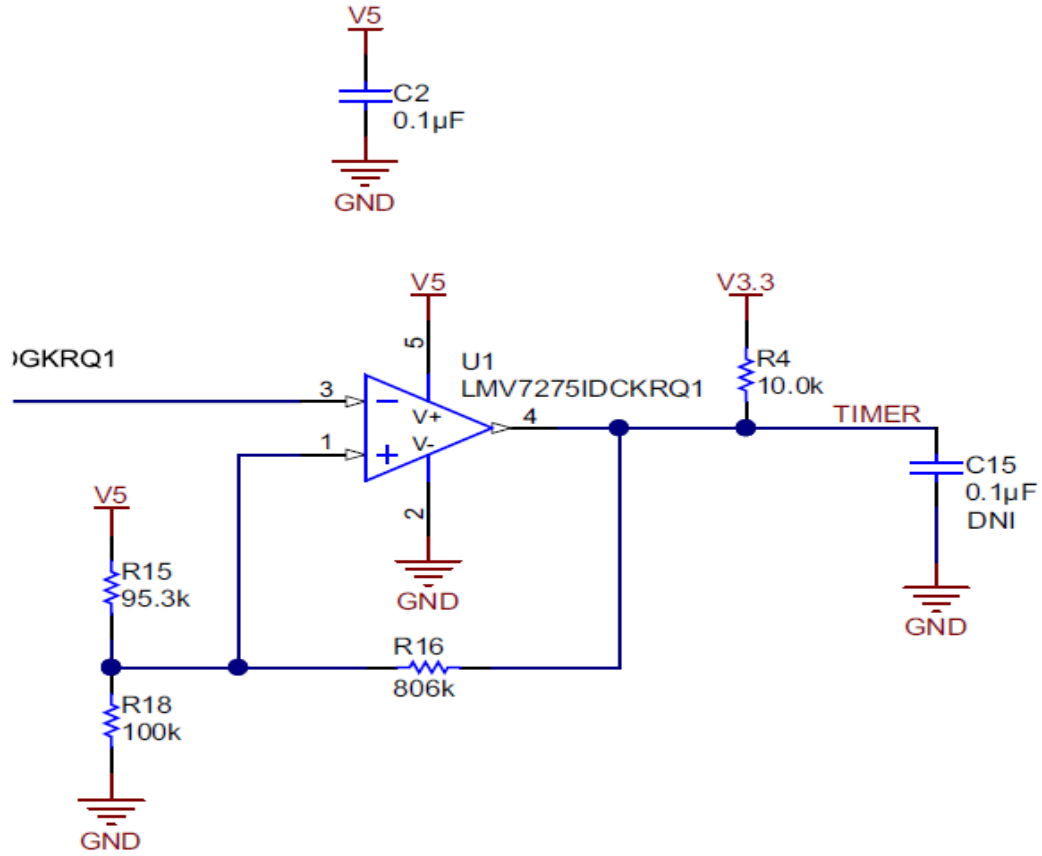


Figure 34: Schematic of Comparator Stage

In order to create an inverting open drain topology, the comparator threshold voltages are computed in the following equations.

$$V_{TL} = ((R18||R16) \times \frac{V_{CC}}{((R18||R16) + R15)}) + (R15||R18) \times \frac{V_{OL}}{((R15||R18) + R16)}$$

$$V_{TH} = ((R18||R16) \times \frac{V_{CC}}{((R18||R16) + R15)}) + (R15||R18) \times \frac{V_{OH}}{((R15||R18) + R16)}$$

For this stage, the V_{OL} equal to 0 V and V_{OH} equal to 5 V that generate a slight offset to concentrate the main biasing point of comparator. As the AC signal is centralized about 2,5 V and the reference point of comparator with feedback resistance is calibrated to permit the V_{TL} and V_{TH} are centralized about 2,5 V.

4.5 Updated System Stages

After the simulation evaluation, it is recognized that some changes can be possible. Therefore, updated system stages have been created. The main purpose of these changes is to reduce cost of all the system. For cost reduction, the differential amplifier was expelled and some stages are changed.

4.5.1 Updated Current-Sense Amplifier Stage

The aim of current sense amplifier is same as previous current sense stage but from cost reduction point of view, the schematic is completely different. In order to reduce cost, instead of INA240-Q1 TLV316 is used. The high side current sensing method is utilized for this stage. Generally, it is chosen applications which are motor monitoring and control, overcurrent protection and supervising circuits, automotive safety systems and battery current monitoring. In the following figure, the circuit is comprised of a single opamp difference amplifier, four external resistances. It increases small current by the gain R_2/R_1 and it converts current to voltage an output of the amplifier.

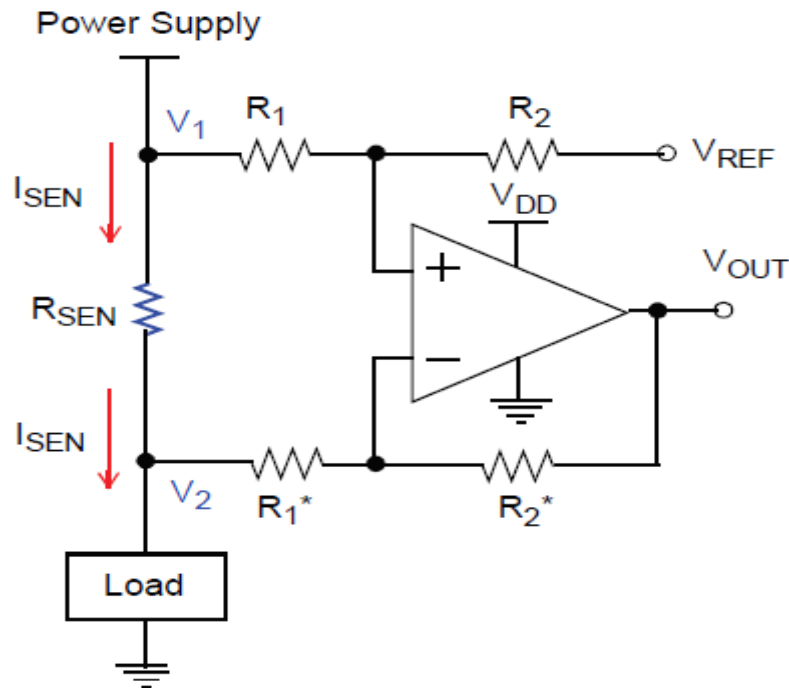


Figure 35: Single Opamp Difference Amplifier

$$R_1 = R_1^* \quad \& \quad R_2 = R_2^*$$

$$R_{SEN} \ll R_1, R_2$$

$$V_{OUT} = (V_1 - V_2) \cdot \left(\frac{R_2}{R_1} \right) + V_{REF}$$

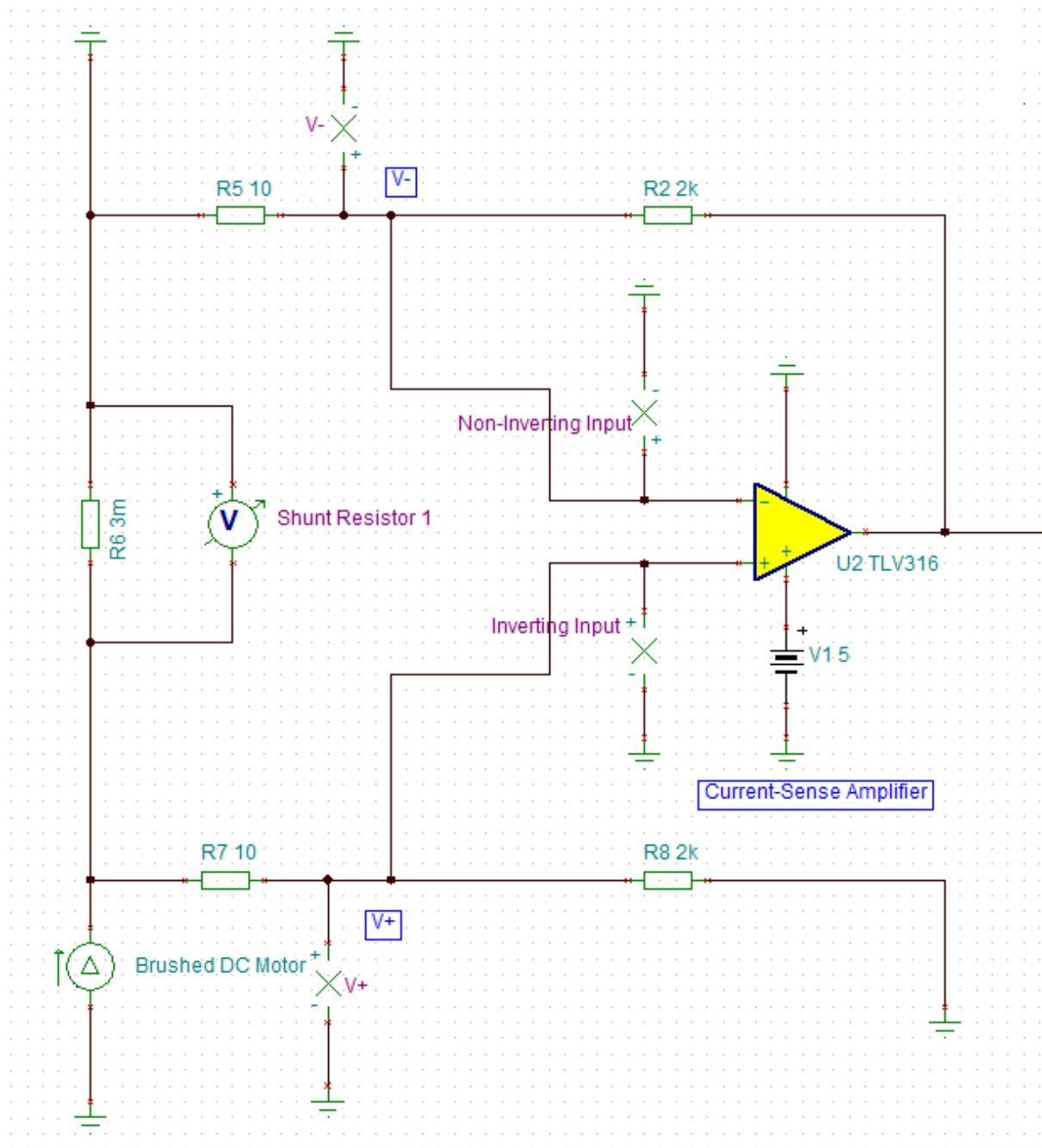


Figure 36: Schematic of Updated Current Sense Amplifier

4.5.2 Updated Band-Pass Filter Stage

The band pass filter stage is completely same as previous band pass filter stage. It can be had some small changes resistor and capacitor values in order to provide better bandwidth. The output of band pass filter is directly connected to input of the comparator.

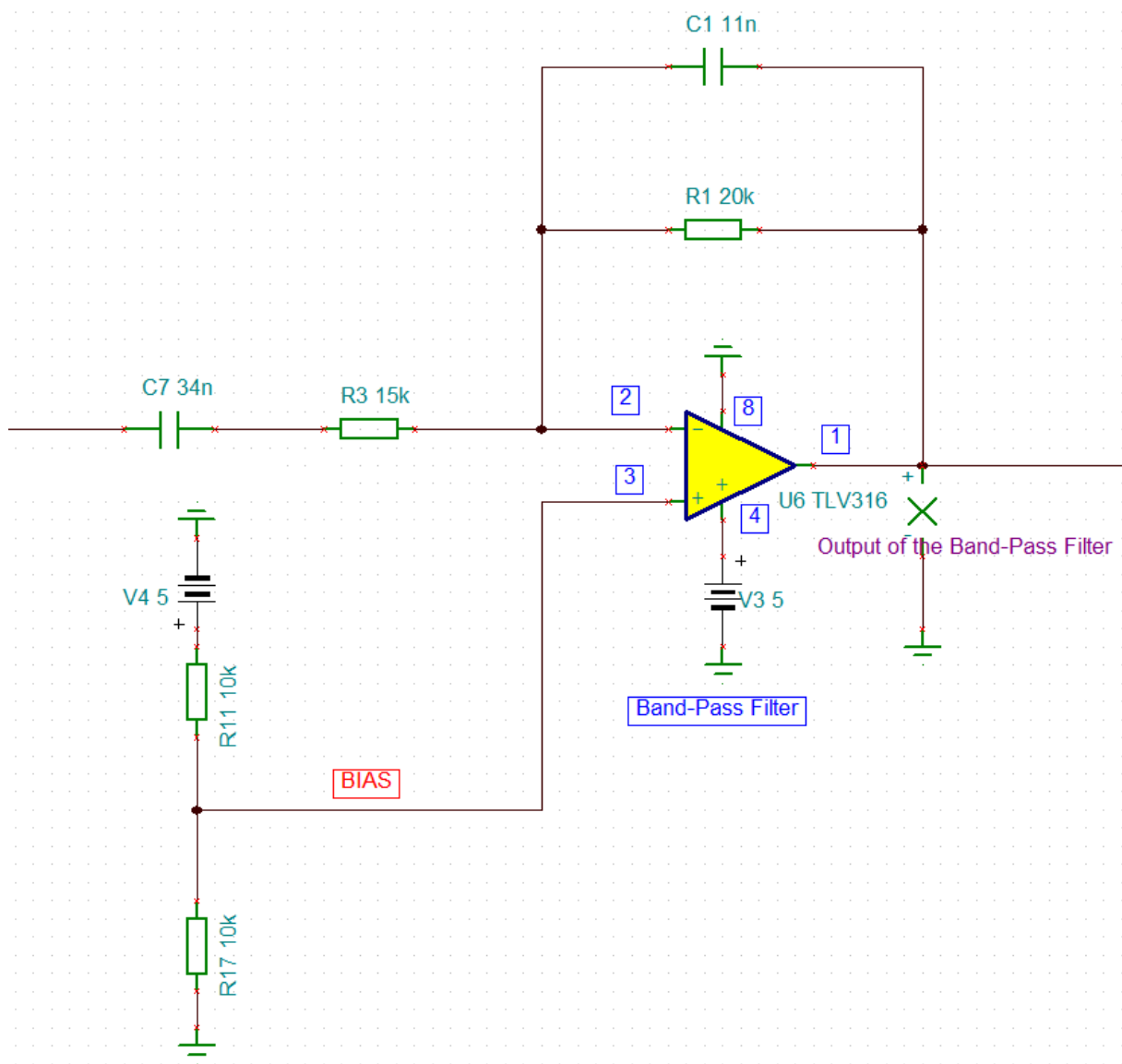


Figure 37: Updated Band-Pass Filter Stage

4.5.3 Updated Comparator Stage

This structure of updated comparator stage is same as previous comparator stage but the input of comparator is connected to output of band pass filter. Therefore, the differential amplifier stage was removed because of cost reduction. Moreover, to regulate threshold voltages according to updated stages, resistances values are altered.

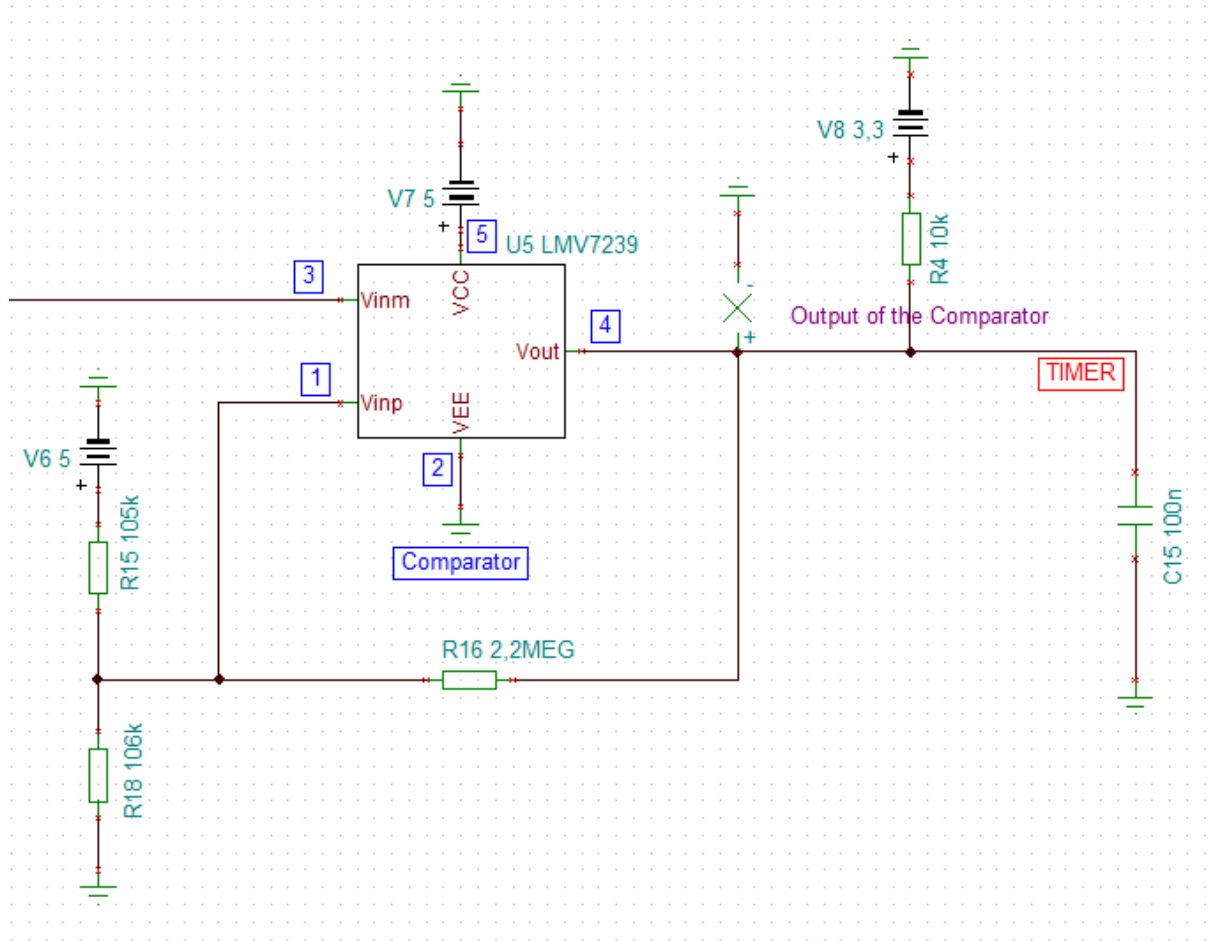


Figure 38: Updated Comparator Stage

5. Circuit Analysis

5.1 Electrical Schematics

5.1.1 Current Sense Amplifier Stage

In this part, each electrical schematic is analysed stage by stage. In the following circuit, the current sense amplifier stage is shown.

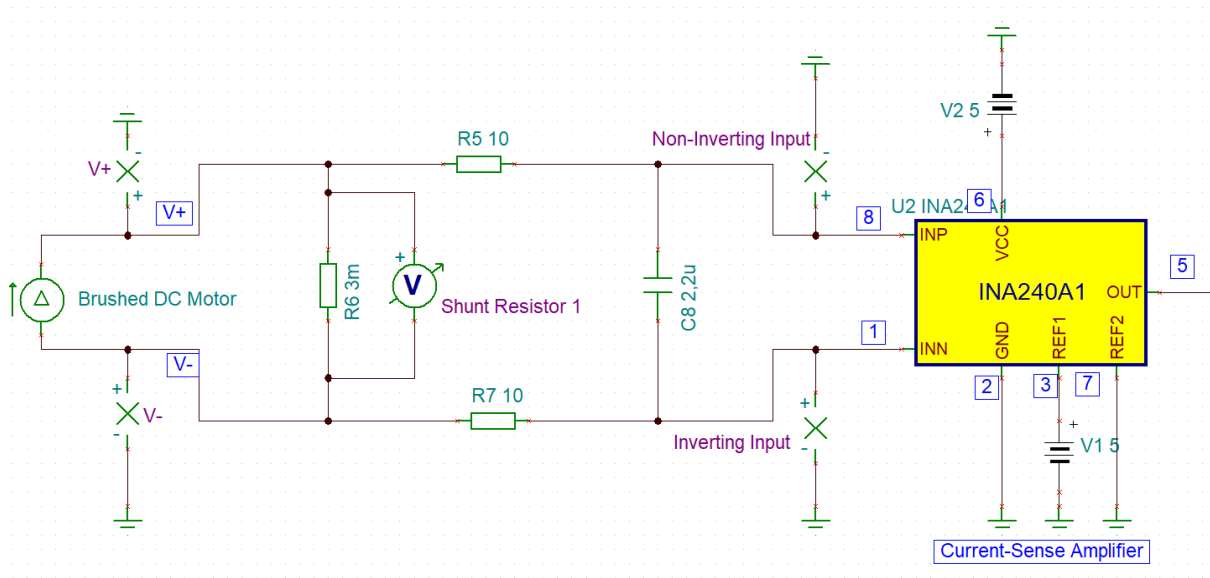


Figure 39: Current Sense Amplifier Circuit

The brushed DC motor is connected shunt resistor in a parallel. The value of shunt resistor was selected in the chapter 4. The maximum current is passed on the shunt resistor. The gain of current sense amplifier is 20 V/V. The output of this amplifier is voltage which is converted from current.

5.1.2 Band Pass Filter Stage

The second stage is band pass filter manages frequency range which represents operational range of complete system. The operational range frequency is inversely relevant that elapsed time for one motor turn that means period of motor. This frequency is also changed when motor is supplied by different voltages. The system is tested with 9 V, 12 V and 16 V for different motions. For each various motion and voltage value, distinct frequency value are obtained. Accordingly, minimum and maximum frequencies are selected. The band pass filter is comprised of low pass filter and high pass filter. For this system, the frequency of low pass filter part of band pass filter is 669 Hz and the frequency of high pass filter part of band pass filter is 333 Hz.

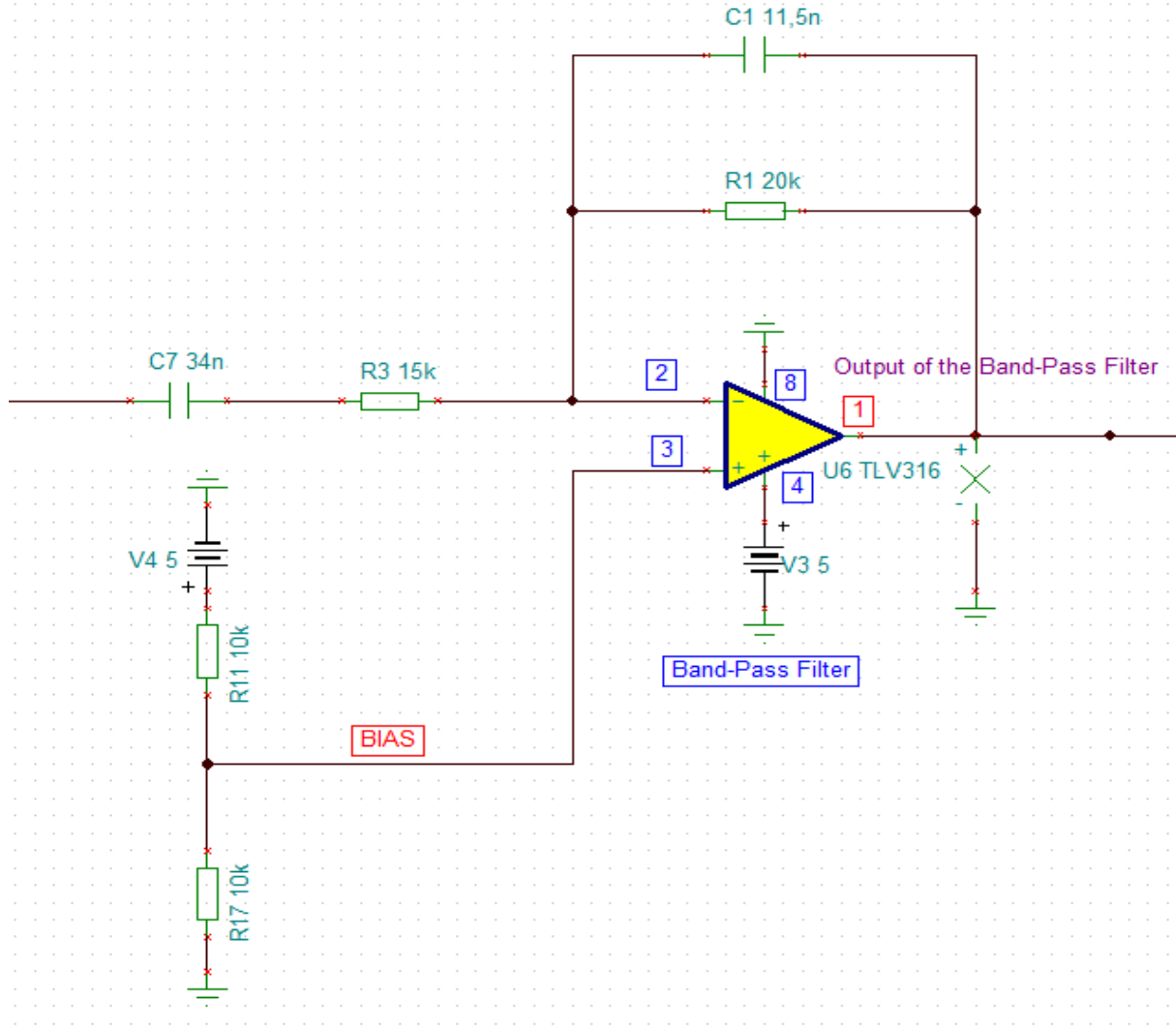


Figure 40: Band Pass Filter Circuit

The both frequencies of low pass filter and high pass filter are calculated separately. In the following equations, it is adequate to compute working frequency. The low pass filter allows to pass the frequency that is lower than limit whereas the high pass filter permits to pass the frequency which is higher than limit. The interval between low pass filter and high pass filter frequencies equal to bandwidth of band pass filter. It means working frequency of complete system.

$$f1 = \frac{1}{(2*\pi*R1*C1)} \quad \text{Frequency of Low Pass Filter}$$

$$f2 = \frac{1}{(2*\pi*R3*C7)} \quad \text{Frequency of High Pass Filter}$$

$$f1 = \frac{1}{(2 * \pi * 20000 * 11,5 * 10^{-9})} = 692 \text{ Hz}$$

$$f2 = \frac{1}{(2 * \pi * 14000 * 34 * 10^{-9})} = 312 \text{ Hz}$$

Bandwidth is between 692-312 Hz. The complete system is working in this interval.

5.1.3 Differential Amplifier Stage

The third stage is differential amplifier that has purpose to generate clean, low noise AC signal. The output of this stage is connected to comparator stage that measure square wave between 0 V to 5 V. The band pass filter starts filtering process but extra particular filter necessity is needed and for the comparator stage it is ensured to convenient biasing. Although both input ports of differential amplifier are linked with output of band pass filter, whereas the one side is filtered by low pass RC filter. This RC filter produces a small phase shift and attenuation of ripple signal.

$$f1 = \frac{1}{(2 * \pi * 1,1 * 10^6 * 210 * 10^{-12})} = 689 \text{ Hz}$$

Normally, the difference between two inputs is nearly zero, by the effect of capacitor is making small difference. The common mode stands equal for both inputs and it is refused by differential amplifier. The output of the differential amplifier is directed by difference of the phase and amplitude between AC signals on the inputs to preserve ripple frequency component. The gain of differential amplifier which is 55 V/V, provokes big variation of signal difference. The DC re-biasing about 2,5 V accepts the output of differential amplifier to generate clean and stable bias point for the signal which is measured by comparator. The output of differential amplifier is connected to input of comparator thus the threshold voltages of comparator are adjusted according to the output of this stage. In the following figure, electrical schematic of differential amplifier is represented.

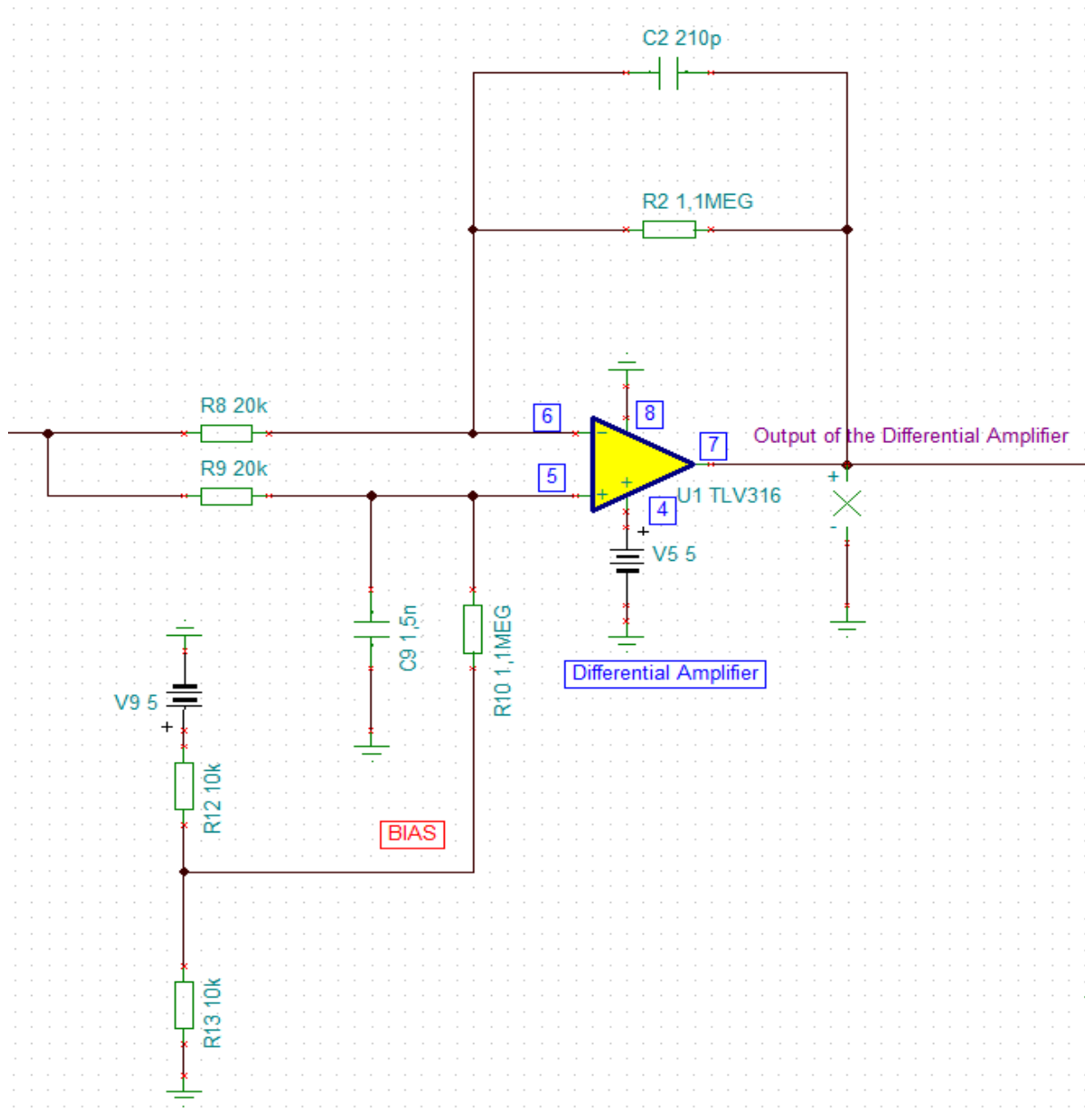


Figure 41: Electrical Schematic of Differential Amplifier

5.1.4 Comparator Stage

The last stage is comparator that generates 0 to 5 V square wave signal in order to count movement of brushed DC motor. An inverting hysteresis topology is used to decrease influence of noise on the input of comparator. The generated square wave by the comparator must be followed the current ripples of motor. According to calculation of number of ripples per revolution, it should be 8 square wave for each complete rotation. These square waves change their rising and falling edges with respect to threshold voltages of comparator. In the following equations that are also mentioned

before in chapter 4, it is used to calculate low threshold voltage and high threshold voltage.

$$V_{TL} = ((R_{18}||R_{16})x \frac{V_{CC}}{((R_{18}||R_{16}) + R_{15})}) + (R_{15}||R_{18})x \frac{V_{OL}}{((R_{15}||R_{18}) + R_{16})})$$

$$V_{TH} = ((R_{18}||R_{16})x \frac{V_{CC}}{((R_{18}||R_{16}) + R_{15})}) + (R_{15}||R_{18})x \frac{V_{OH}}{((R_{15}||R_{18}) + R_{16})})$$

$V_{CC}= 5\text{ V}$ $V_{OL}= 0\text{ V}$ $V_{OH}= 5\text{ V}$ R_{15} , R_{16} and R_{18} these are unknowns resistance values V_{TL} and V_{TH} , threshold voltages that are determined with respect to maximum and minimum points of differential amplifier output. For example, for this configuration V_{TL} is specified 2,53 V and V_{TH} is adjusted 2,57 V. According to these threshold voltages, there are many possibilities for resistances but following values are selected.

$R_{15}= 91\text{k}\Omega$ $R_{16}= 7\text{ M}\Omega$ $R_{18}= 95\text{ k}\Omega$

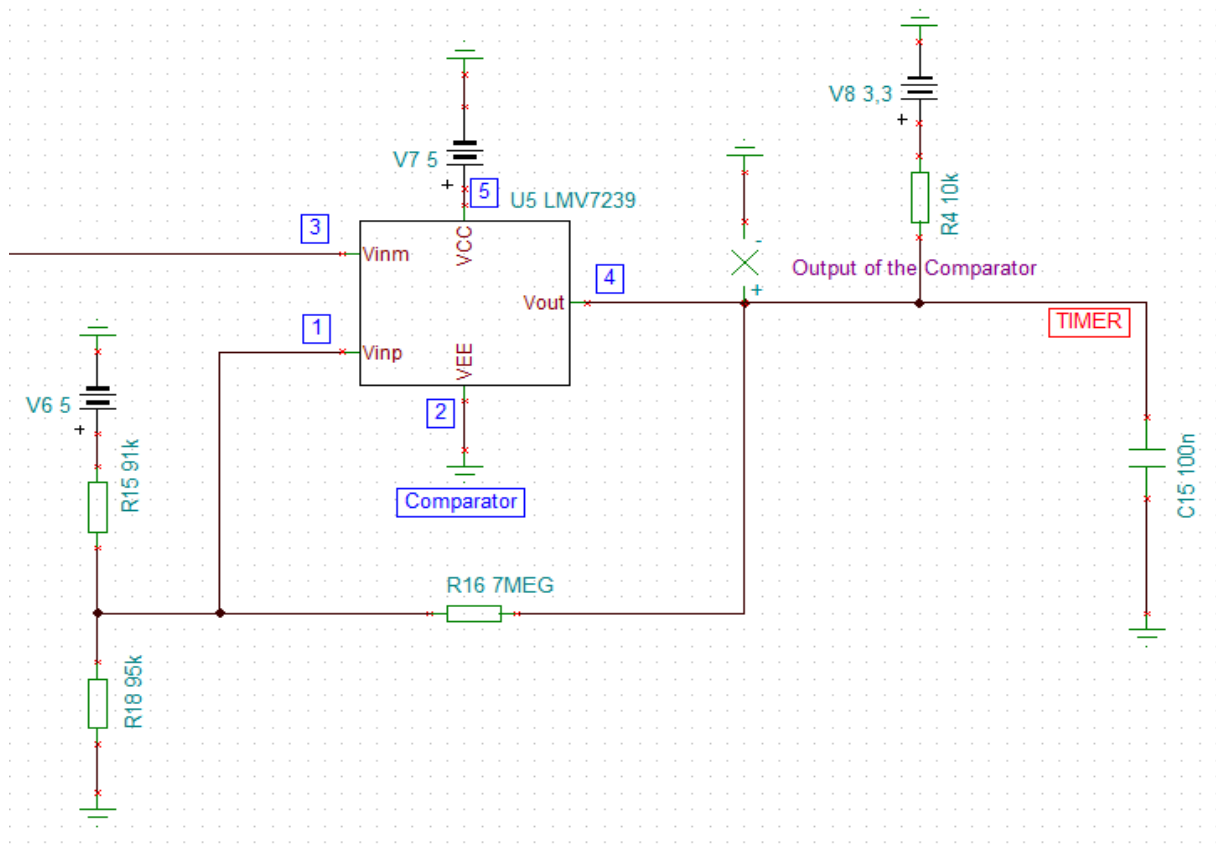


Figure 42: Electrical Schematic of Comparator

5.2 Updated Electrical Schematic

5.2.1 Updated Current Sense Amplifier Stage

After modifying system, the current sense amplifier stage is completely changed. Instead of INA240-Q1, TLV316 is applied with respect to cost reduction. New configuration of this stage is explained in chapter 4. In the following figure, the electrical schematic is demonstrated.

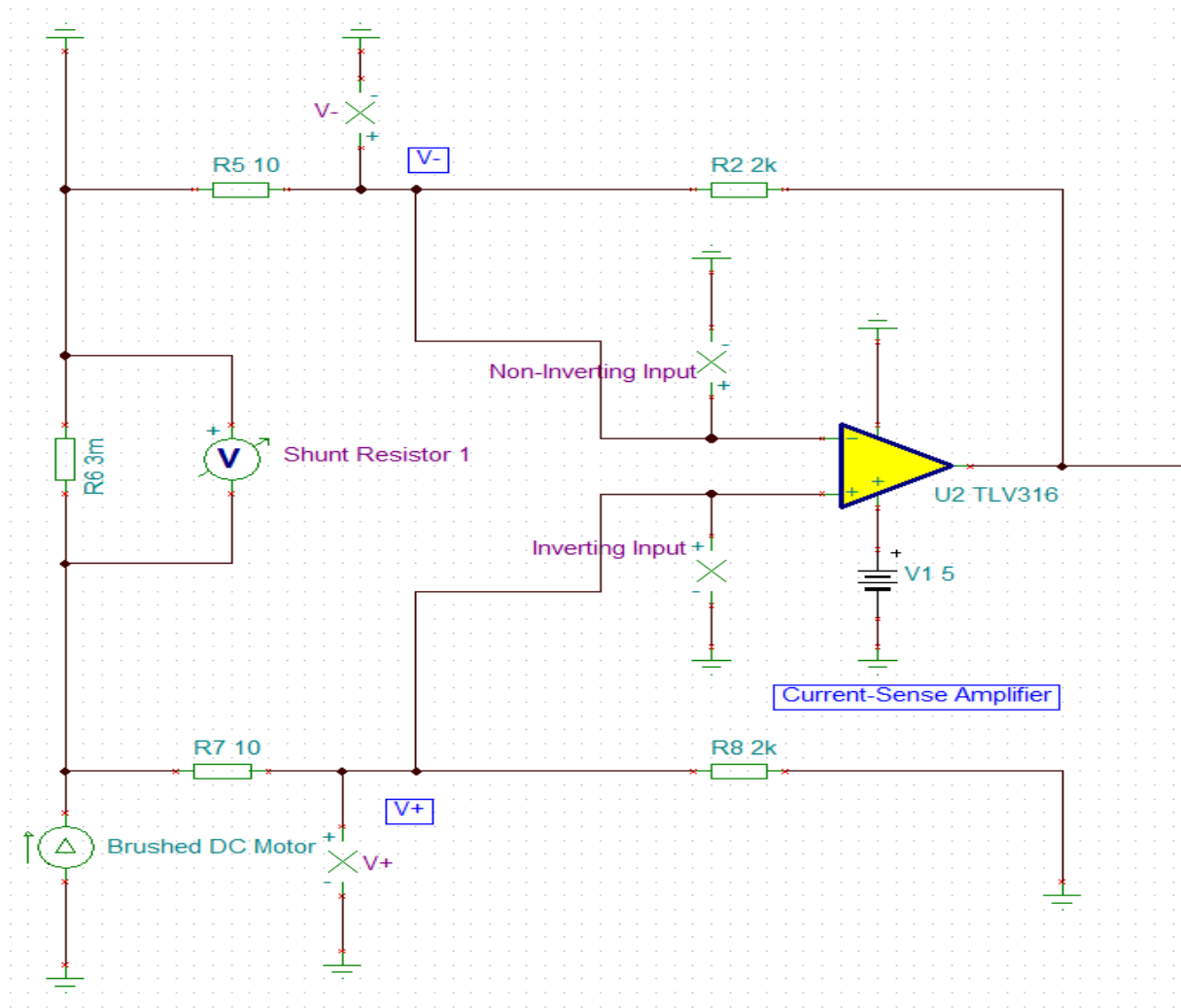


Figure 43: Updated Electrical Schematic of Current Sense Amplifier

Shunt resistor was not changed, it is remained as 3 mΩ. Before the updated stage, the gain of this stage was 20 V/V but then it is adjusted 200 V/V to get sufficient output that provide for next stage. It is calculated in the following equation.

$$Gain = \frac{R8}{R7} = \frac{2k}{10} = 200 \text{ V/V}$$

5.2.2 Updated Band Pass Filter Stage

For new configuration, the same structure of band pass filter is adopted. Only working frequencies are slightly changed hence capacitor and resistance values are adjusted to provide new frequency values. The updated electrical schematic of this stage is displayed below.

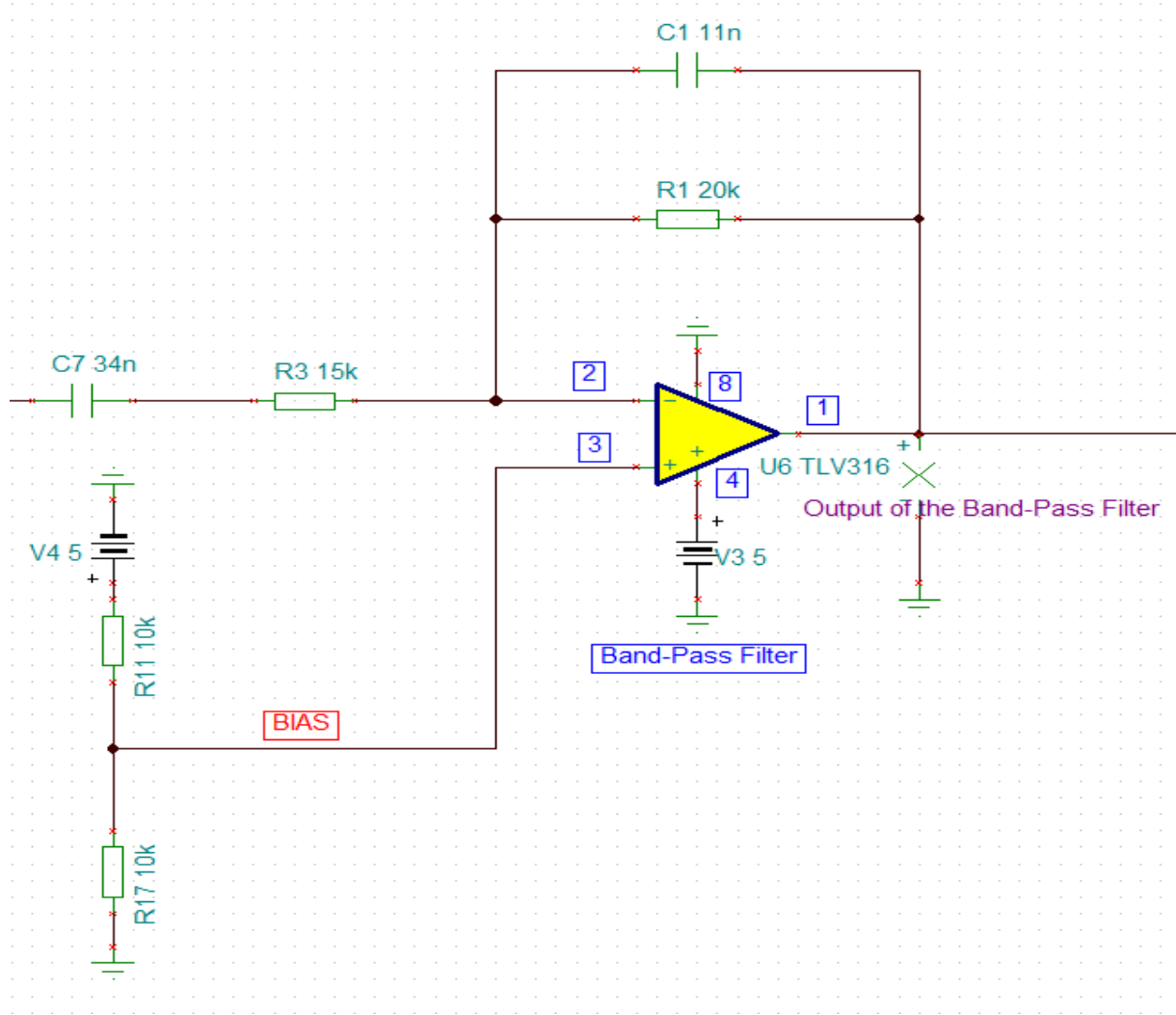


Figure 44: Updated Electrical Schematic of Band Pass Filter

According to updated band pass filter test result, the frequency of low pass portion is found 669 Hz and the frequency of high pass portion is seen 318 Hz. In order to provide these frequency values, following equations are applied.

$$f1 = \frac{1}{(2 * \pi * 20000 * 11 * 10^{-9})} = 723 \text{ Hz}$$

$$f_2 = \frac{1}{(2 * \pi * 15000 * 34 * 10^{-9})} = 312 \text{ Hz}$$

The bandwidth is between 723-312 Hz. The system operates in this interval.

5.2.3 Updated Comparator Stage

For the updated version of comparator stage, the circuit structure remains same as previous one. Only threshold voltages are modified to count every current ripples. It is calculated with same equations that are mentioned for previous comparator stage.

$$V_{TL} = ((R_{18}||R_{16})x \frac{V_{CC}}{((R_{18}||R_{16}) + R_{15})}) + (R_{15}||R_{18})x \frac{V_{OL}}{((R_{15}||R_{18}) + R_{16})})$$

$$V_{TH} = ((R_{18}||R_{16})x \frac{V_{CC}}{((R_{18}||R_{16}) + R_{15})}) + (R_{15}||R_{18})x \frac{V_{OH}}{((R_{15}||R_{18}) + R_{16})})$$

$$V_{CC} = 5 \text{ V} \quad V_{OL} = 0 \text{ V} \quad V_{OH} = 5 \text{ V}$$

Three unknown resistance values are computed to follow every motor movement.

$$R_{15} = 105 \text{ k}\Omega \quad R_{16} = 2,2 \text{ M}\Omega \quad R_{18} = 106 \text{ k}\Omega$$

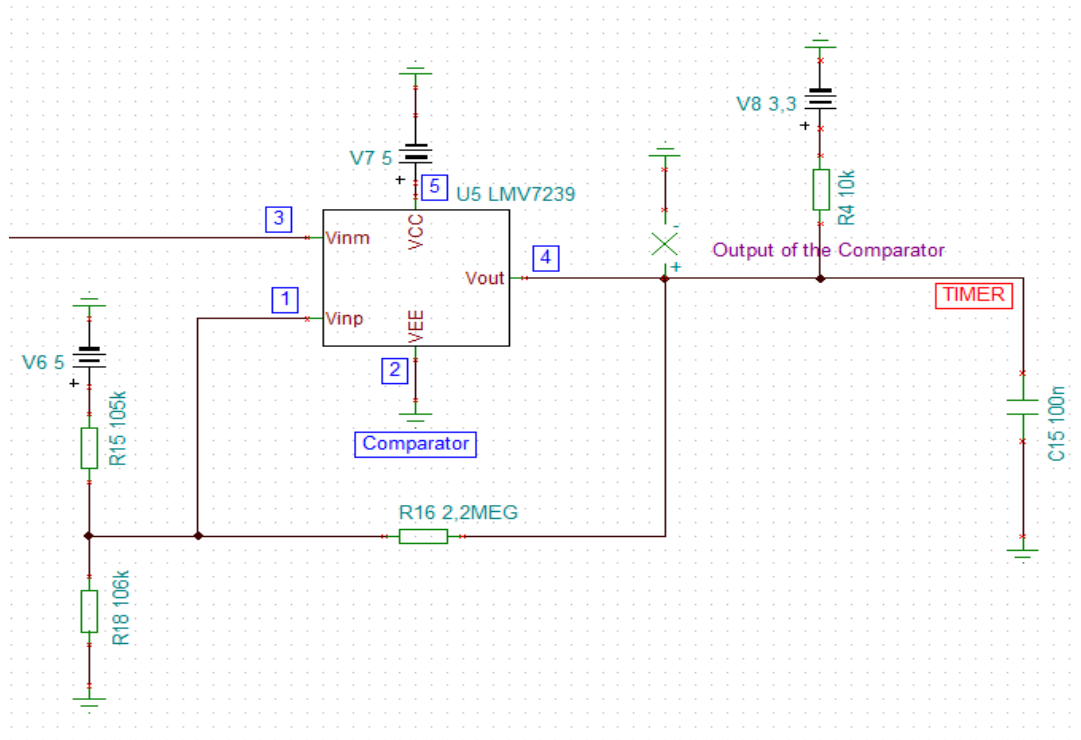


Figure 45: Updated Electrical Schematic of Comparator Stage

5.3 Test & Simulation Result

In this part, analysis of complete system are performed to provide sensorless approach in proper way. For automotive applications, 9 V, 12 V, 16 V three different voltage values were applied as a power supply. Moreover, the vehicle seats have various movement capability which are backward, forward, upward, downward, tilt angle up and down. These 6 distinct movements are ensured 3 different brushed DC motors assembled to the test bench. For this project, backward and forward motions, upward and downward motions are examined. The test procedure of this project, firstly sensed electric adjustment was tested in the laboratory with test bench then obtained test results were uploaded software tool(TINA) and sensorless approach was simulated. In the following sections, each tests are analyzed deeply.

5.3.1 9 V Backward

In this test, the brushed DC motor that is driven by 9 V power supply, is connected with sensed electronic board and it is tested. Obtained test results are uploaded to software tool. The maximum current of motor reaches 9 A. In the following graph, it is seen that transient analysis of sensorless approach of electrical adjustment.

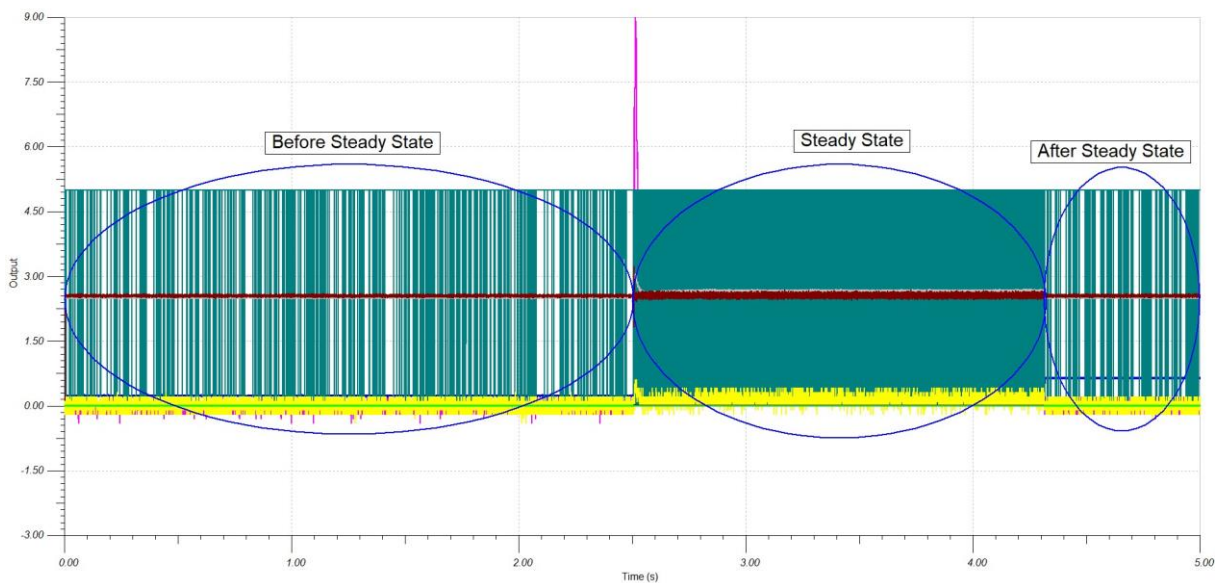


Figure 46: Transient Analysis of 9 V Backward

It is easily recognized that there are 3 different regions which are represented in the graph with respect to motor condition. First region is called “before steady state”(before start the motor) that means interval from time 0 to time of starting of motor. Second region which illustrates steady state, includes that from time of starting motor to time of stopping motor. Third region, after steady state that describes time interval from time of stopping the motor to final time of test.

In the following graph, every input and output values are clearly seen.

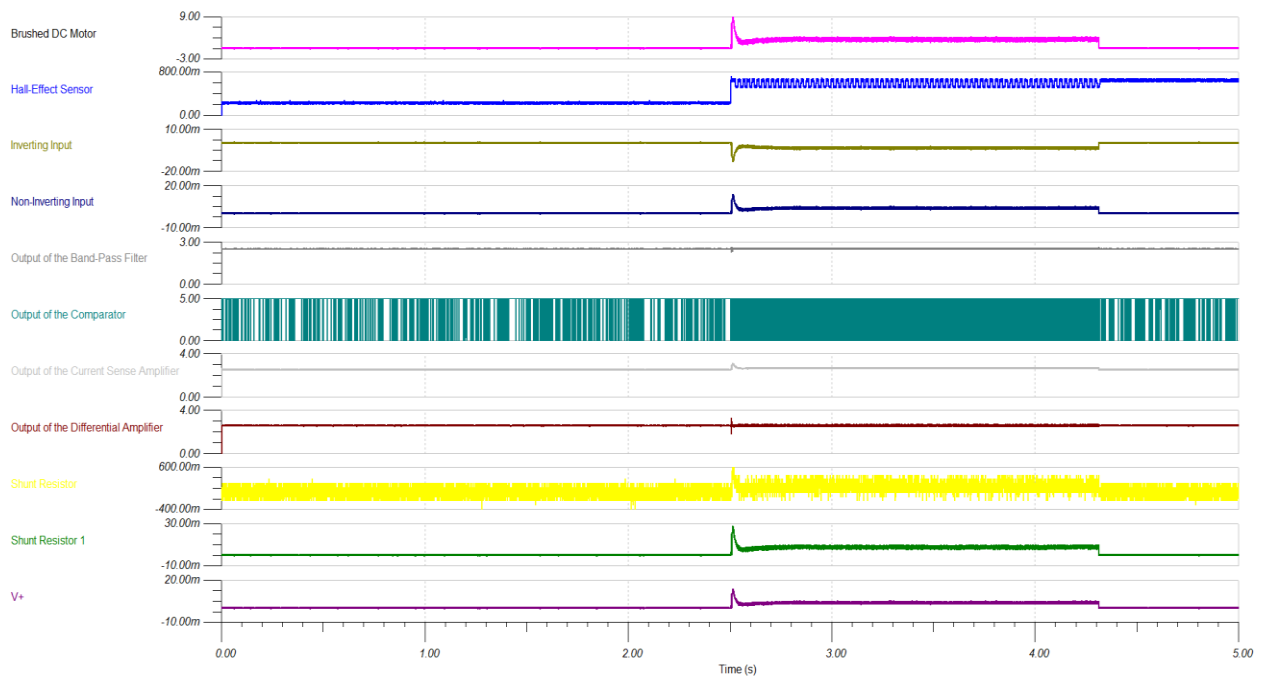


Figure 47: 9 V Backward Each Stage Analysis

In this graph, the output of comparator that is represented teal colour, follows movement of brushed DC motor. The logic of comparator ripples, while the motor is running, the comparator ripples pursue motion of motor whereas when motor stops or does not run, there should not be any ripple. Therefore, comparator ripples should be only in steady state region, in before and after steady state there should not be any ripple because there is not any motion in these regions. However, there are some unwanted comparator ripples in these regions as in order to provide a good solution for 3 voltage values. The solution should be as follows.

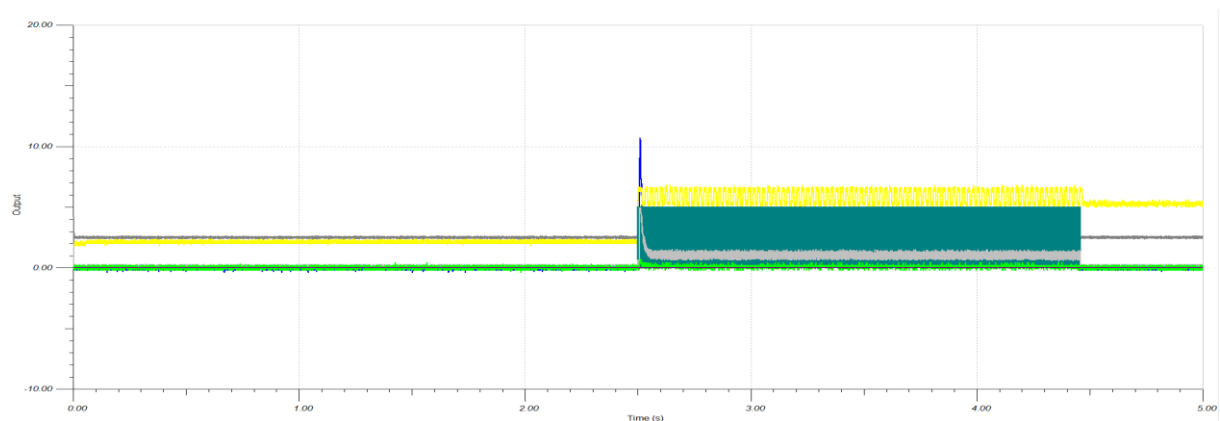


Figure 48: Test Sample for 9 V

As it is mentioned previous page, this solution can not be provided for every voltage values hence this graph is showed as a sample. The critical region is steady state because the comparator must follow all the movement of motor. There should not be any missing and additional comparator ripples inside this region to determine exact position of motor. As already calculated in the chapter 3.2.1, 8 comparator ripples correspond a complete rotation of motor. Nonetheless, thanks to number of comparator ripples position of motor is easily computed. In the following figure, to see better it is zoomed in steady state region.

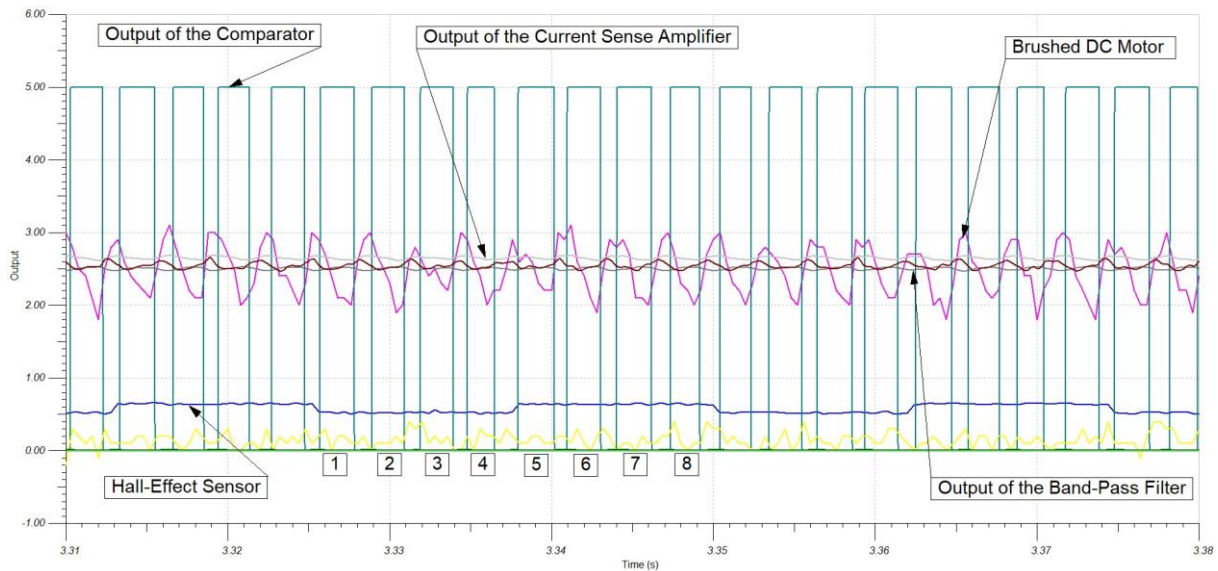


Figure 49: 9 V Backward Steady State Region Details

The blue line represents hall-effect sensor movement and a period of this corresponds a complete turn of motor hence there are 8 comparator ripples (represented in teal colour) in this period. The motor movement is represented by fuchsia line and it is seen that every movement of motor is followed by comparator ripples. However, these comparator ripples are adjusted with respect to output of differential amplifier (represented in maroon colour) by threshold voltages of comparator.

5.3.2 9 V Forward

In the second test, brushed DC motor is also driven by 9 V supply but motion is different. When the motion is different, also current of motor is various. For this test maximum current of motor approaches 9,2 A. It is a little bit higher than backward motion because it is moving against to mass and spring. The same test procedure is applied for this motion. In the following graph, 3 different regions are represented.

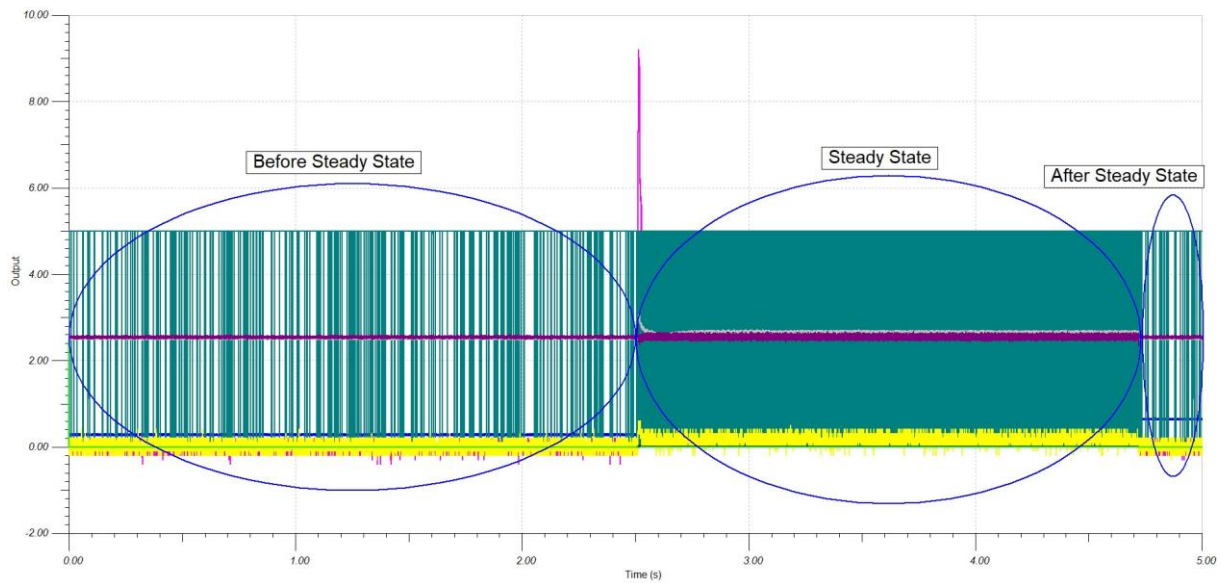


Figure 50: Trasient Analysis of 9 V Forward

Generally test time is fixed but this steady state region seems a bit longer than 9 V backward, because start and stop operation of motor is performed by manually. In before and after steady state regions, there are still some unwanted comparator ripples but it seems less ripples than previous test. In order to check every variable, it is needed to separete all the inputs of outputs. In the following page, each phases inputs and outputs are analyzed.

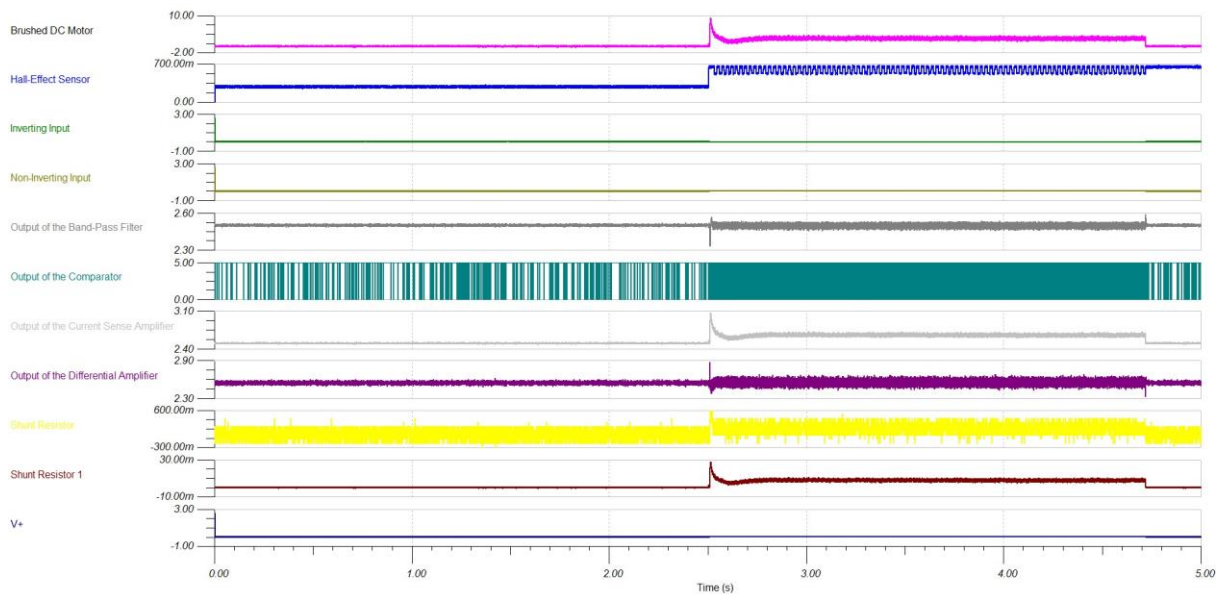


Figure 51: 9 V Forward Each Stage Analysis

Particularly, brushed DC motor, hall-effect Sensor, shunt resistor 1 are working in steady state region and also current sense amplifier, band pass filter, differential

amplifier, comparator are active in this region. The reason of unwanted comparator ripples in before and after steady state, there are some noise and disturbances in this region and comparator threshold voltages are too close each other due to follow and count all the movement of motor, hence the comparator counts these noise and disturbances as a motor movement. In steady state region, it is needed to zoom in to check counts of motor motion by comparator ripples.

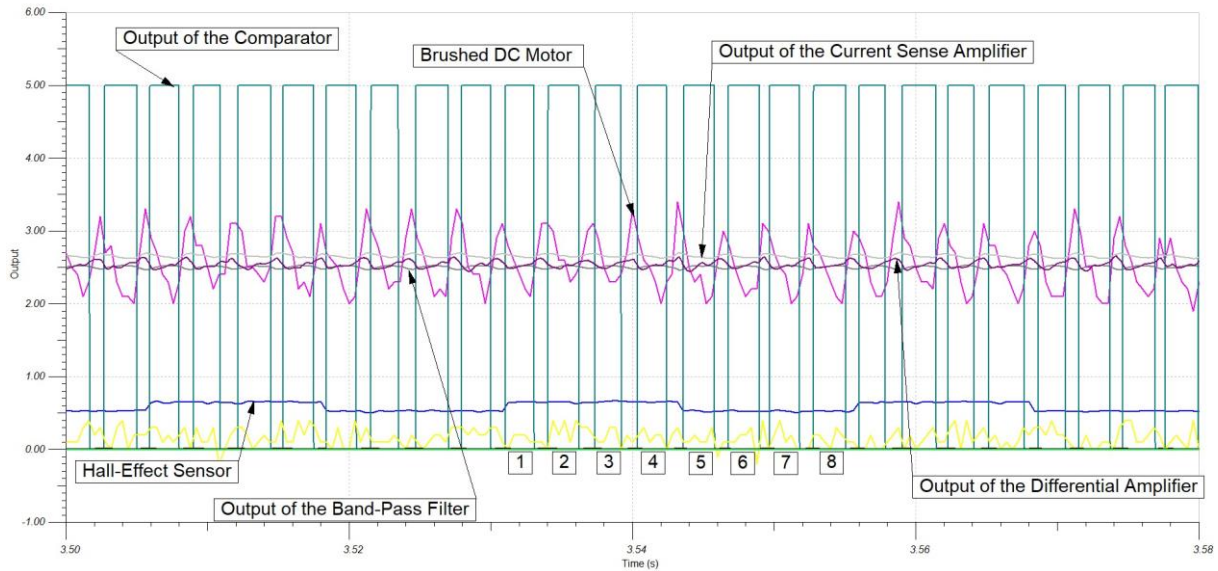


Figure 52: 9 V Forward Steady State Region Details

As seen, there are 8 comparator ripples that correspond a complete rotation of motor.

5.3.3 12 V Backward

The second voltage value, the brushed DC motor is supplied by 12 V. For this test, the maximum current increases up to 14,3 A. When voltage is increased, vehicle seat completes its motion early because motor turns rapidly. However, test duration is manually adjusted in the laboratory and simulation of test is fixed to 5 seconds. The 3 various regions are demonstrated in the following page.

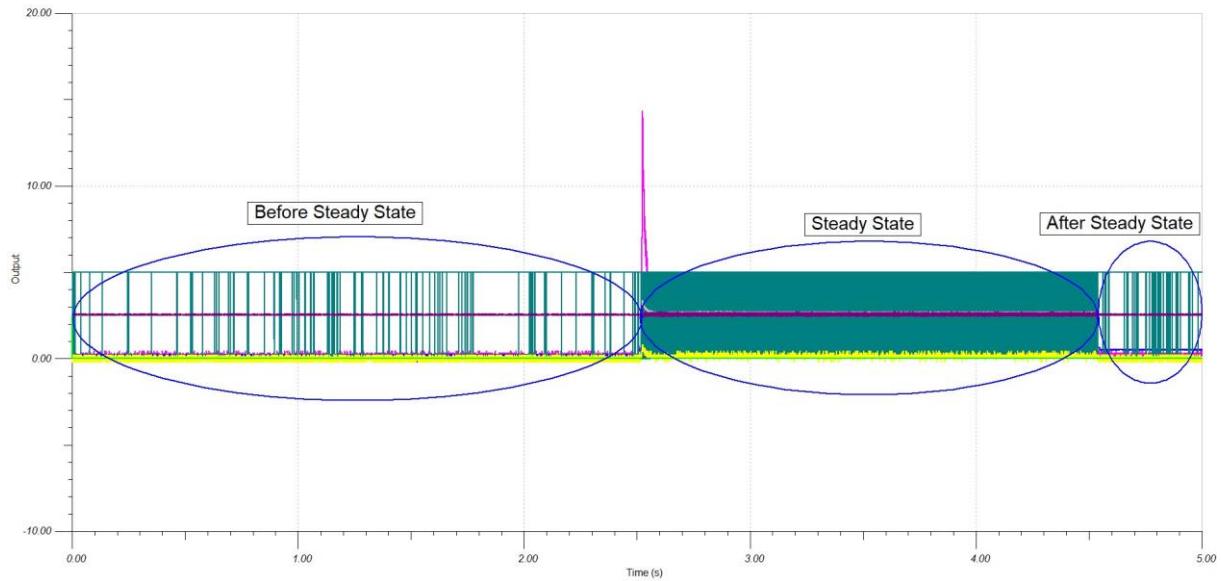


Figure 53: Transient Analysis of 12 V Backward

In before and after steady state regions, there are less unwanted comparator ripples in contrast to 9 V tests because 9 V is the lowest value for this application and to provide every voltage values for it can be encountered more ripples for 9 V. The desired solution should be similar as that was represented in figure 48. Nevertheless, as it was told before, due to ensure good solution for steady state region that means the comparator ripples should follow all the motor movement, there are some unwanted ripples can be occurred in the before and after steady state.

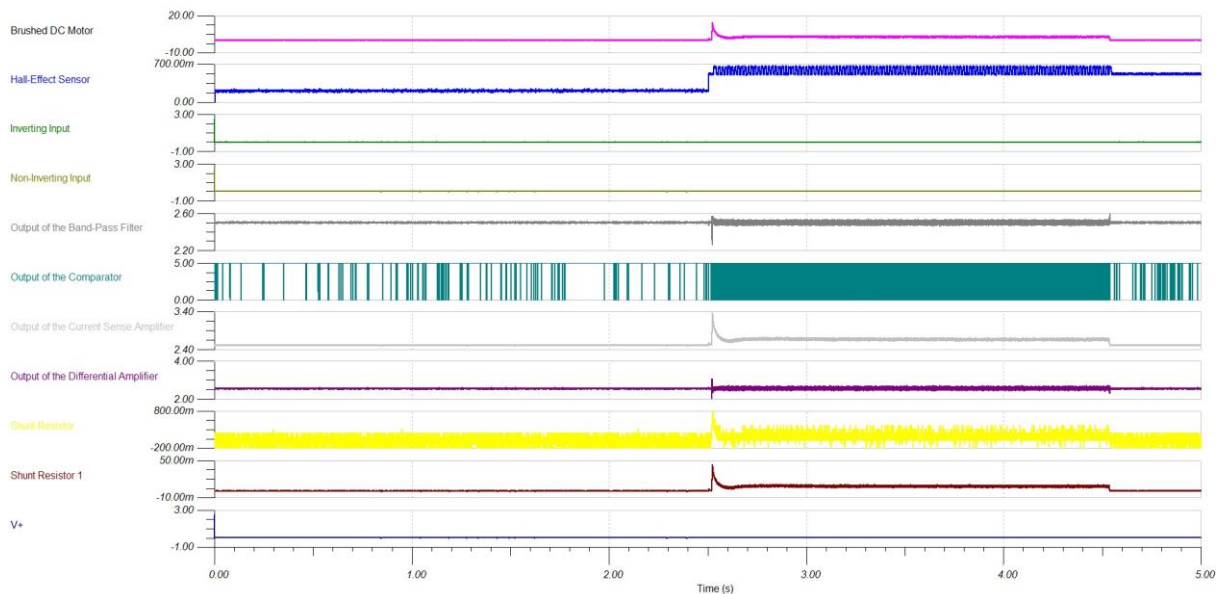


Figure 54: 12 V Backward Each Stage Analysis

The output of current sense amplifier and brushed DC motor current are higher than 9 V tests. The output of band pass filter and the output of differential amplifier do not change more in contrast to 9 V tests. The comparator behaviour is different than previous tests because supply voltage is greater. It is gotten closer into steady state region to check comparator ripples work properly.

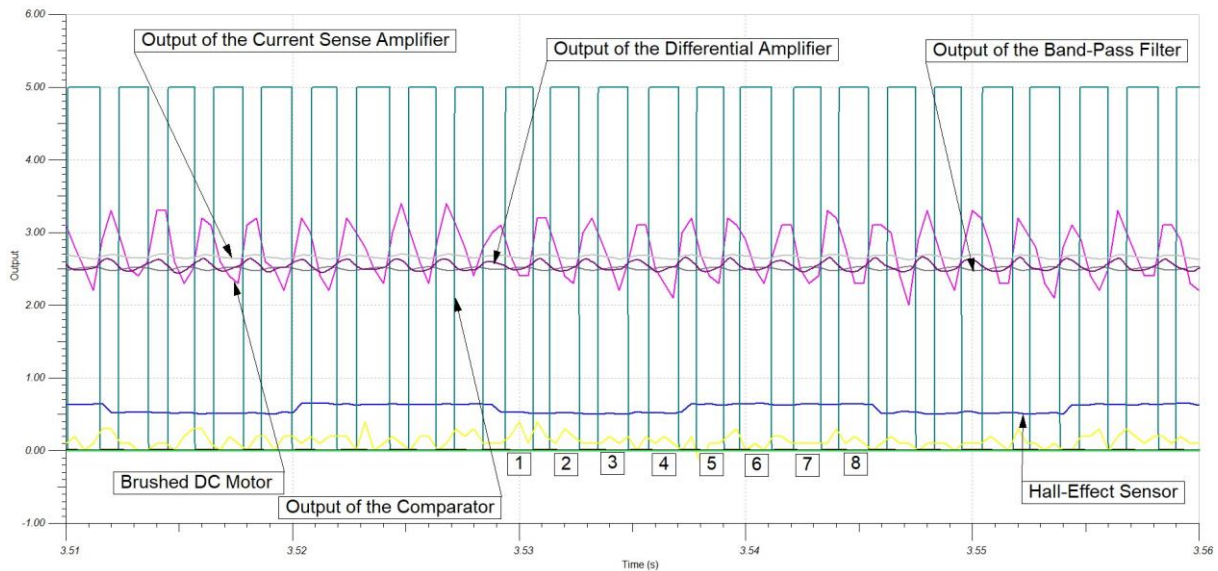


Figure 55: 12 V Backward Steady State Region Details

There are 8 comparator ripples for each complete turn and there is not any additional and missing ripples so comparator follows all the movement of motor.

5.3.4 12 V Forward

Second motion is forward that the brushed DC motor is supplied by 12 V power supply. The maximum current reaches 14,4 A for this test. The vehicle seat finishes its motion more or less as same time as 12 V backward motion. The simulation time of test is set 5 seconds. The general view for test is illustrated in the following figure.

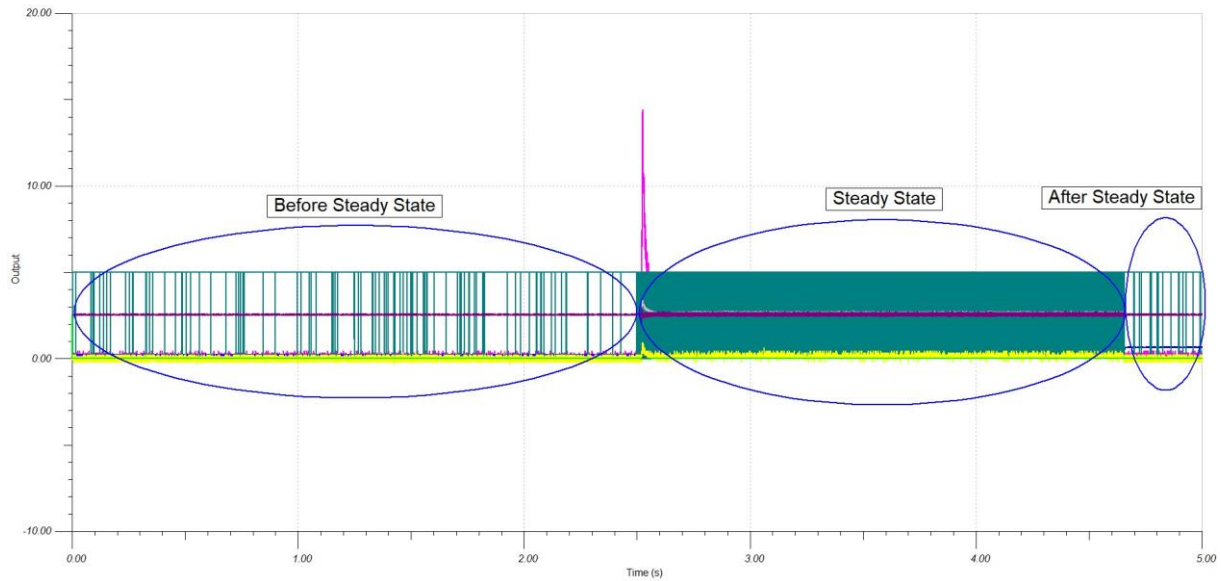


Figure 56: Transient Analysis of 12 V Forward

In contrast to 12 V backward test in before and after steady state regions, it seems less unwanted comparator ripples in test of 12 V forward but it does not make a difference. The steady state region is more important to follow every motor movement. Also, all the variables, inputs and outputs are shown in the following figure.

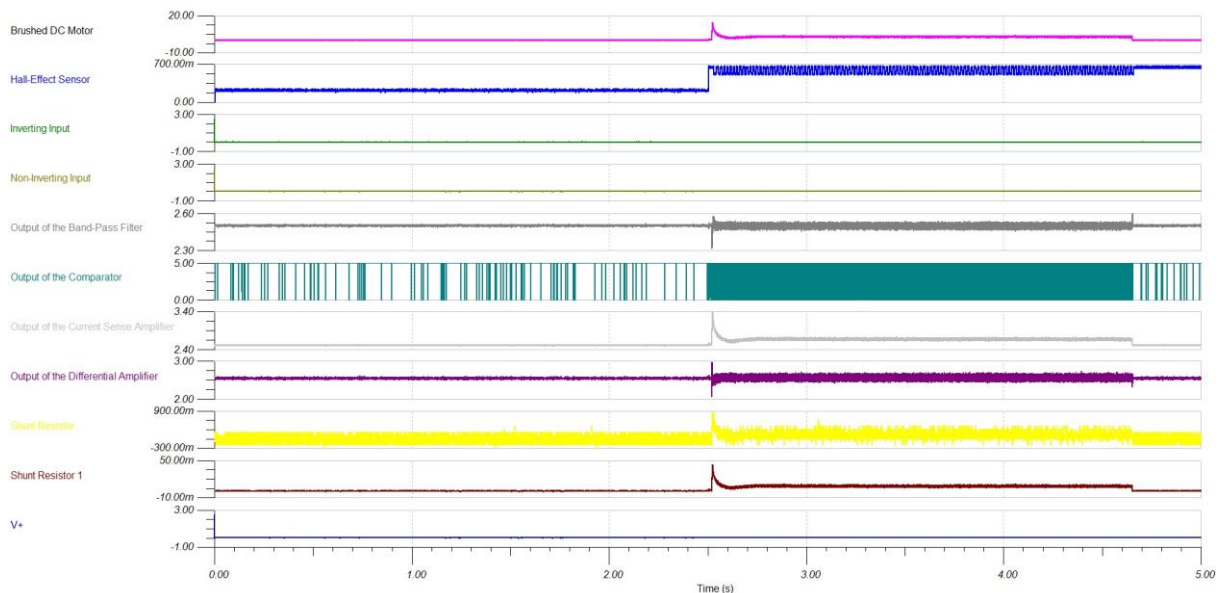


Figure 57: 12 V Forward Each Stage Analysis

The first 3 stages output, output of current sense amplifier, output of band pass amplifier, output of differential amplifier are nearly same as test of 12 V backward because supply voltage is equivalent. Only comparator ripples are a bit different because of motor movement.

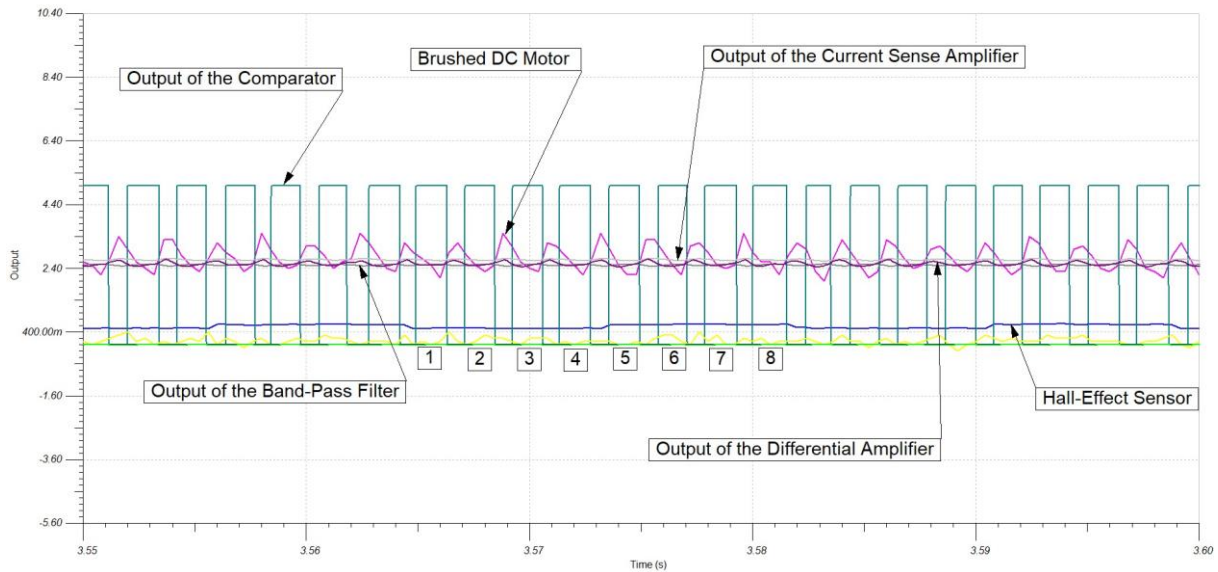


Figure 58: 12 V Forward Steady State Region Details

As clearly seen from the graph, comparator ripples follow every motor movement and there is not any additional and missing comparator ripples in steady state region. In a period of hall-effect sensor, there are 8 comparator ripples that correspond a complete turn of motor.

5.3.5 16 V Backward

Third voltage value, the brushed DC motor is supplied by 16 V. The maximum current value is 19,4 A for this test. The vehicle seat completes its movement faster than other voltage levels thanks to the highest voltage for this application. The all test and simulation procedures are same as previous tests.

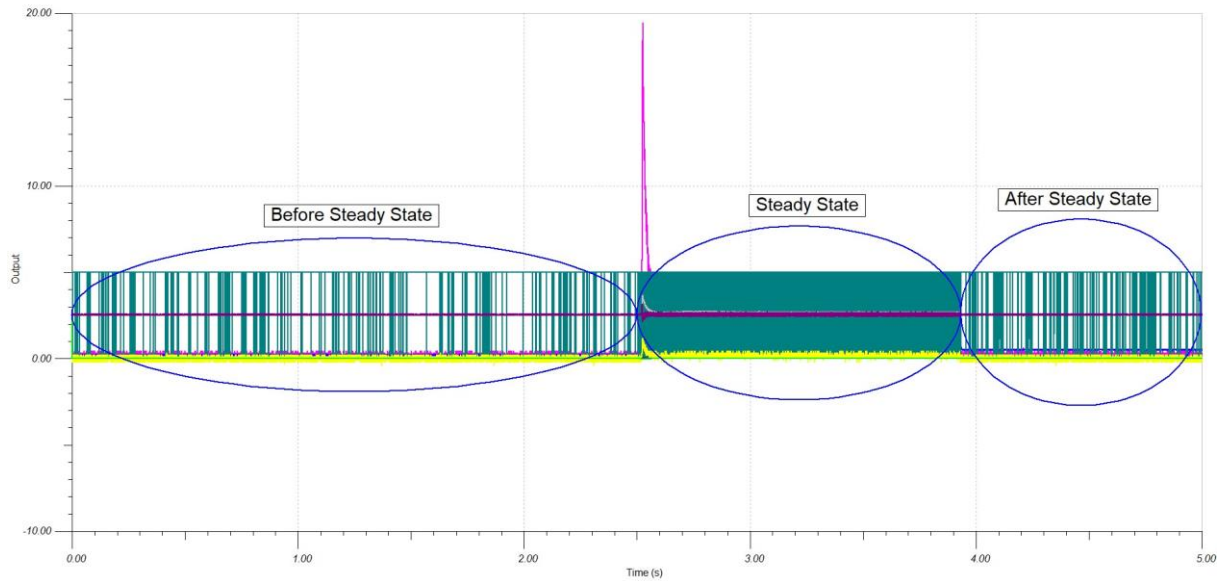


Figure 59: Transient Analysis of 16 V Backward

As it is seen in the graph of transient analysis, there are 3 different phases that are valid for previous tests. In before and after steady state phase, unwanted comparator ripples are still exist and they seem more than 12 V tests. When analysing these 3 voltage levels, 9 V and 12 V tests behave similar each other but 16 V test behaviour is a little bit different than other two levels. That means more or less with same threshold voltages provides similar result between 9 V and 12 V but to obtain similar result for 16 V when threshold voltages are changed more.

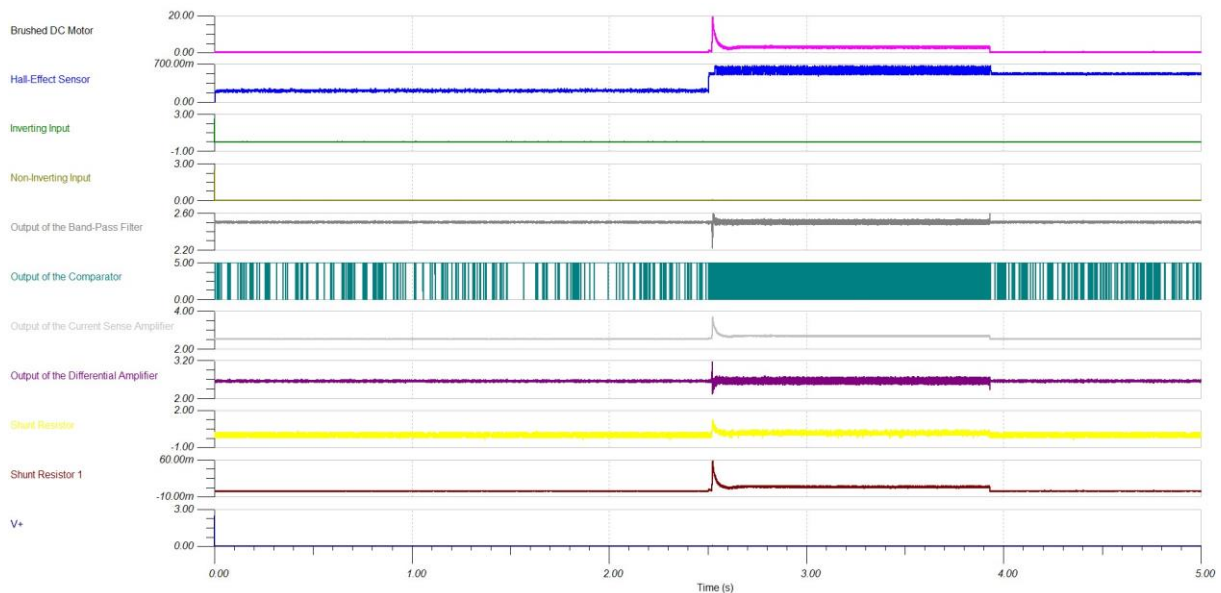


Figure 60: 16 V Backward Each Stage Analysis

There are some differences occur when it is compared to 12 V, the output of current sense amplifier and brushed DC motor current increased a bit and the output of band pass filter and the output of differential amplifier are nearly same. Besides, the comparator ripples behave differently due to supplying higher voltage.

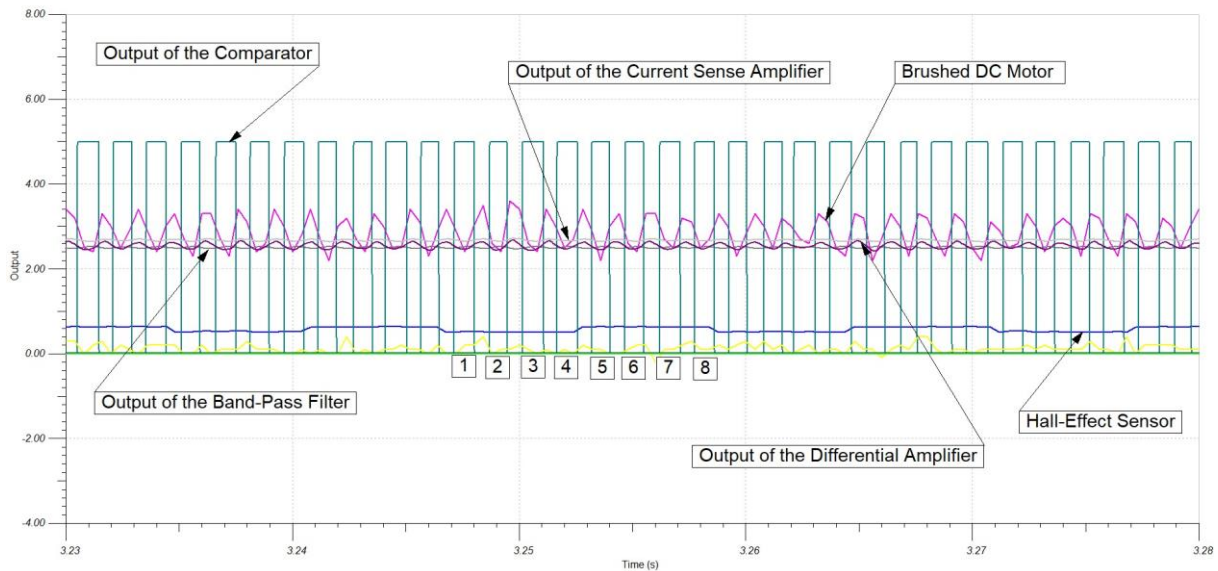


Figure 61: 16 V Backward Steady State Region Details

For this test, it was not easy to success to follow all the motor movements at the beginning but then it regulated for 16 V. In the graph every variables are seen explicitly and the comparator ripples pursue all the motor movement without additional ripples.

5.3.6 16 V Forward

Second motion by supplied 16 V is forward. The maximum current of this motion approaches 16,6 A. The motion of forward is completed its movement nearly same duration as backward motion. In the following figure is represented general view of transient analysis of 16 V forward.

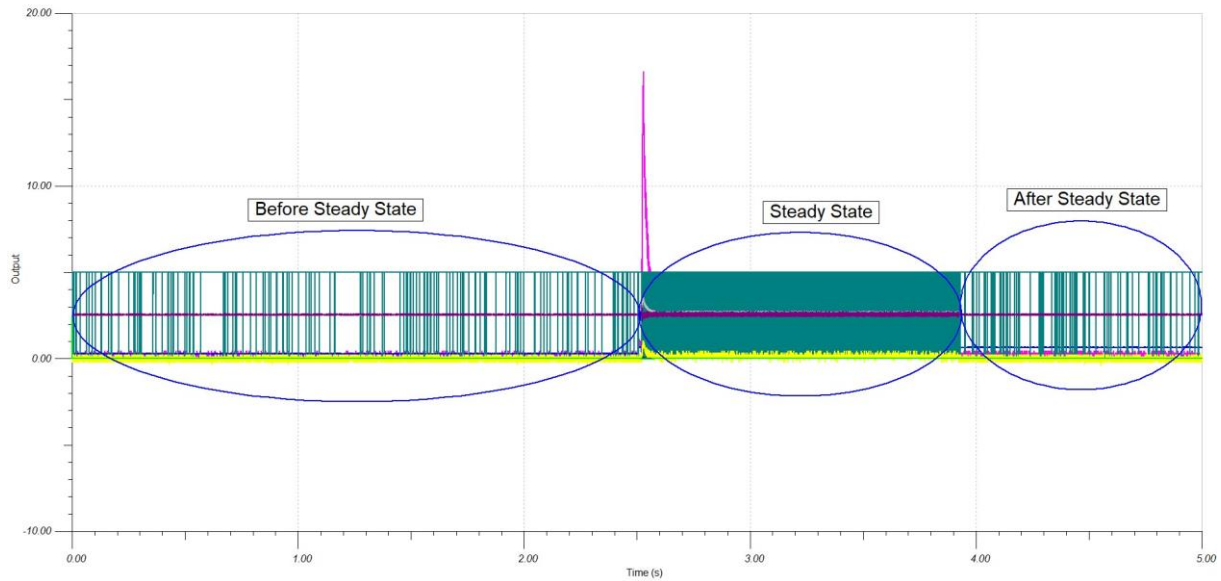


Figure 62: Transient Analysis of 16 V Forward

The 3 different phases are easily seen in the graph. When results are compared to previous motion, in before and after steady state regions, there are less comparator ripples and in steady state there is not any missing and additional ripples. In order to examine each variables, the system separated into different graphs in the following figure.

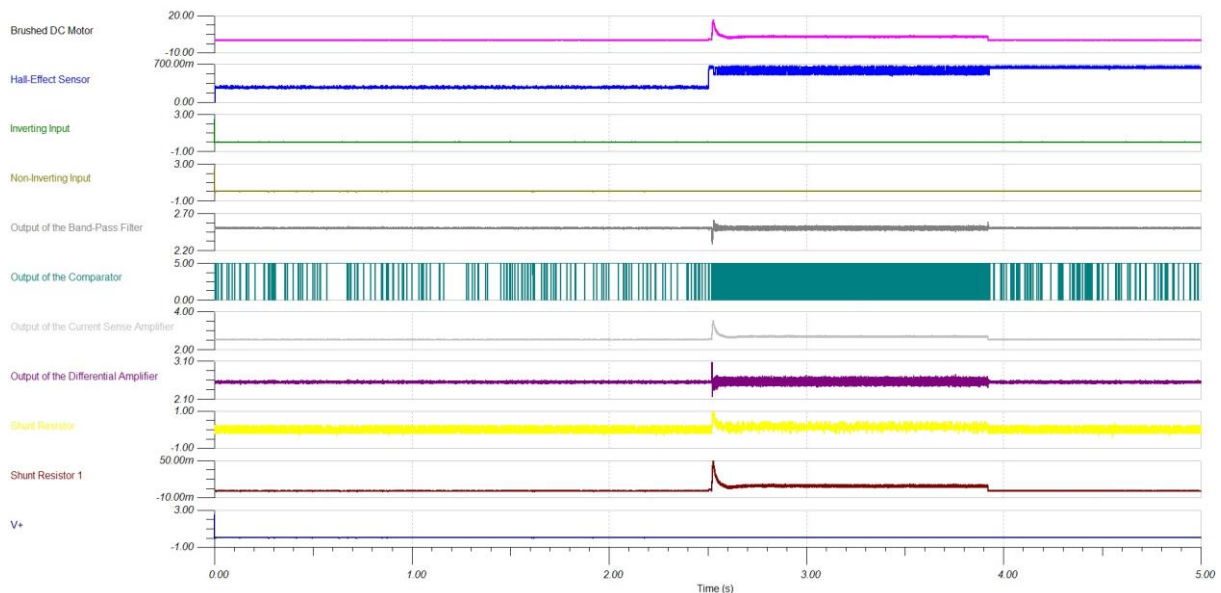


Figure 63: 16 V Forward Each Stage Analysis

The brushed DC motor is higher than previous test the other outputs except comparator output are nearly same as backward motion. The comparator ripples are a bit different because of motion.

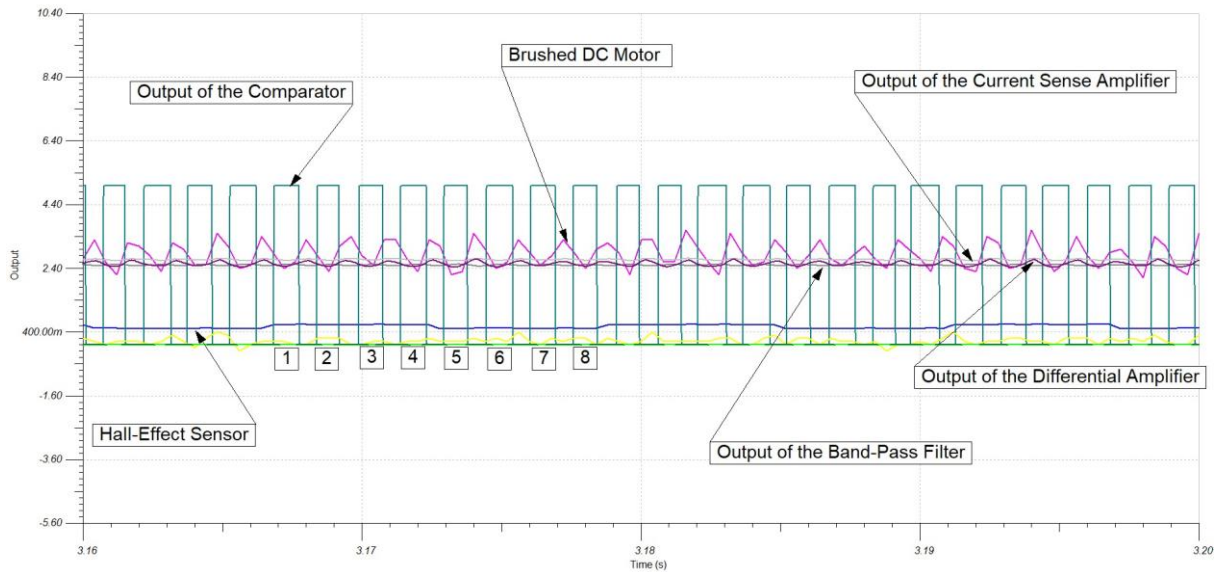


Figure 64: 16 V Forward Steady State Region Details

Each stage variable is demonstrated above. When analysing steady state phase, comparator ripples pursue all the motor motions without any losses. There is a period of hall-effect sensor that corresponds a complete turn of motor, also equal to 8 comparator ripples.

5.4 Downward-Upward Motion

There are 3 different motors to adjust various movements in the test bench. For downward and upward motion, another brushed DC motor was used in contrast to backward and forward motion. For this reason, some modifications are needed for band-pass filter stage, differential amplifier stage to regulate for this motion. In the following figure it is shown the electrical schematic of band pass filter.

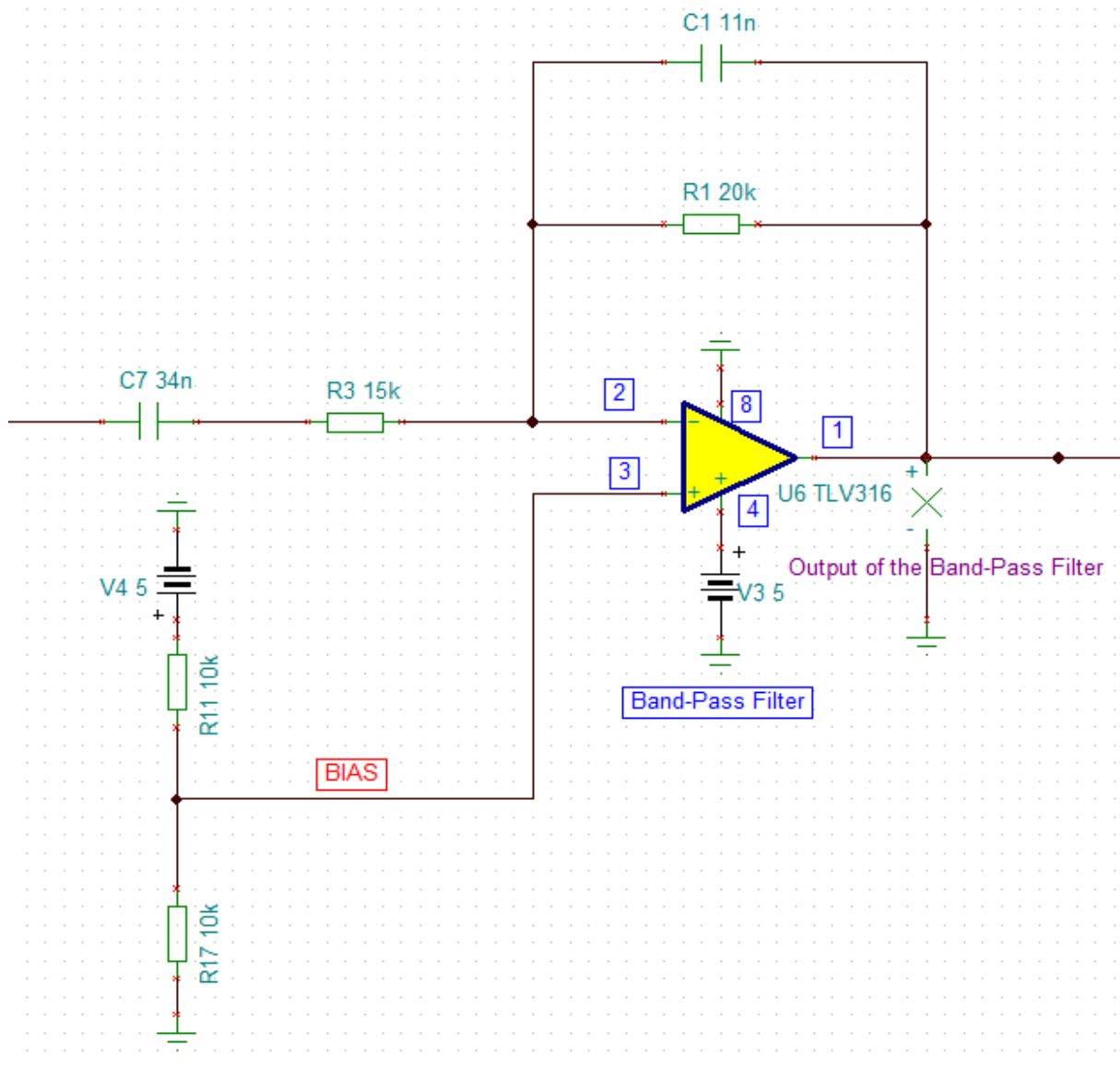


Figure 65: Band Pass Filter Electrical Schematic for Upward-Downward Motion

When it is done comparison between motion of forward-backward to upward-downward only capacitor C1 was changed because operating frequency was altered a bit. In the following page, the electrical schematic of differential amplifier stage is demonstrated.

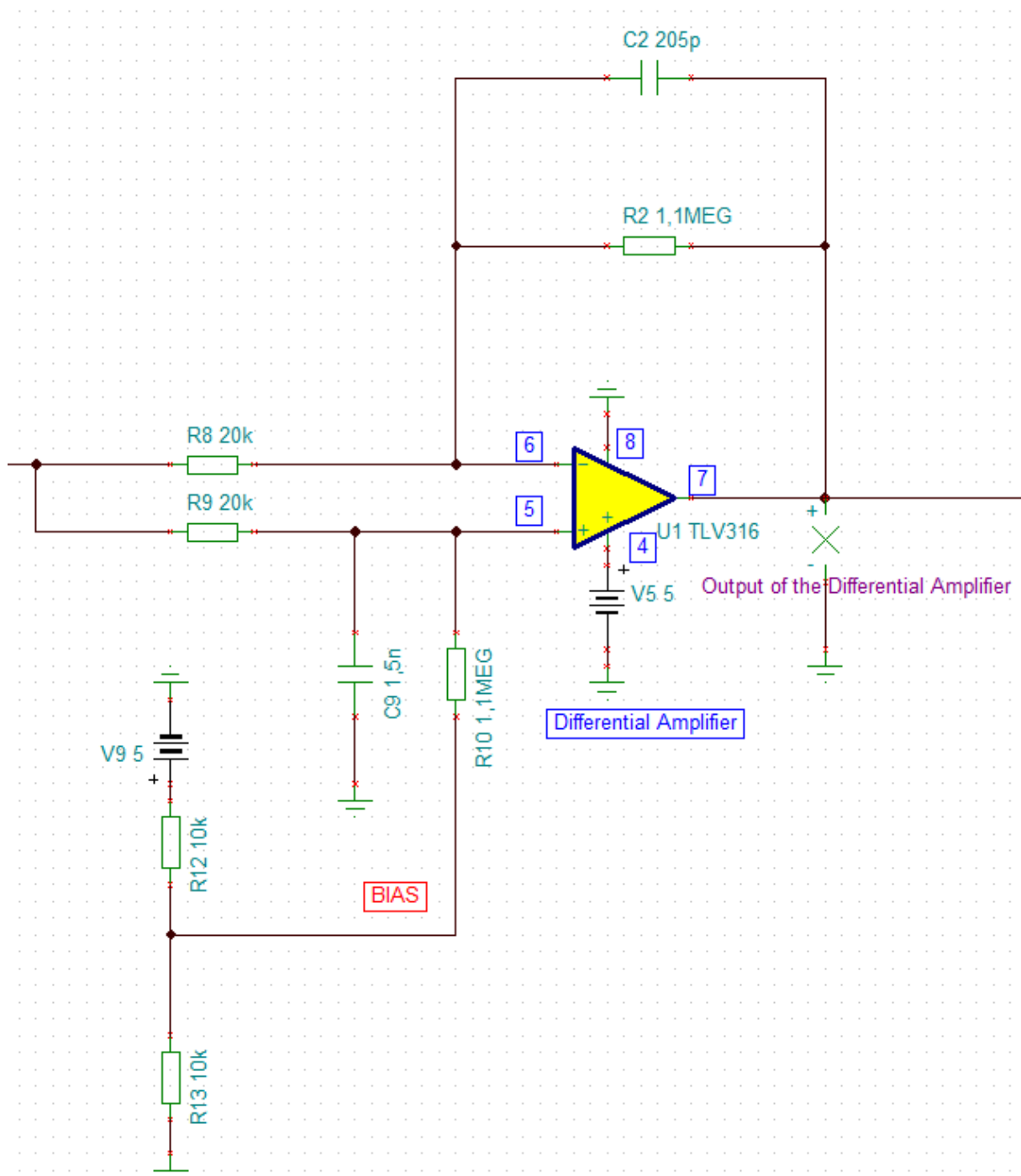


Figure 66: Differential Amplifier Electrical Schematic for Upward-Downward Motion

For this stage, capacitor C2 was altered compared to previous motion to adjust operating range.

5.4.1 9 V Downward

For this test, this motion is provided by another brushed DC motor in comparison with forward-backward motion. The test is applied same as previous motion first it is tested with sensed electronic board then acquired test results are uploaded on the simulation program. The motor is supplied by 9 V and the maximum current reaches to 11,2 A. The transient analysis of sensorless approach that is performed on the simulation tool(TINA), is represented below.

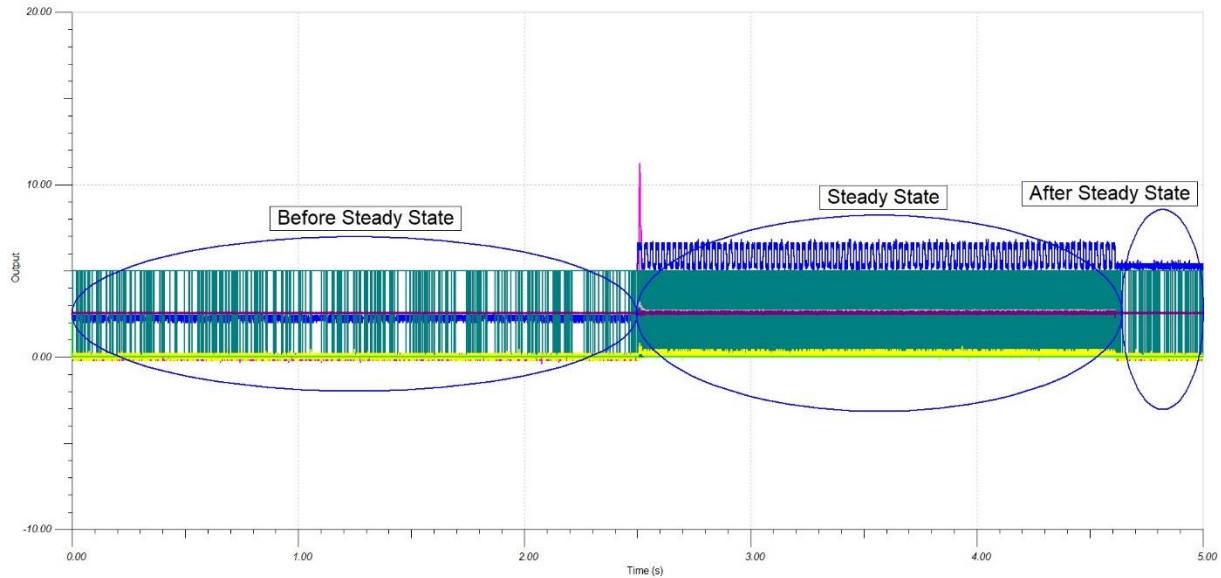


Figure 67: Transient Analysis of 9 V Downward

As clearly seen, there are 3 various stages that are separated according to motor condition. In first stage, before steady state there are many unwanted comparator ripples thanks to some noises and disturbances. In second stage, steady state there is not missing ripples so sensorless method follows all the movements of motor in this stage and there are few number of additional comparator ripples by virtue of unexpected current rise and fall. In third stage, in after steady state many unwanted ripples are seen after stop the motor by means of noises of disturbances. To examine each stage, inputs and outputs are separated in the following page.

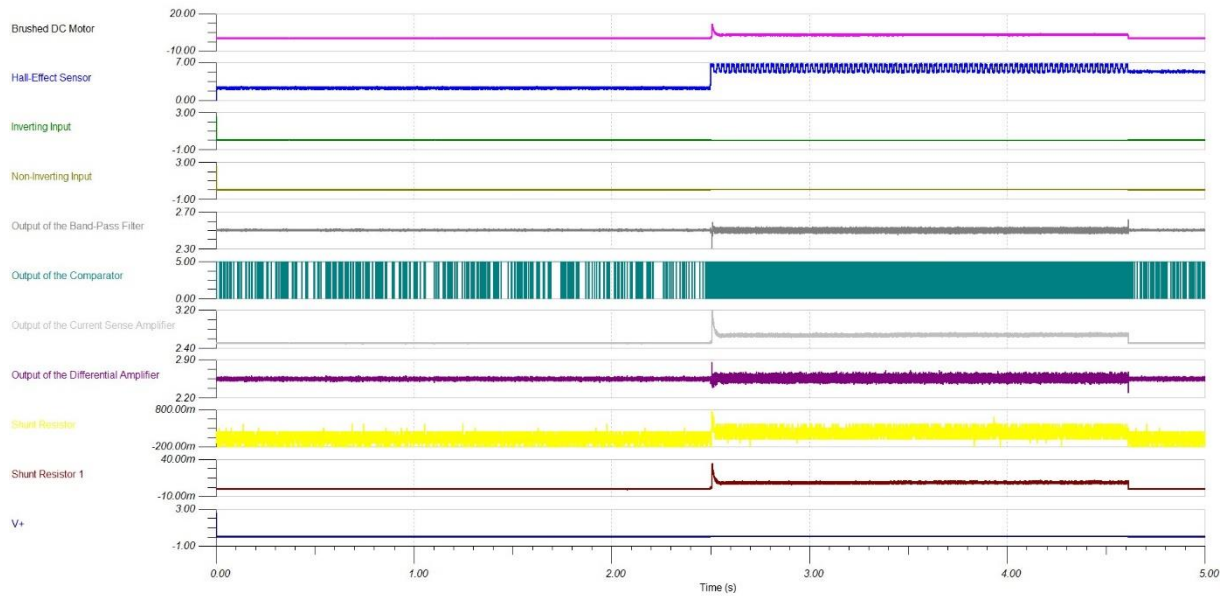


Figure 68: 9 V Downward Each Stage Analysis

In this figure, every variable is seen roughly. Generally, it is easily analysed change of each variable stage by stage. In before steady state, the current of brushed DC motor is 0, so hall-effect sensor does not work at this period. Output of first three stages that are current sense amplifier, band pass filter, differential amplifier, are lower in this region. There are some unwanted comparator ripples in this stage because of noises of disturbances. In steady state region, the first three stages increase their outputs as circuit is driven by motor and comparator increases its ripples to count every movement. Last region, after steady state the outputs of first three stages decrease and number of comparator ripples decrease.

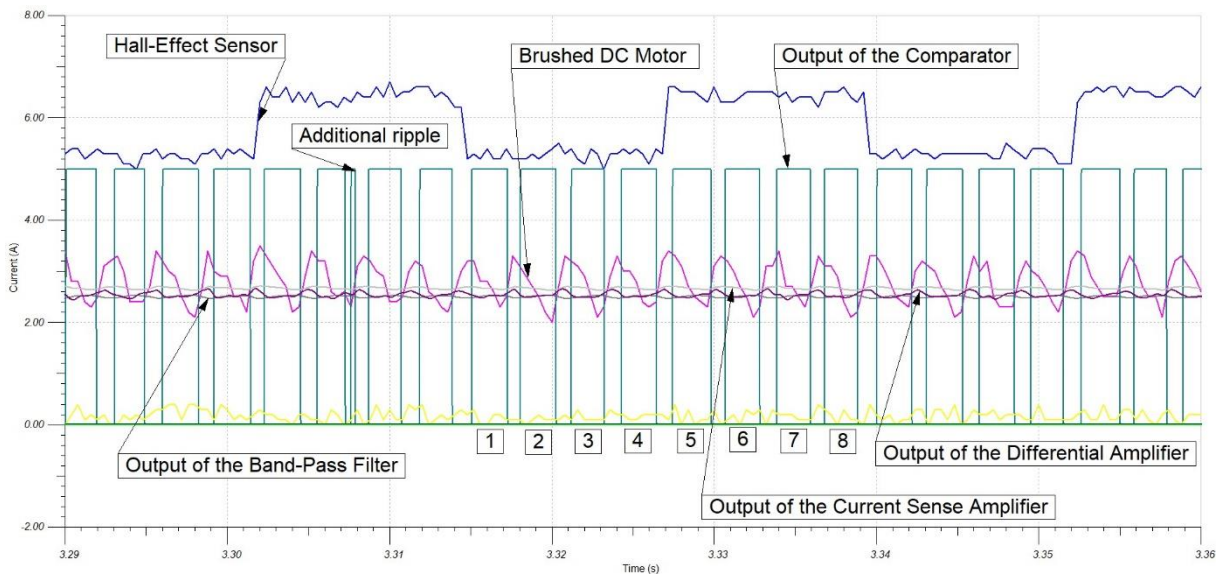


Figure 69: 9 V Downward Steady State Region Details

As clearly seen, each stage variable was represented in the previous figure. When examining steady state, there is not missing comparator ripple so every motor movement is pursued by comparator ripples. However, it should be 8 ripples for a period of hall-effect sensor that corresponds a complete rotation of motor but in this test it is happened some additional ripples because of unexpected change of brushed DC motor.

5.4.2 9 V Upward

Second motion is applied by 9 V power supply that is to upward. The maximum current of motor that is lower than downward motion, approaches 10,7 A. To examine generally, transient analysis is performed and three states are seen in the following figure.

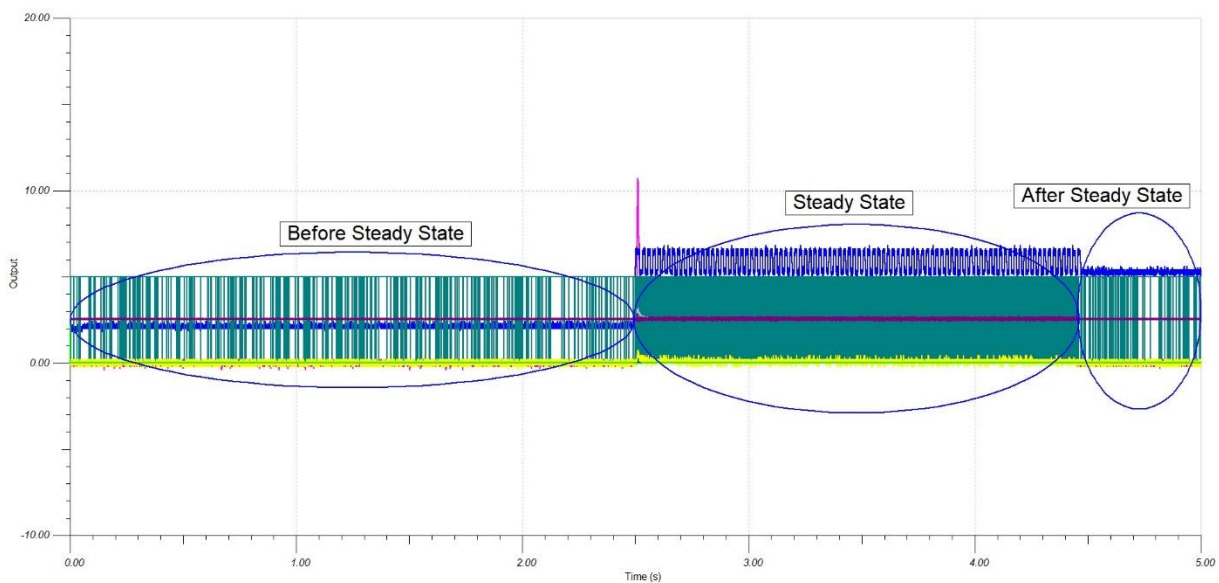


Figure 70: Transient Analysis of 9 V Upward

In before steady state, it is seen many unwanted comparator ripples because output of differential amplifier is caught by threshold voltages of comparator. To check steady state it is need to zoom in to this region. In after steady state there are many unwanted ripples because of same reason as before steady state. The graph is separated into each variable in the following page.

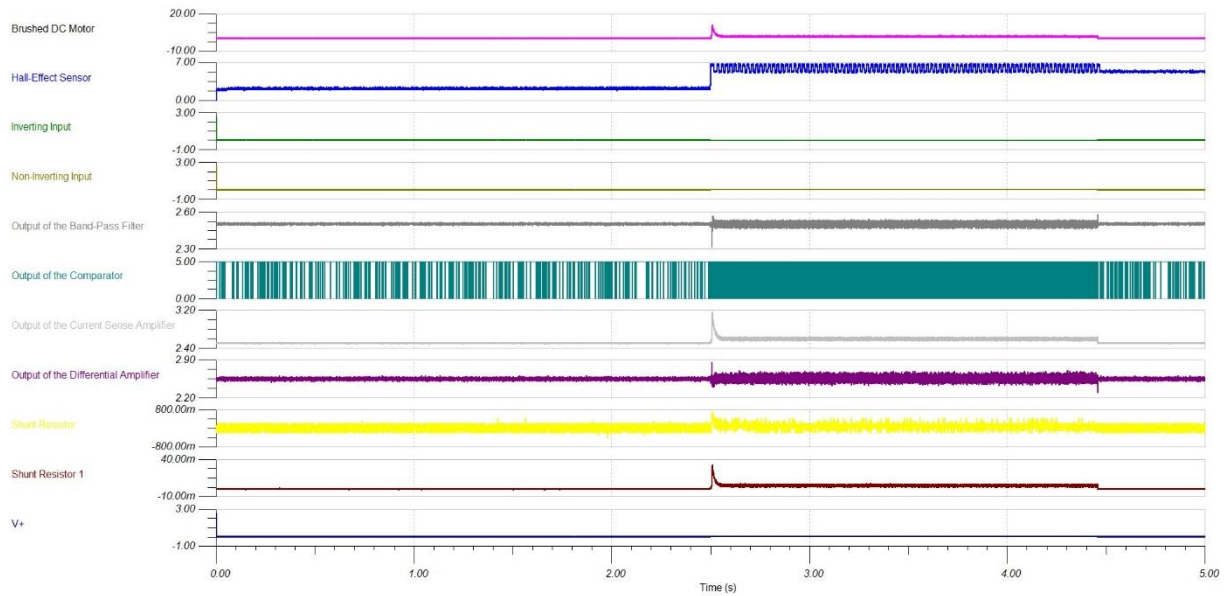


Figure 71: 9 V Upward Each Stage Analysis

The alteration of each variable is understood in this graph. The current of brushed DC motor is 0 before steady state and hall-effect sensor is not active in this state because motor is not rotating. The output current sense amplifier is lower in this region. For this reason, following two stages output are low. Normally comparator ripples are adjusted according to steady state region but for before steady state some voltage values of differential amplifier are caused by unwanted ripples. In steady state region, each stage variable increases and comparator ripples is been more often to catch every movement of motor. After steady state, each stage variable decreases and comparator ripples become less because brushed DC motor stops.

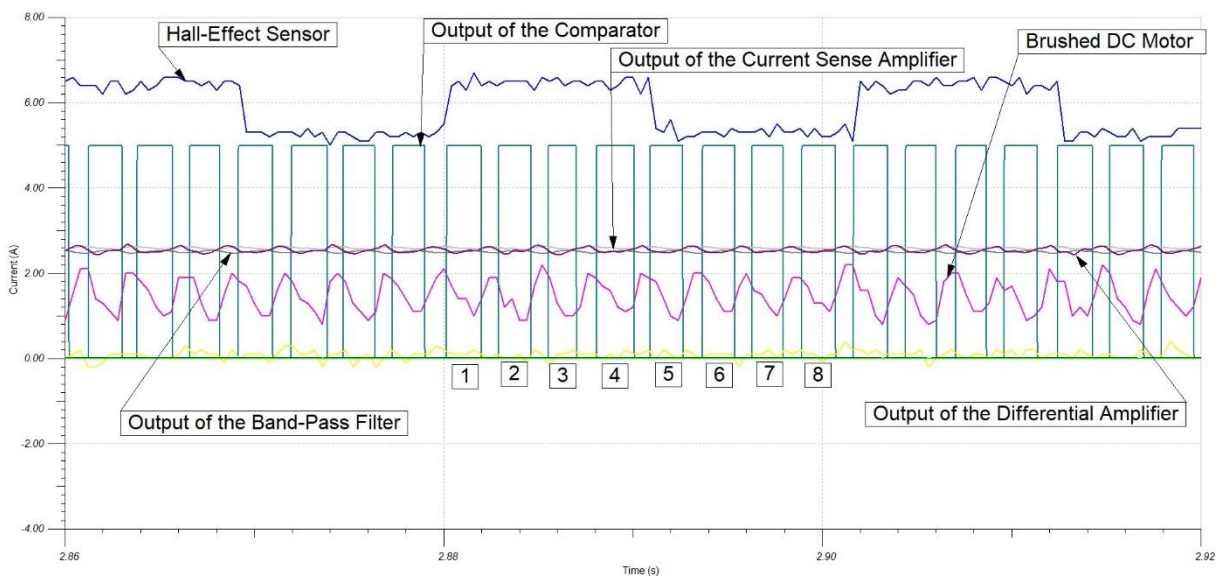


Figure 72: 9 V Upward Steady State Region Details

Every stage variable is shown in the previous page. In this state, it is not found any missing ripple and any additional ripple. That means all the motor movements are followed by comparator ripples. There are 8 ripples that correspond for each rotation of motor.

5.4.3 12 V Downward

The second voltage level, the brushed DC motor is driven by 12 V power supply. The maximum current of motor approximates 11,8 A. When voltage level is increased, test bench finishes its movement fastly. Nonetheless, the test time is set by hand in the laboratory but the simulation of test is always fixed 5 seconds. The 3 different states are illustrated in the following figure.

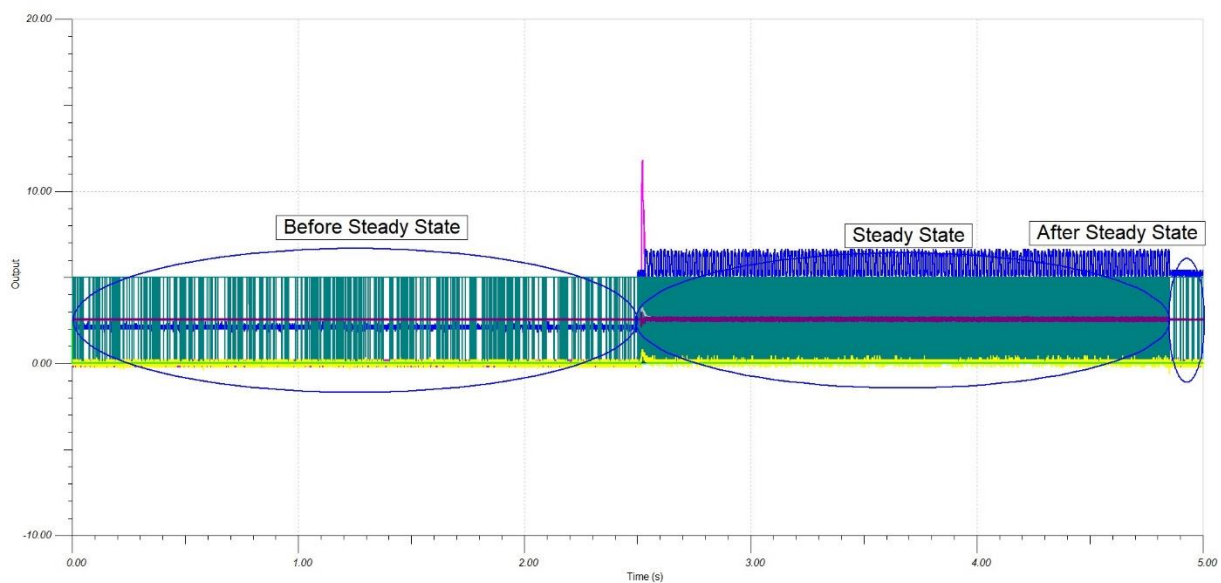


Figure 73: Transient Analysis of 12 V Downward

First state, before steady state many unwanted comparator ripples are appeared thanks to low level of output voltage of differential amplifier. To understand steady state, it requires to examine deeply. For after steady state, there are many comparator ripples by virtue of same reason of before steady state. In order to examine each variable, it is separated into inputs and outputs in the following page.

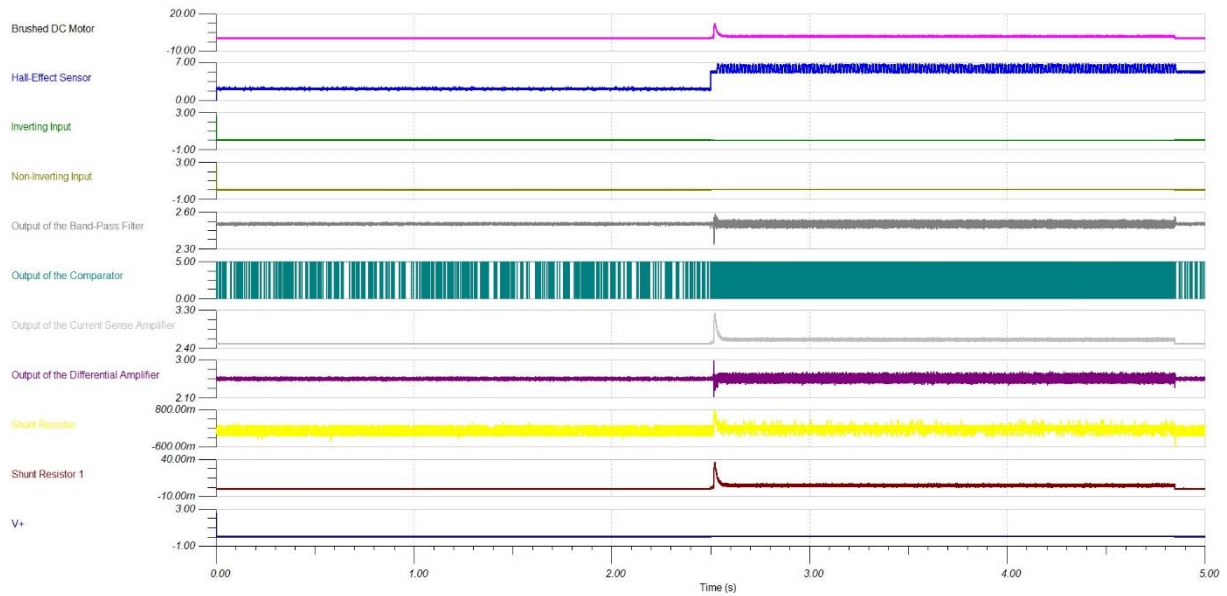


Figure 74: 12 V Downward Each Stage Analysis

In this graph, each stage is clearly shown. In before steady state, the brushed DC motor is not working so current of motor is 0 and hall-effect sensor is not active. The outputs of first 3 stages that are current sense, band pass filter and differential amplifier, are low in this state because the system does not supply by motor. Normally it should not be any comparator ripples in this state but they are sparse because of low level voltage of differential amplifier. In steady state, brushed DC motor is rotating and its current increases also hall-effect sensor follows motor movements. The outputs of first 3 stages increase and comparator ripples are intense to pursue all the motor movements. In after steady state, the first 3 stages outputs decrease and comparator ripples are infrequent again.

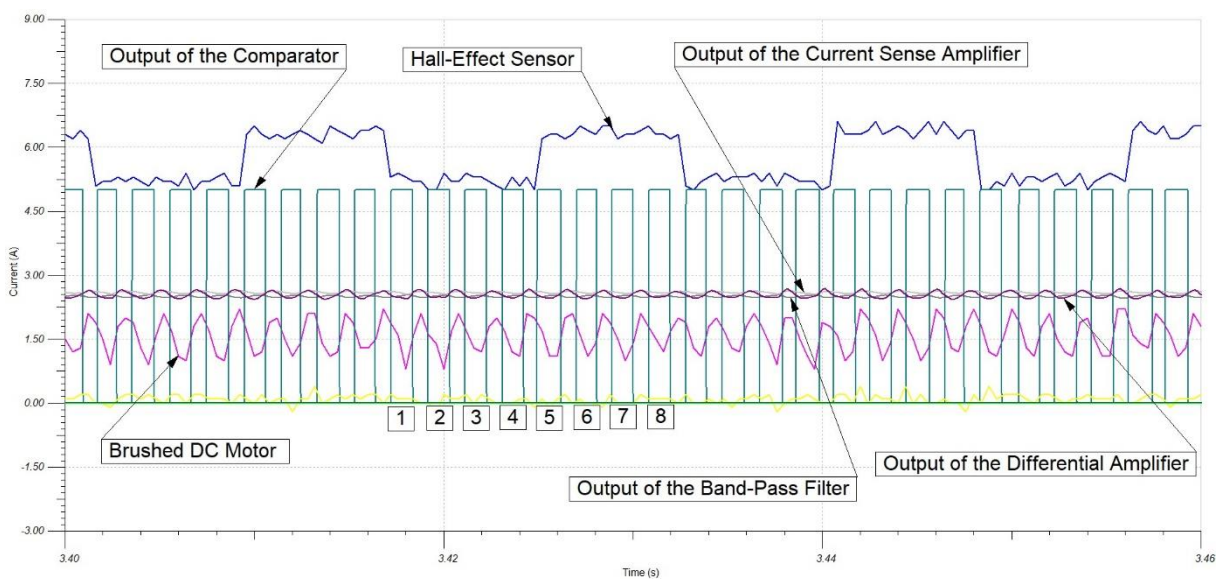


Figure 75: 12 V Downward Steady State Region Details

Each stage variable was represented in the previous page. There is not any missing and additional ripple. Thereby, comparator ripples follow each motor movement. It is shown that 8 comparator ripples equal to complete rotation of motor.

5.4.4 12 V Upward

The second motion of supplying motor by 12 V is to upward. The maximum current of motor increases up to 11,8 A. The current level is nearly same as test of 12 V downward. In the following figure, 3 different states are demonstrated according to motor condition.

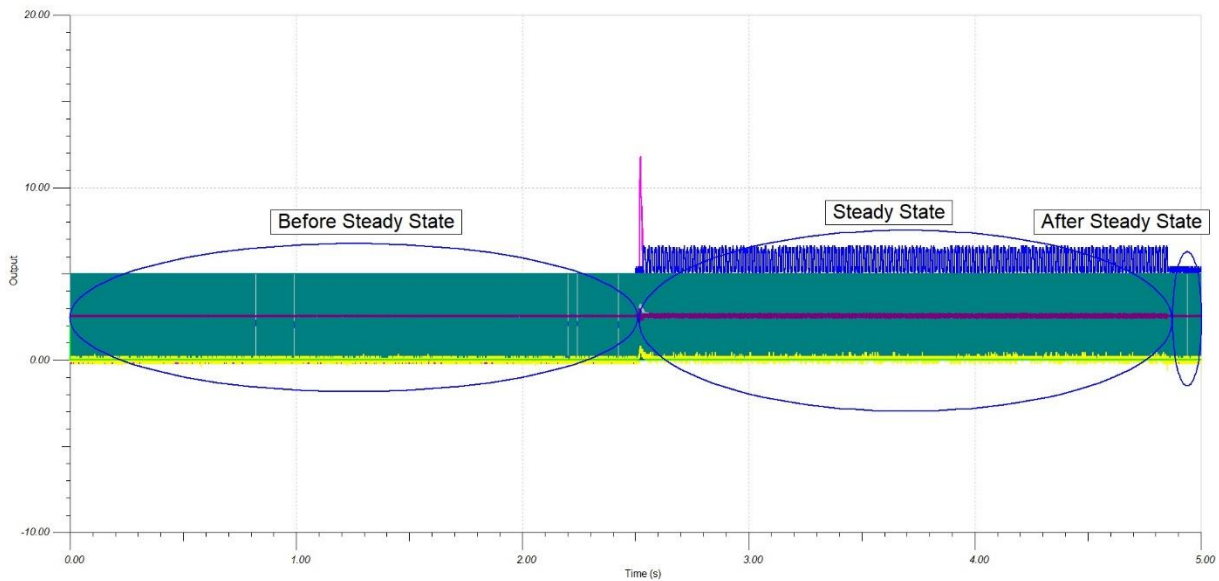


Figure 76: Transient Analysis of 12 V Upward

In before steady state, there are many comparator ripples but number of ripples are nearly as intense as in steady state. Before steady state normally, it should be less ripples or no ripple. In steady state there are more ripples but to examine detailed way, it is needed to zoom in. After steady state, the comparator ripples become lower. In the following page each stage variable is illustrated.

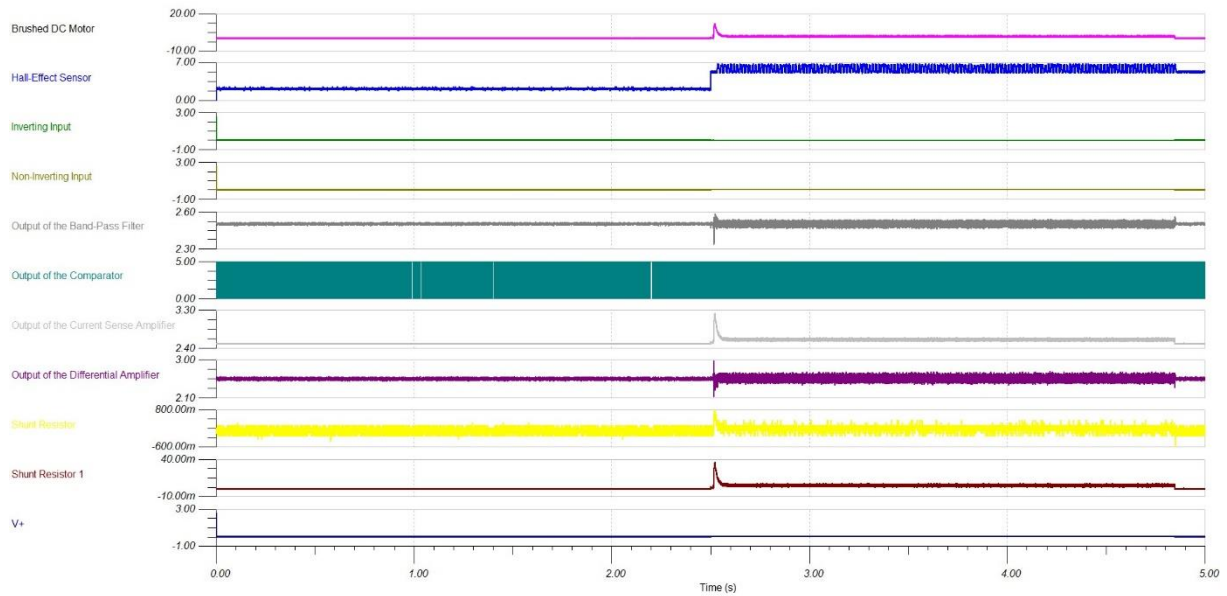


Figure 77: 12 V Upward Each Stage Analysis

Each stage variable is seen in this graph. When analysing state by state, in before steady state current of brushed DC motor is 0, current of hall-effect sensor is not 0 but inactive, the first 3 stages are unloaded condition so they are low and number of comparator ripples are more than 12 V downward motion. In steady state region, the outputs of first 3 stages increase, the current of brushed DC motor increases, hall-effect sensor becomes active and generate square wave to follow motor movement also comparator ripples increase to catch movement of motor. After steady state, the outputs of first 3 stages decrease, current of brushed DC motor and hall-effect sensor voltage lower, number of comparator ripples decrease. In the following graph the steady state is analyzed deeply.

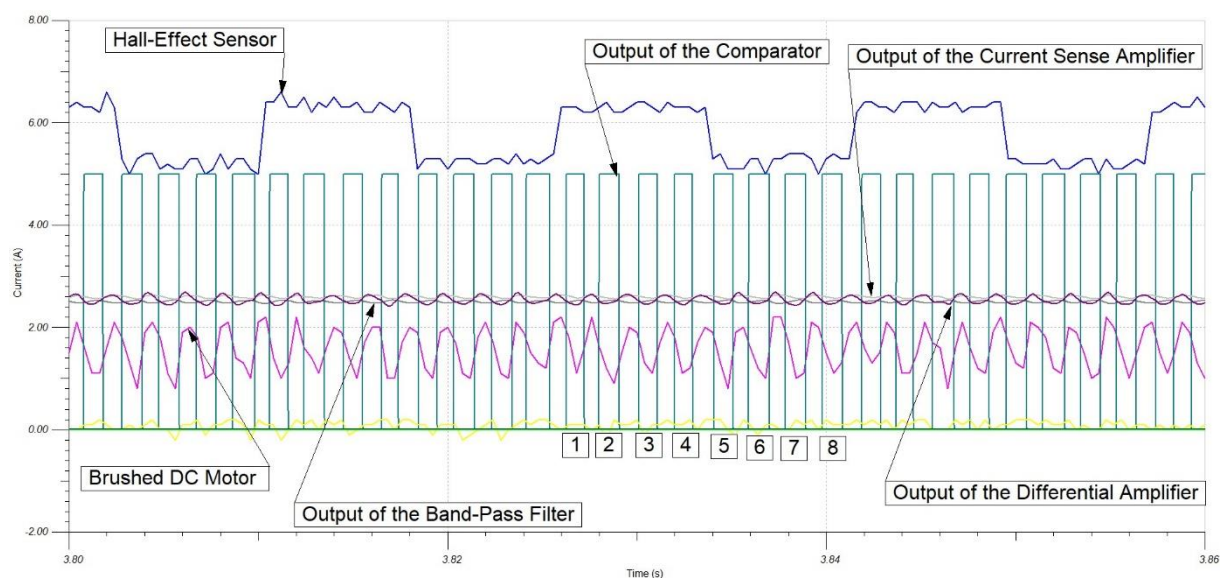


Figure 78: 12 V Upward Steady State Region Details

Every stage variable was stated in the previous page. It is not found any missing and additional comparator ripple. This means, motor movements are followed by comparator ripples. Also, it is indicated 8 comparator ripples correspond a rotation of motor.

5.4.5 16 V Downward

The third voltage level, the brushed DC motor is supplied by 16 V power supply and motion is downward. The maximum current of motor reaches 19,3 A. The motor states which are before steady state, steady state, after steady state shown in the following figure.

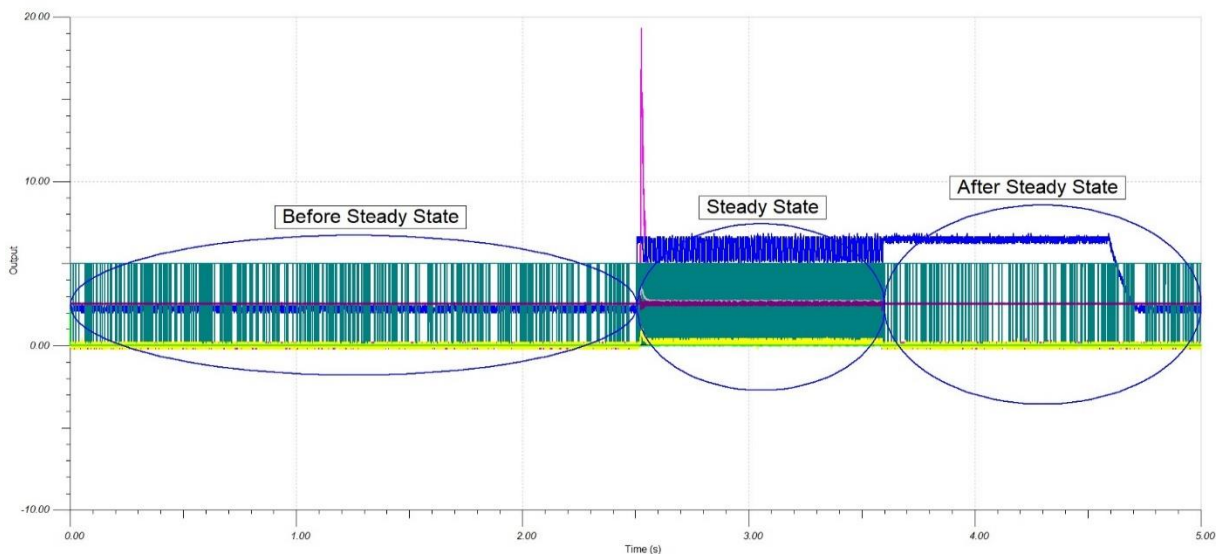


Figure 79: Transient Analysis of 16 V Downward

In the first state, before steady state many comparator ripples have been observed. In steady state, comparator ripples become frequent to follow all the motor movements. It should be zoomed in to check details of steady state. After steady state, comparator ripples become sparse. Each stage variable is shown in the following page.

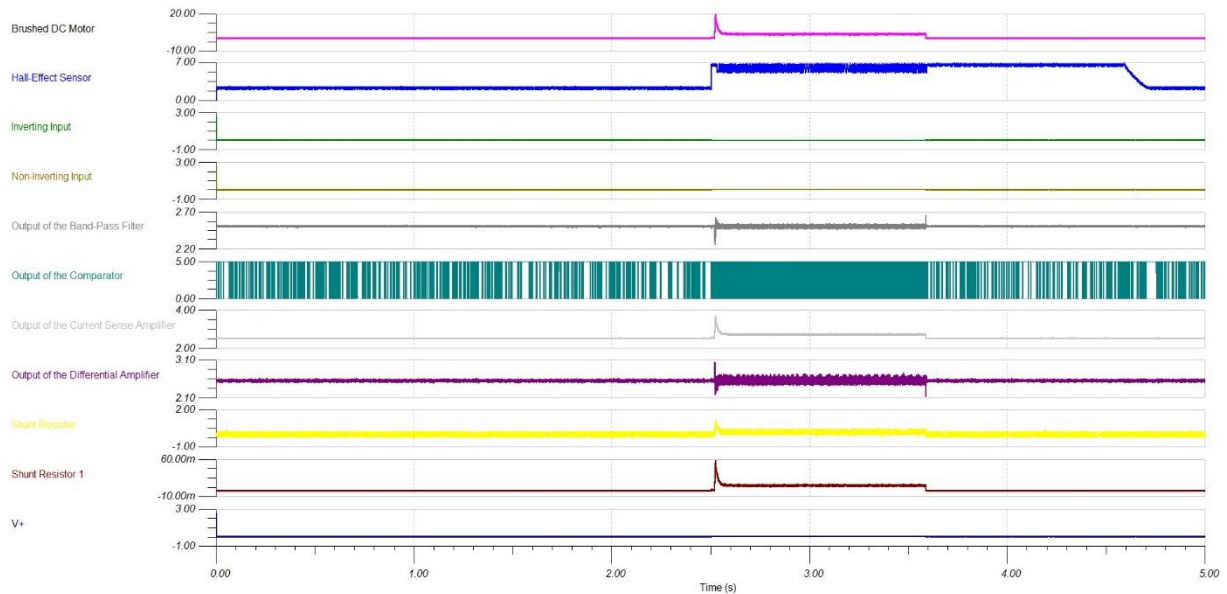


Figure 80: 16 V Downward Each Stage Analysis

All inputs and outputs are represented in this graph. In the first state, before steady state the current of motor is 0, hall-effect sensor is not active, output of current sense amplifier, output of band pass filter, output of differential amplifier are low and the number comparator ripples are low. In steady state, the current of brushed DC motor increases and voltage of hall-effect sensor increases and follows motor movements, the first 3 stages outputs increase, the comparator ripples become intense to pursue motor movements. In the last state, after steady state, the first 3 stages outputs decrease, the current of brushed DC motor lower, hall-effect sensor voltage lower and comparator ripples decrease. In the following figure the steady state is examined.

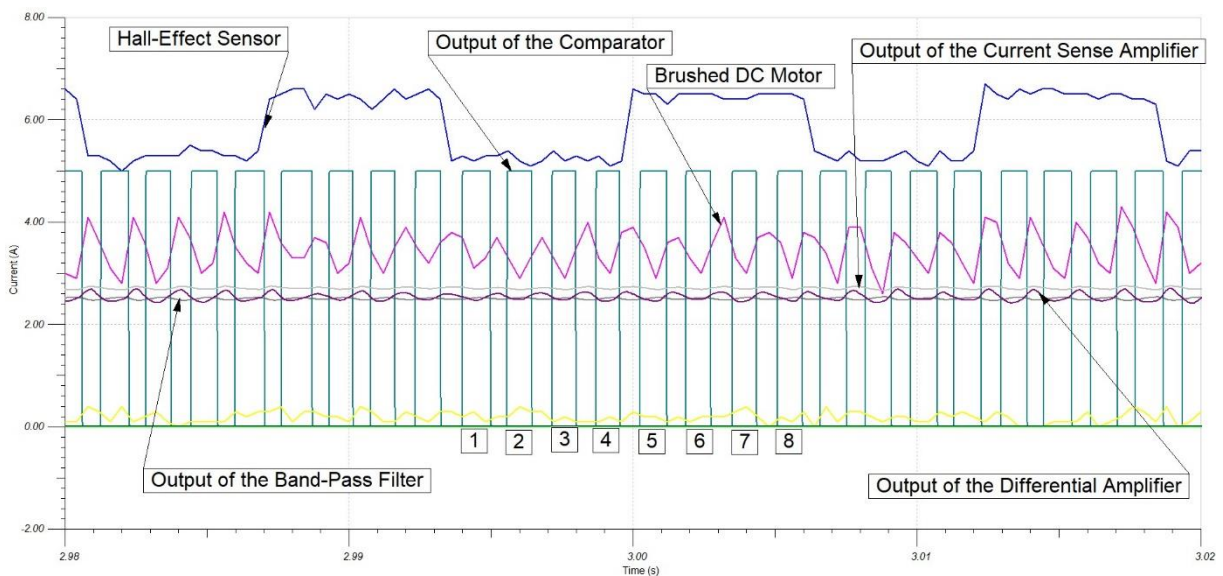


Figure 81: 16 V Downward Steady State Region Details

All inputs and output were demonstrated in the previous page. There is not any missing and comparator ripple in this region. Therefore, the ripples pursue all the motor movements and 8 comparator ripples equal to complete rotation of motor.

5.4.6 16 V Upward

The second motion of applying motor by 16 V is to upward. The maximum motor current approaches 16,5 A. The maximum current is less than 16 V downward. The general view of transient analysis is shown in the following graph.

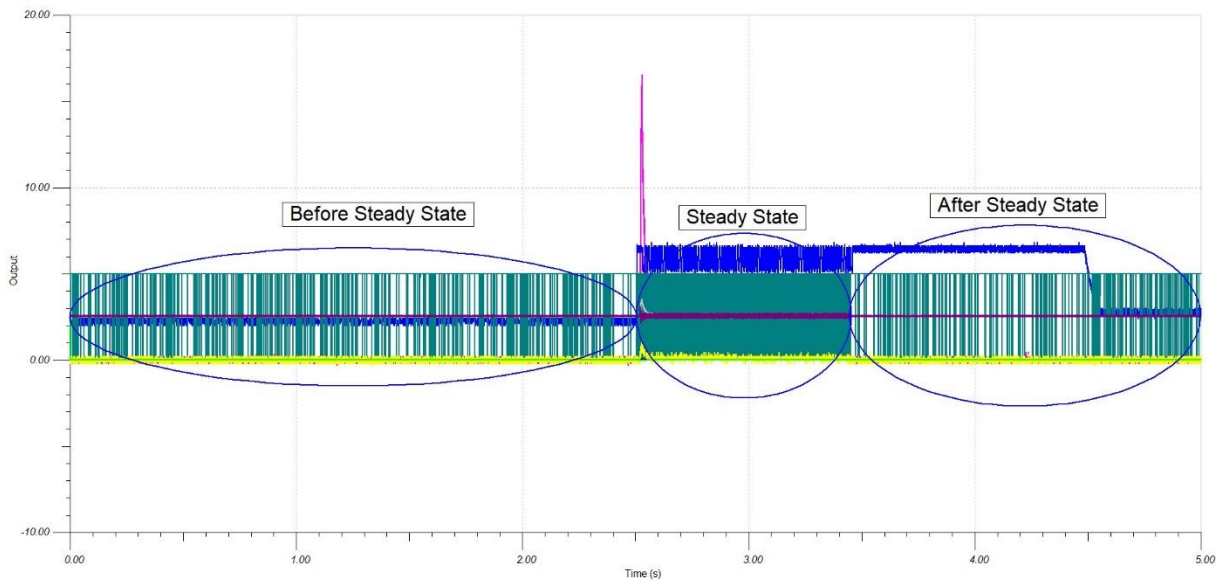


Figure 82: Transient Analysis of 16 V Upward

In before steady state, there are many unwanted comparator ripples and it seems nearly similar as analysis of 16 V downward. In steady state, the comparator ripples increase to follow every motor movement. In after steady state, number of comparator ripples decrease because motor is not driven. In the following page each stage variable is illustrated.

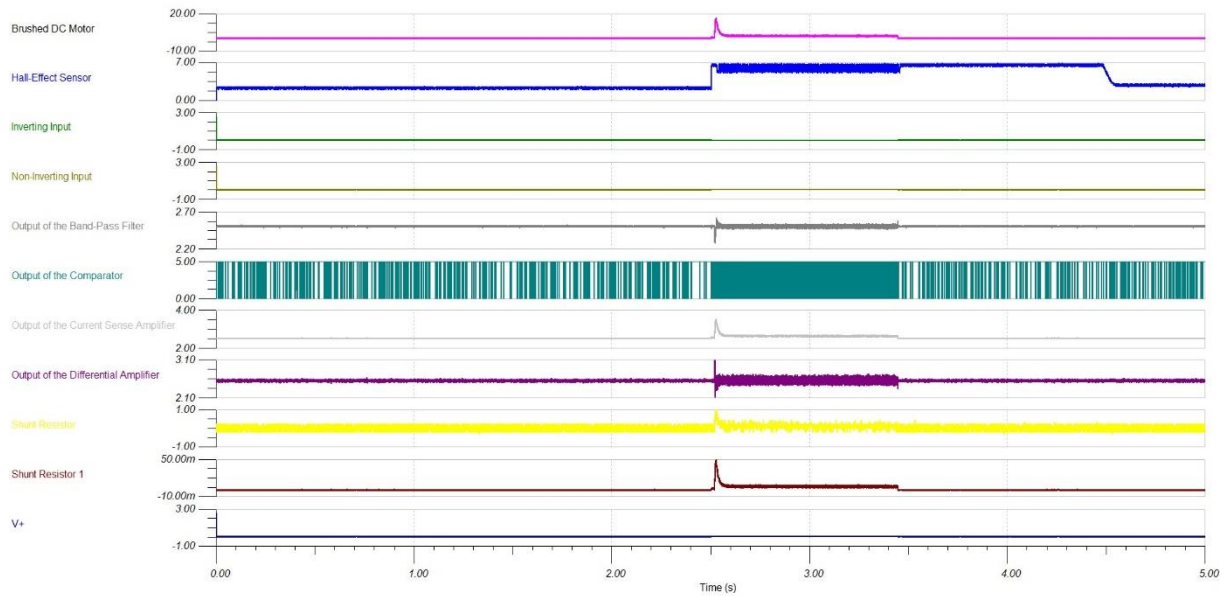


Figure 83: 16 V Upward Each Stage Analysis

Each stage variable is observed in this graph. Before steady state, the current of motor is 0, hall-effect sensor is not active, the first 3 stages outputs are low because they are not driven by motor, the comparator ripples are sparse. In steady state, the motor current increases and hall-effect sensor pursues motor movements, the first 3 stages outputs increase, the number of comparator ripples increase to follow motor movements. After steady state the motor current decreases, voltage of hall-effect sensor decreases, the first 3 stages outputs decrease, the comparator ripples decrease. In the following figure, the steady state is analyzed with details.

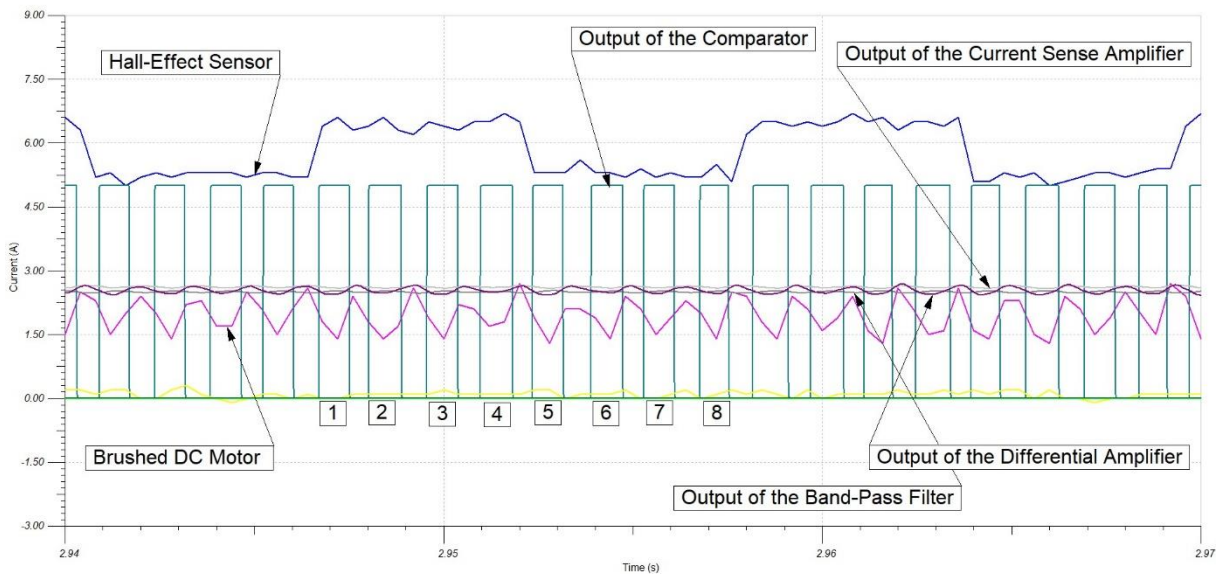


Figure 84: 16 V Upward Steady State Region Details

In steady state, comparator ripples have to follow motor movements, so the number of ripples are increased. Any missing and additional comparator ripple has not been observed in this state. Hence, the comparator follows every motor movement and 8 comparator ripples correspond a complete rotation of motor.

5.5 Updated System Test

The updated system is comprised of the current sense amplifier, the band pass filter, the comparator. In the current sense amplifier stage, the amplifier was changed instead of INA240-Q1, TLV316 is used to reduce cost so the structure of current sense amplifier was completely changed.

The structure of band pass filter is same as old version of band pass filter stage, but only C1 is changed to adapt frequency range.

The comparator stage, only threshold voltages is need to adjust because in updated system band pass filter is directly connected to comparator so input of comparator changes.

5.5.1 9 V Downward Updated

In this test, the same procedure and test value are applied for downward-upward motion but varieties of system stages and structure cause different test result. The brushed DC motor is driven by 9 V and the maximum current of motor approximates 11,2 A. The general overview of transient analysis of sensorless approach is demonstrated in the following figure.

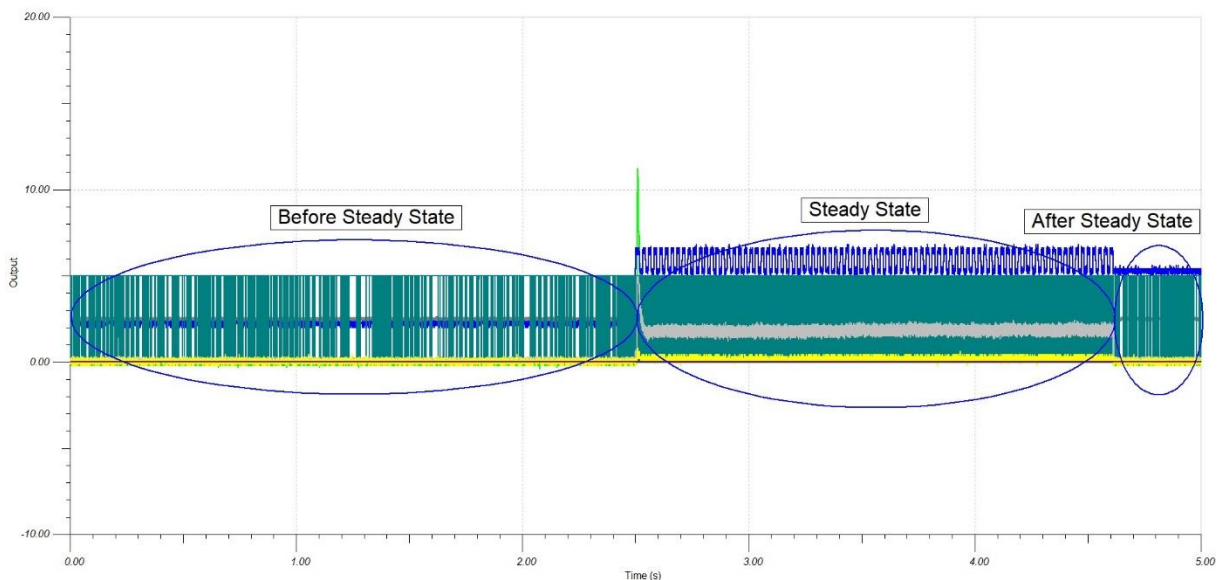


Figure 85: Transient Analysis of 9 V Downward Updated

In this graph, it is clearly realized intensive comparator ripples form, at the beginning of test there were less ripples also for 9 V and 12 V tests but in order to provide good result in the steady state of 16 V tests, threshold voltages were adjusted for every voltage level. In before steady state, there are many unwanted ripples seen because the output of band pass filter is detected by comparator. It is need to analyse closely steady state region to check whether every movement of motor is followed. In after steady state, the intensive unwanted comparator ripples are occurred because of same reason as before steady state. In the graph below, all variables are separated for better viewing.

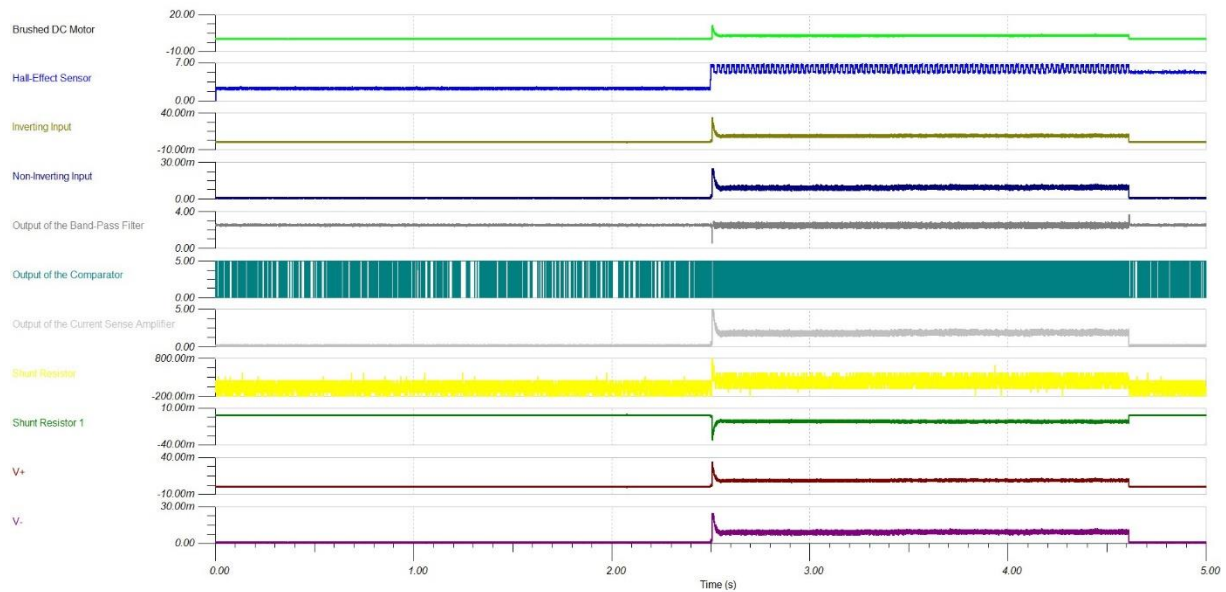


Figure 86: 9 V Downward Updated Each Stage Analysis

All variables are in sighted clearly in this graph. As done before, each stage is examined according to 3 different states. Before steady state, the current of brushed DC motor is 0, hall-effect sensor is not active. Output of first two stages that are current sense amplifier, band pass filter, are depressed in this state. It is seen many unwanted comparator ripples thanks to low level of output voltage of band pass filter. In steady state, the first two stages rise their inputs because motor is supplied in this period and comparator ripples increase to follow each motor movement. In after steady state, motor current, voltage of hall-effect sensor, the outputs of first two stages and comparator ripples diminish.

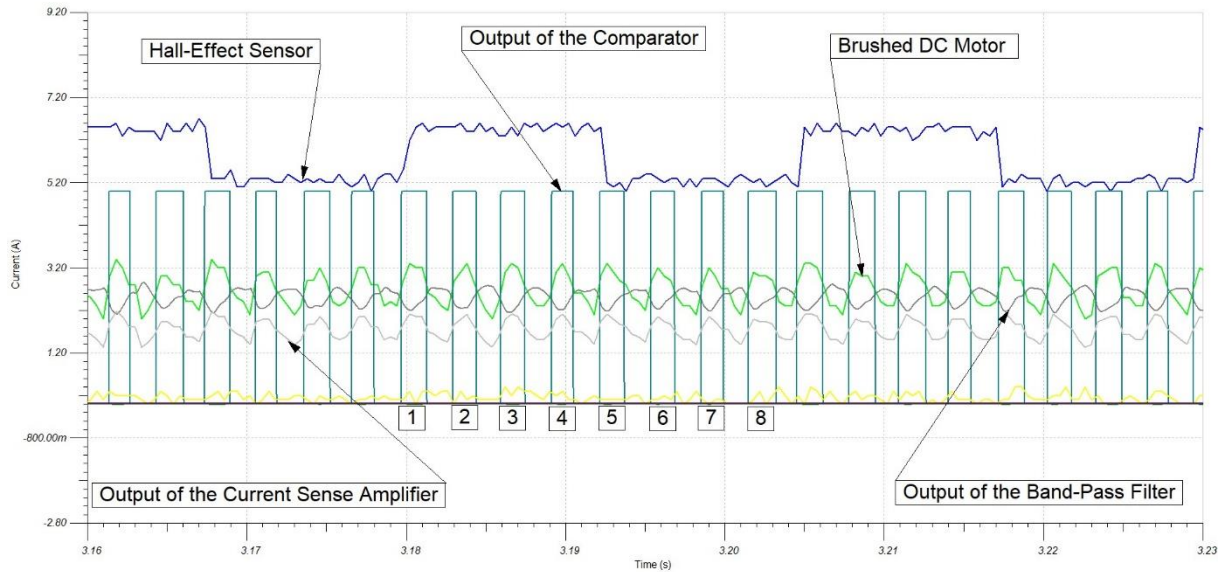


Figure 87: 9 V Downward Updated Steady State Region Details

In this graph, colours of lines are different but it is represented above. While analysing steady state, the most important thing is that comparator ripples should follow all the motor movements. Also, during a complete rotation of motor there should be 8 ripples. As understood from graph, these two important things are realized.

5.5.2 9 V Upward Updated

Second motion of updated version is to upward by applying 9 V. The maximum current of motor reaches 10,7 A. The general overview of transient analysis is illustrated in the following figure.

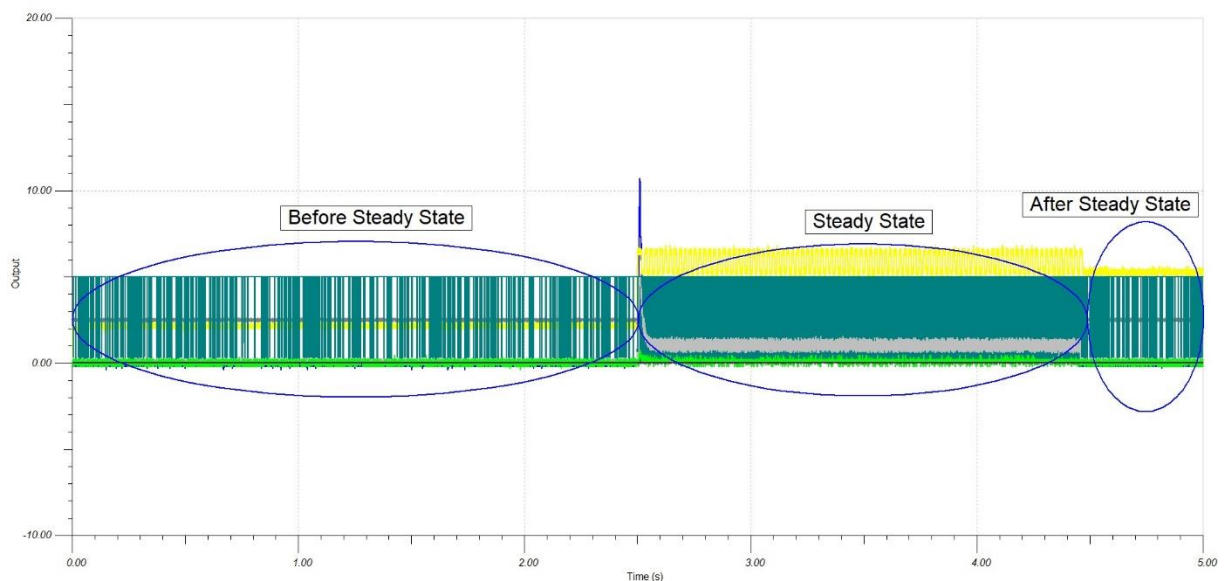


Figure 88: Transient Analysis of 9 V Upward Updated

Before steady state, there are many unwanted comparator ripples seen and it is realized that the ripples are more intense than old version of 9 V upward. Steady state region is analyzed deeply later. After steady state many unwanted comparator ripples are seen. Each stage variable is shown clearly in the following graph.

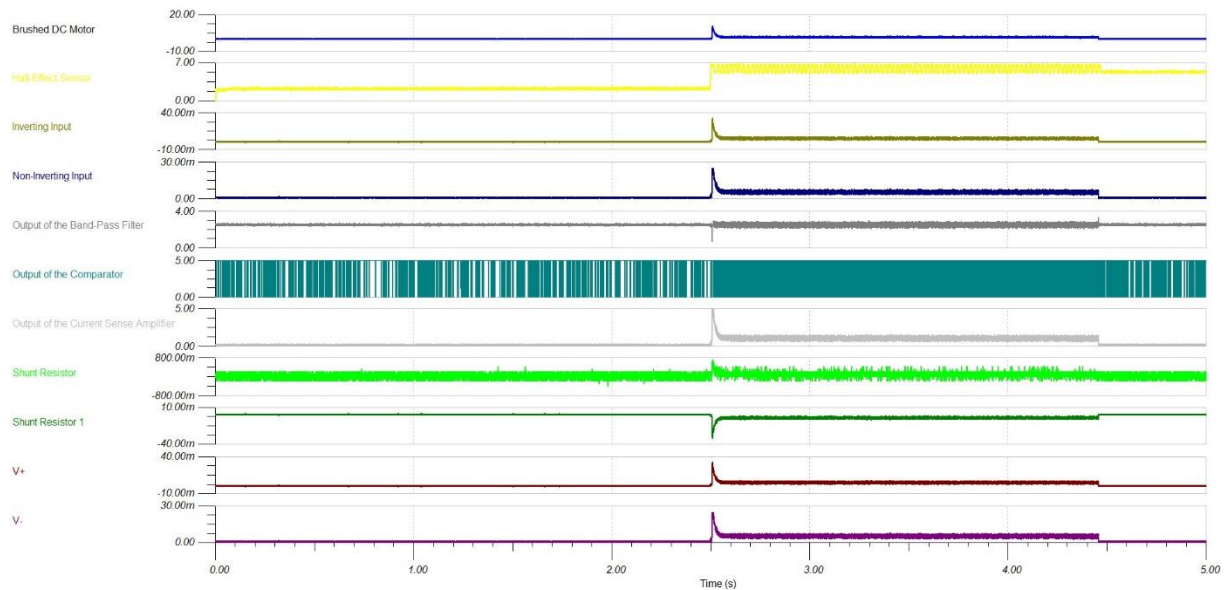


Figure 89: 9 V Upward Updated Each Stage Analysis

The change of each stage variable is stated in this graph. In before steady state, current of motor is null, hall-effect sensor is constant. Output of first of two stages are low in this state. There are many unwanted comparator ripples are realized as low level of output voltage of band pass filter cause these ripples. In steady state, motor starts to turn and motor current rises and hall-effect sensor follows motor movement, also comparator ripples pursue motor motion. In after steady state region, current of motor, hall-effect sensor voltage, outputs of first two stages and comparator ripples decrease.

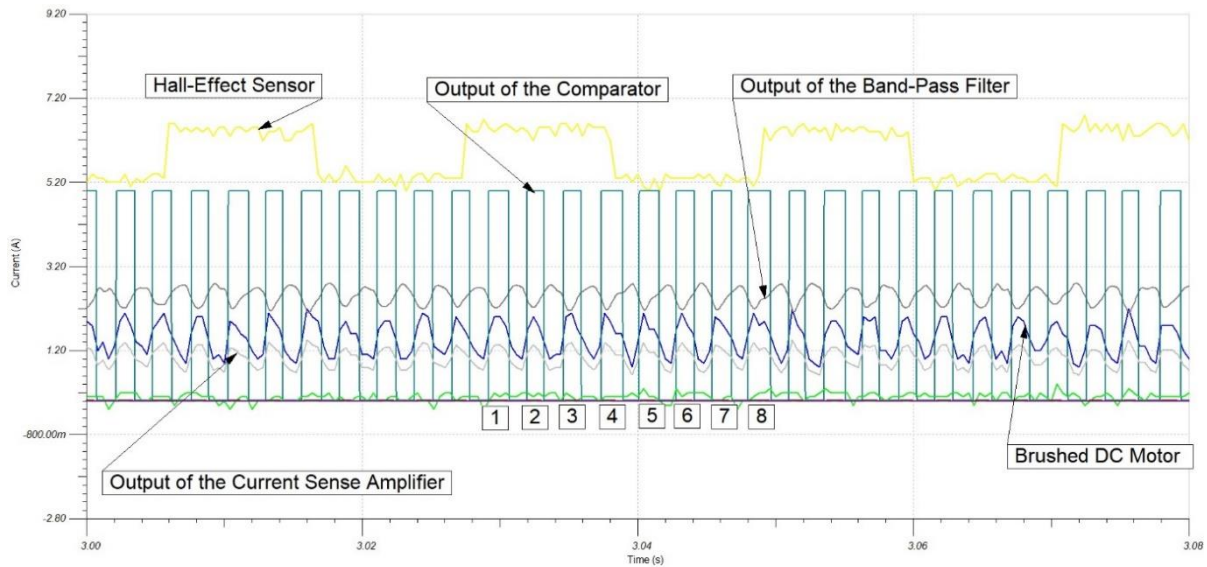


Figure 90: 9 V Upward Updated Steady State Region Details

In steady state, it is focused on comparator ripples that should follow all the motor movements. Besides, there is not any additional comparator ripples and 8 ripples correspond a complete rotation of motor.

5.5.3 12 V Downward Updated

The second voltage value of downward-upward motion is driven by 12 V power supply. The maximum current of motor approaches 11,8 A. When voltage increases from 9 V to 12 V, test bench completes its motion faster. The general view of transient analysis is shown below.

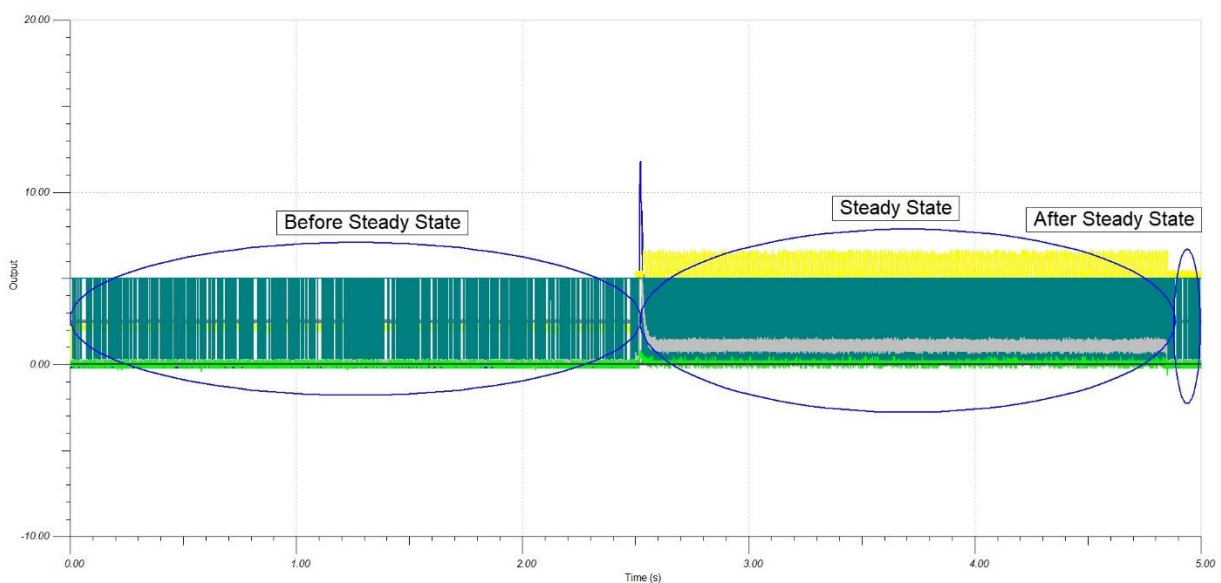


Figure 91: Transient Analysis of 12 V Downward Updated

Before steady state, many unwanted comparator ripples are seen by virtue of low level of band pass filter output. Steady state comparator ripples become intensive to catch all motor movements. In after steady state, many comparator ripples are realized. In the following graph, each stage variable is demonstrated.

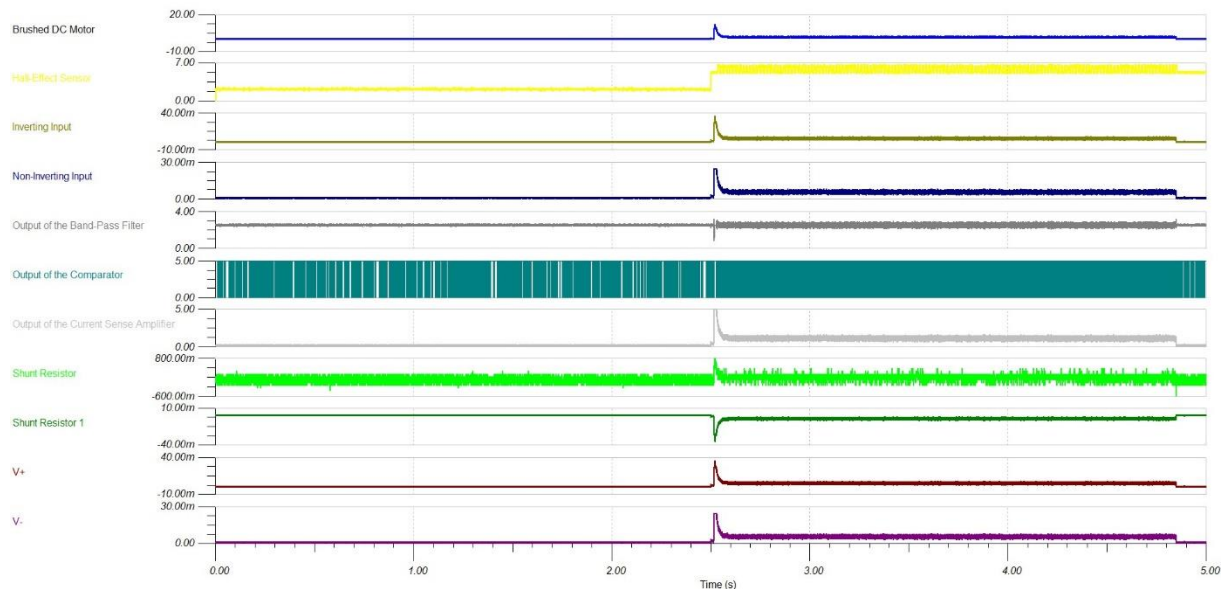


Figure 92: 12 V Downward Updated Each Stage Analysis

In this figure, each stage variable is seen clearly. Before steady state, motor current is 0, hall-effect sensor voltage is constant. The outputs of first two stages are depressed and there are many unwanted comparator ripples seen by means of low level voltage of band pass filter. In steady state, the motor is running and it increases its current also hall-effect sensor pursues motor motions. The outputs of first two stages rise and comparator ripples rise to catch all the motor movements. After steady state, the first two stages outputs diminish and comparator ripples decrease because motor is not supplied by power.

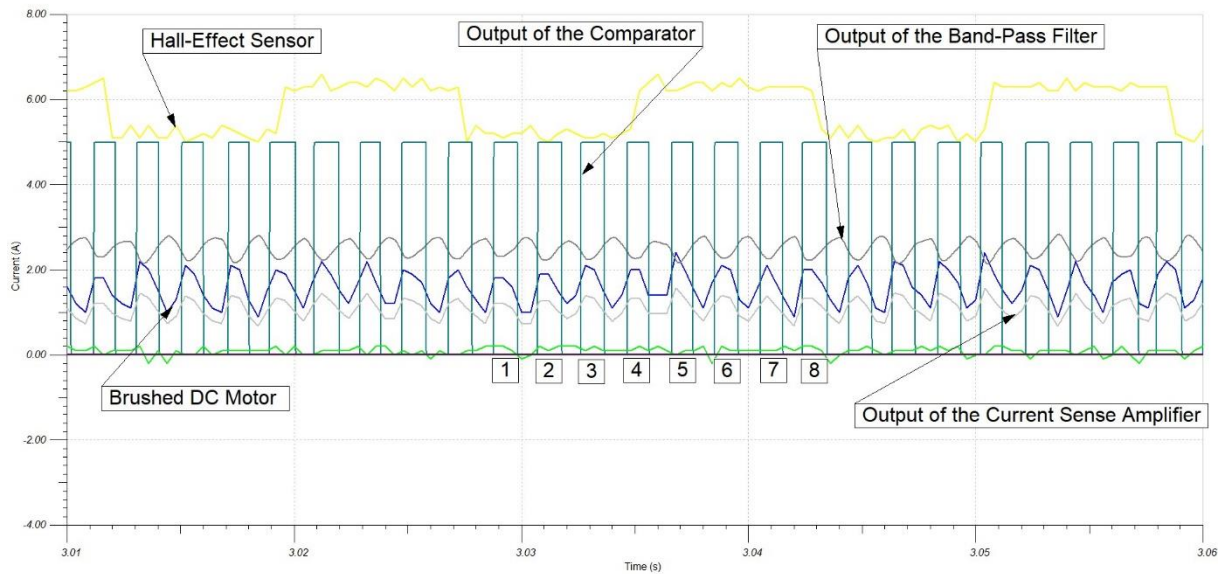


Figure 93: 12 V Downward Updated Steady State Region Details

All stage variables are shown clearly. As seen comparator ripples follow all the motor movements and there is not any additional ripples. It is realized that 8 comparator correspond complete turn of motor.

5.5.4 12 V Upward Updated

The second movement of applying motor by 12 V is to upward. The maximum motor current increases up to 11,8 A. The current is a bit higher than 12 V downward. In the following figure, the transient analysis with general overview of three states are shown.

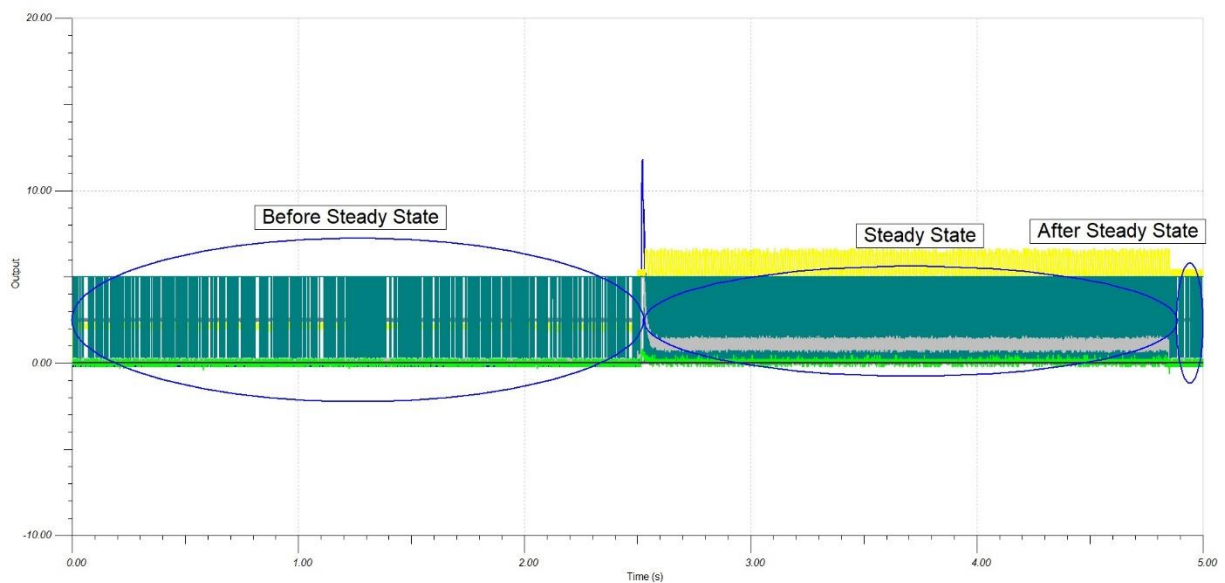


Figure 94: Transient Analysis of 12 V Upward Updated

It is seen that there are many comparator ripples thanks to low level of band pass filter voltage. In steady state, comparator ripples increase to follow all the motor motions. After steady state, comparator ripples decrease. Each stage variable is represented in the following page.

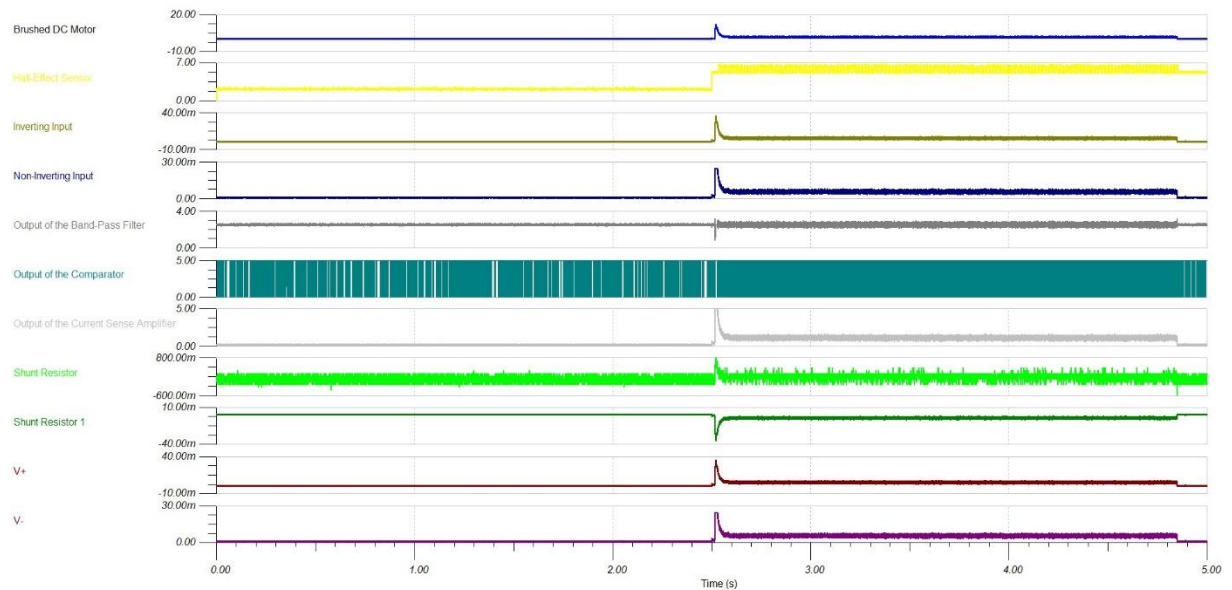


Figure 95: 12 V Upward Updated Each Stage Analysis

All variables are clearly shown in this graph. In before steady state, motor current is 0, hall-effect sensor is not active, outputs of first 2 stages are low, many comparator ripples are seen because of low voltage level of band pass filter. In steady state, the motor is working so the current of motor increases, hall-effect sensor follows to motor motions, the first two stages outputs increase, the comparator ripples also increase to catch all the motor motions. After steady state, motor current decreases, hall-effect sensor is constant, the first two stages outputs decrease, comparator ripples diminish.

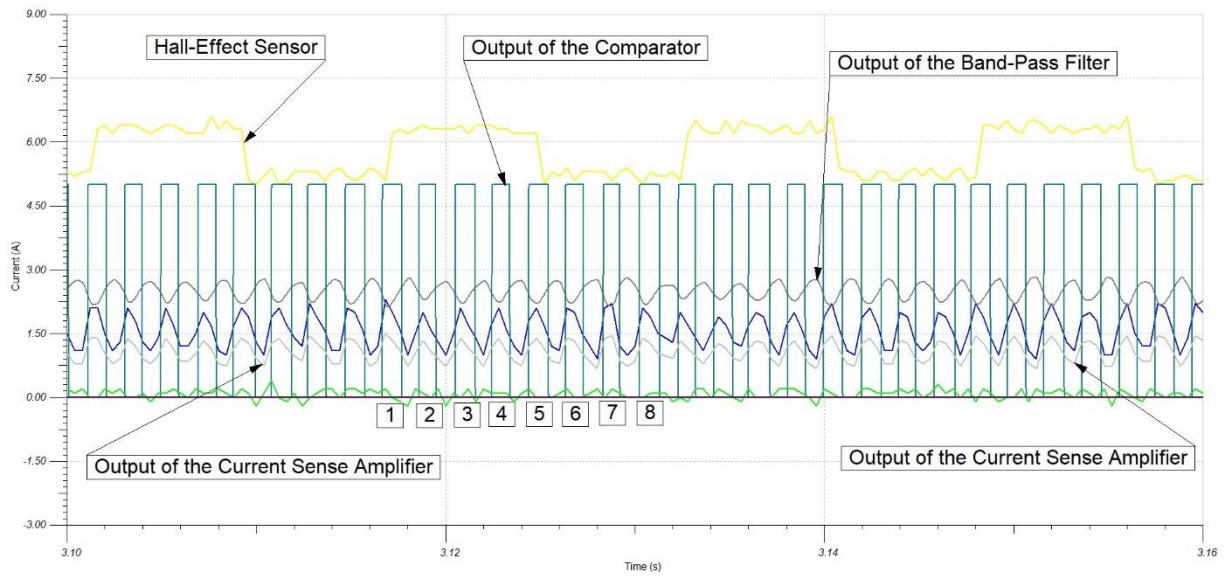


Figure 96: 12 V Upward Updated Steady State Region Details

Each stage variable was shown in previous page. It is understood that comparator ripples follow all the motor ripples. There is not any additional ripples in this state also 8 comparator ripples equal to complete rotation of motor.

5.5.5 16 V Downward Updated

The third voltage value, the motor is driven by 16 V power supply and test bench moves to downward. The maximum motor current reaches 19,3 A. The motor conditions that are before steady state, steady state, after steady state are represented in following figure.

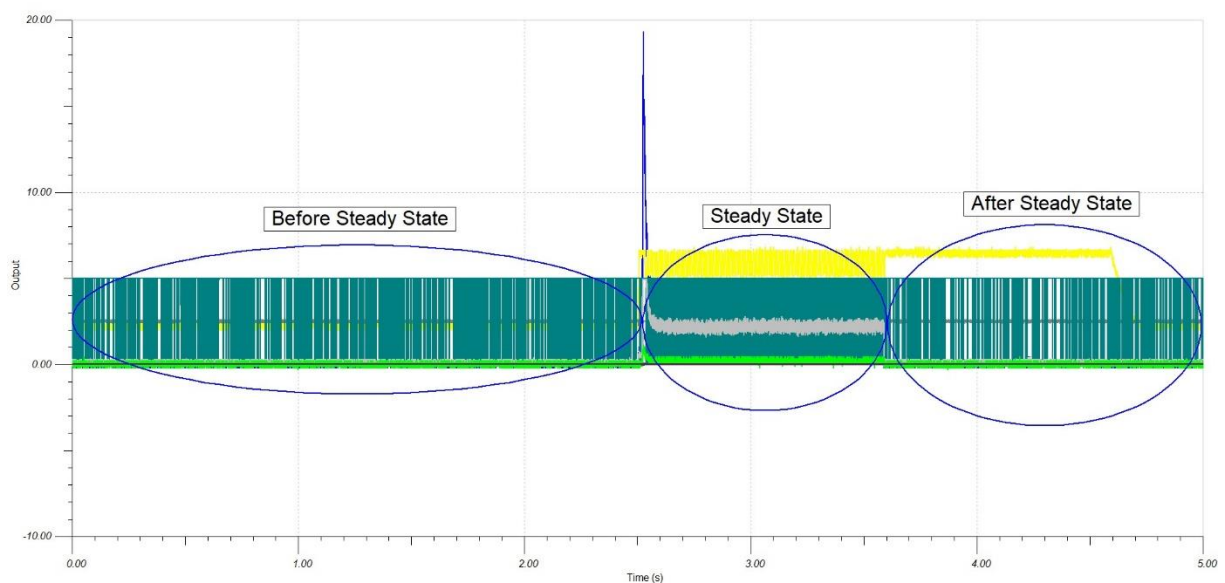


Figure 97: Transient Analysis of 16 V Downward Updated

Before steady state, many comparator ripples are observed by means of low voltage level of band pass filter. In steady state, the comparator ripples increase to pursue every motor motion. After steady state, comparator ripples decrease because motor is not running in this state and input voltage of comparator is low.

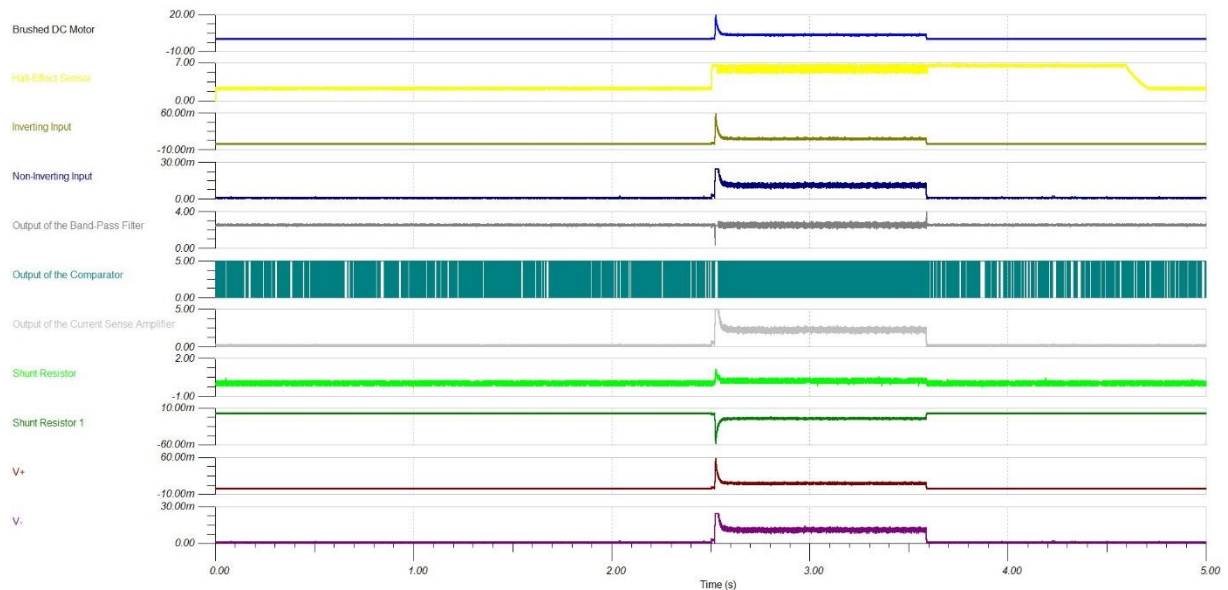


Figure 98: 16 V Downward Updated Each Stage Analysis

Each stage variable is shown in this graph. Before steady state, the motor current is 0, the signal of hall-effect sensor is constant, outputs of first two stages are low and many comparator ripples are seen because of low output voltage of band pass filter. In steady state, motor rotates and motor current increases, hall-effect sensor is active to follow motor movements, outputs of first two stages outputs increase, the number of comparator ripples increase to follow motor motions. After steady state, motor current diminishes, the signal of hall-effect sensor is constant again, outputs of first two stages lower, comparator ripples reduce. In the following figure the steady state is analyzed.

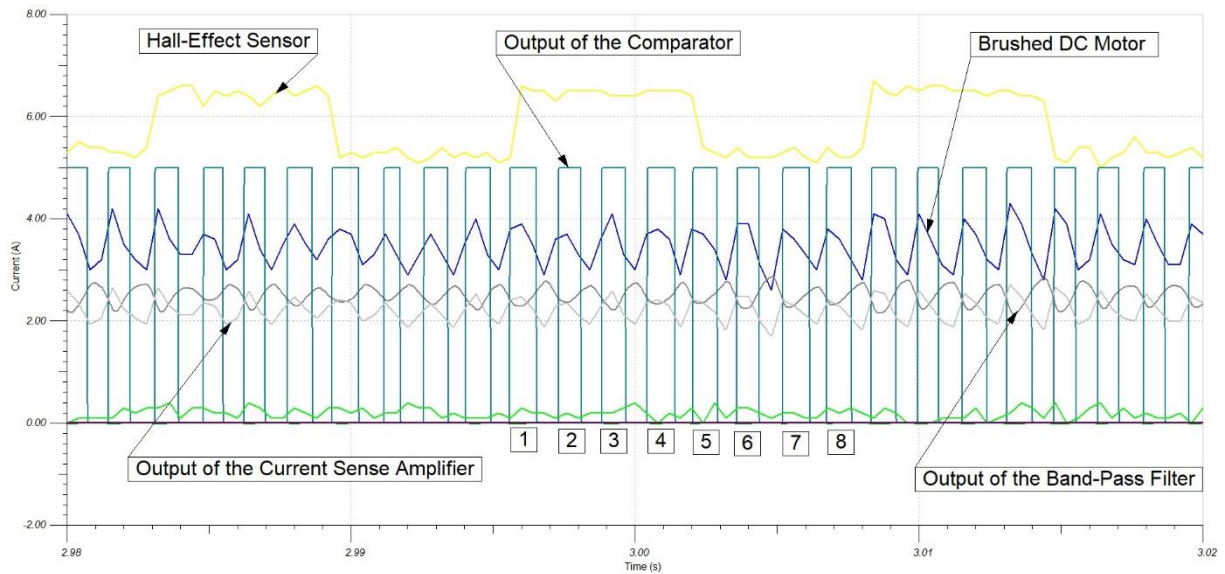


Figure 99: 16 V Downward Updated Steady State Region Details

All stage variables were shown in the previous page. It is observed that comparator ripples follow all the motor movements and there is not any additional ripples found. Corresponding complete rotation of motor, there are 8 comparator ripples.

5.5.6 16 V Upward Updated

The second motion supplying motor by 16 V is to upward. The maximum motor current approximates 16,5 A. This current value is less than 16 V downward. In the following graph, the overview of transient analysis is demonstrated.

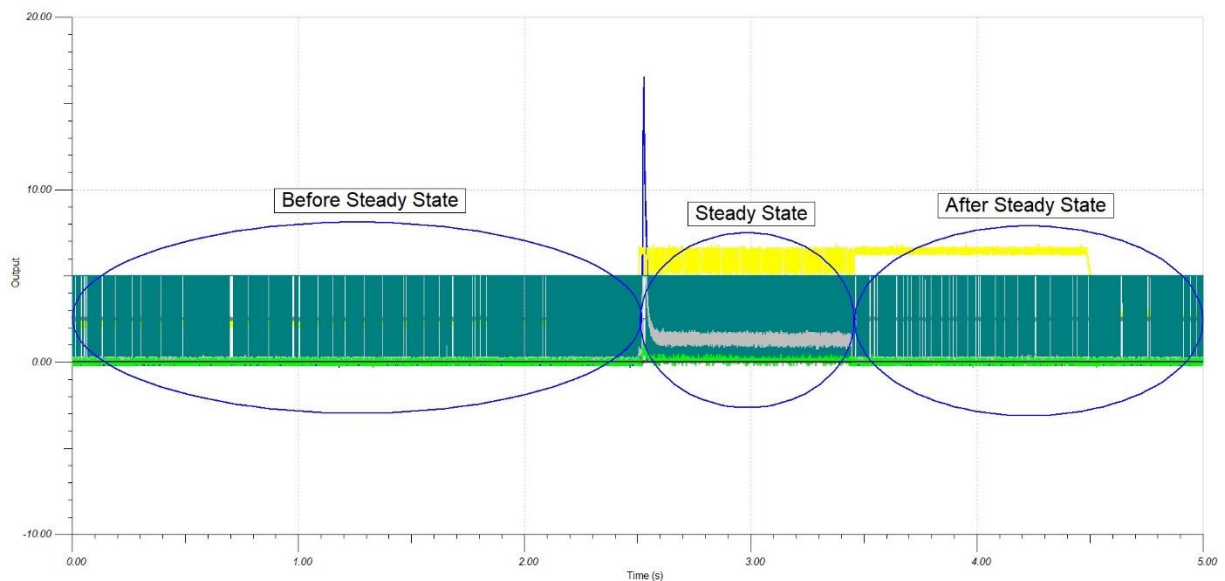


Figure 100: Transient Analysis of 16 V Upward Test

Before steady state, many comparator ripples are seen because of low level output voltage of band pass filter. In steady state, the number of comparator ripples rise to pursue all the motor movements. After steady state, number of comparator ripples decrease as motor is not supplied. Each stage variable is examined in the following page.

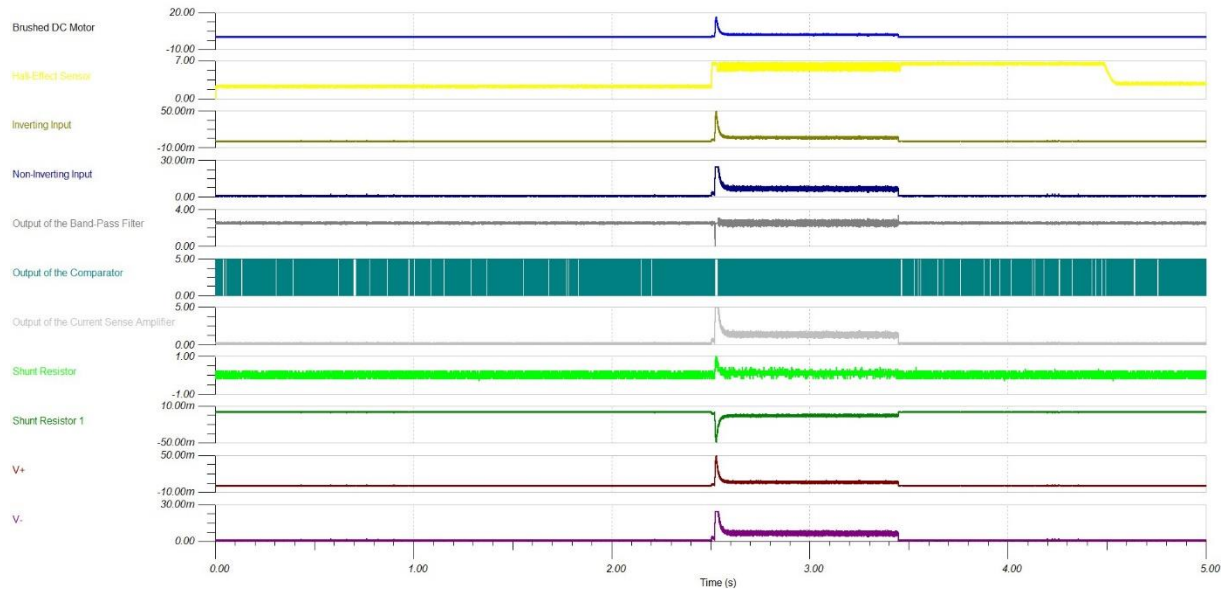


Figure 101: 16 V Upward Updated Each Stage Analysis

All stage variables are seen in this figure. In before steady state, the motor current is 0, hall-effect sensor voltage is low, the first 2 stages outputs are low as they are not supplied by motor, many unwanted comparator ripples are observed by virtue of low level output voltage of band pass filter. In steady state, the motor rotates and its current increases, hall-effect sensor generates square wave to follow motor movements, the first 2 stages outputs increase, the number of comparator ripples rise to pursue each motor motion. After steady state the motor stops and its current decreases up to 0, hall-effect sensor is not active, outputs of first two stages diminish, the number of comparator ripples decrease. The steady state is examined deeply in the following figure.

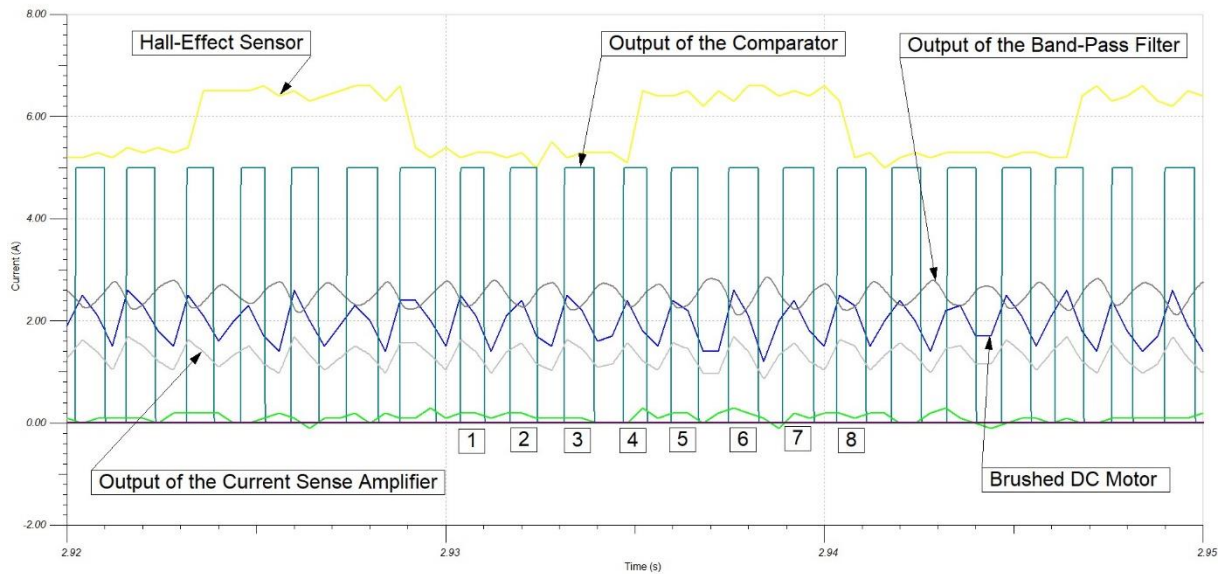


Figure 102: 16 V Upward Updated Steady State Region Details

The comparator ripples must pursue every motor motion in steady state, hence the number of ripples increase. There is not any missing and additional ripple observed in this state. Therefore, the comparator ripples pursue all the motor movements also complete rotation of motor corresponds 8 ripples.

6. Conclusion & Future Work

The sensorless method of vehicle seat adjustment is research project of Bitron Electronic Division. The company has already produced sensed method so this project will be an alternative for sensed approach. Also, aims of sensorless method are to get similar or same results as sensed method, and to reduce to cost account.

In order to provide these aims, the project was separated into two that are hardware electronic design and software design. I and my company tutor were responsible for hardware part.

Initially, simulation test of sensorless method was applied on TINA programme. This step was performed in order to understand how the sensorless approach works and it was an example to provide some required results.

After receiving brushed DC motor assembled on test bench, test procedure was started.

Firstly, the sensed method was tested in the laboratory and obtained test results were uploaded TINA programme so by using these results the sensorless method was simulated in this programme. These results which were acquired by simulation, did not give us the desired system behaviour. In order to make an improvement, some computational works were done. For sensorless approach, motor movements were followed by comparator ripples in steady state region that means when motor is

rotating. However, before motor rotates and after motor stops, there should not be any comparator ripples because there is no motor movement at that time. In these tests, in steady state region seemed good but there were some unwanted comparator ripples in before and after steady state region.

Secondly, the sensed electronic board that was product of Bitron, was utilized to get better and accurate signal from comparator output. By using this board, the same test procedure was applied. This test helped to get better and realistic result.

Thirdly, the system stages were modified to reduce cost of method. For this operation, the first stage was completely change and third stage was removed and remaining parts were remained same as previous stages. After these modifications similar results were obtained as previous results.

Finally, according to all test results motor movements were pursued in steady state so while motor was rotating, comparator was followed by comparator ripples. However, some unwanted ripples were seen in before and after steady state. Normally, it should not be these unwanted comparator ripples but in order to follow all the motor movements in steady state three different voltage levels, it could occurred some ripples. These unwanted ripples could be removed by software side because so motor was not driven by power supply and motor was not rotating so there were low level voltage in these states. By using software these low voltage level could be cleared away from before and after steady states.

In future, it can be possible that various structure of electronic circuit can be applied with different components and type of motor, also by supplying software part it could be gotten better results for this application.

7. Appendix

7.1 Datasheets



INA240-Q1

SBOS808C –AUGUST 2016–REVISED NOVEMBER 2018

INA240-Q1 Automotive, Wide Common-Mode Range, High- and Low-Side, Bidirectional, Zero-Drift, Current-Sense Amplifier With Enhanced PWM Rejection

1 Features

- AEC-Q100 Qualified for Automotive Applications
 - Temperature Grade 1: -40°C to $+125^{\circ}\text{C}$ Ambient Operating Temperature Range
 - Temperature Grade 0: -40°C to $+150^{\circ}\text{C}$ Ambient Operating Temperature Range
 - HBM ESD Classification Level H2
 - CDM ESD Classification Level C5
- Enhanced PWM Rejection
- Excellent CMRR:
 - 132-dB DC CMRR
 - 93-dB AC CMRR at 50 kHz
- Wide Common-Mode Range: -4 V to 80 V
- Accuracy:
 - Gain Error: 0.20% (Maximum) With 2.5 ppm/ $^{\circ}\text{C}$ (Maximum Drift)
 - Offset Voltage: $\pm 25\text{ }\mu\text{V}$ (Maximum) With 250 nV/ $^{\circ}\text{C}$ (Maximum Drift)
- Available Gains:
 - INA240A1-Q1: 20 V/V
 - INA240A2-Q1: 50 V/V
 - INA240A3-Q1: 100 V/V
 - INA240A4-Q1: 200 V/V

2 Applications

- Electronic Power Steering
- Stability and Traction Control
- Motor and Actuator Control
- Solenoid and Valve Control

3 Description

The INA240-Q1 device is an automotive-qualified, voltage-output, current-sense amplifier with enhanced PWM rejection that can sense drops across shunt resistors over a wide common-mode voltage range from -4 V to 80 V , independent of the supply voltage. The negative common-mode voltage allows the device to operate below ground, accommodating the flyback period of typical solenoid applications. Enhanced PWM rejection provides high levels of suppression for large common-mode transients ($\Delta V/\Delta t$) in systems that use pulse width modulation (PWM) signals (such as motor drives and solenoid control systems). This feature allows for accurate current measurements without large transients and associated recovery ripple on the output voltage.

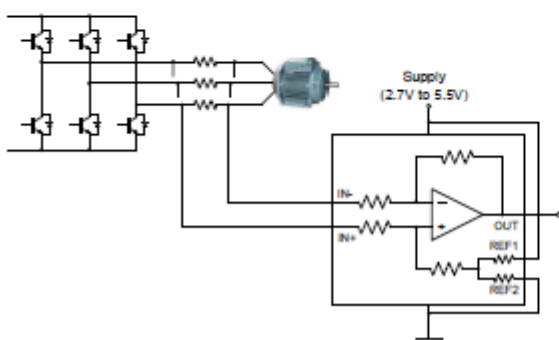
This device operates from a single 2.7-V to 5.5-V power supply, drawing a maximum of 2.4 mA of supply current. Four fixed gains are available: 20 V/V, 50 V/V, 100 V/V, and 200 V/V. The low offset of the zero-drift architecture enables current sensing with maximum drops across the shunt as low as 10-mV full-scale. Grade 1 versions are specified over the extended operating temperature range (-40°C to $+125^{\circ}\text{C}$) and are offered in an 8-pin TSSOP and 8-pin SOIC packages. Grade 0 versions are specified over the extended operating temperature range (-40°C to $+150^{\circ}\text{C}$) and are offered in an 8-pin SOIC package.

Device Information⁽¹⁾

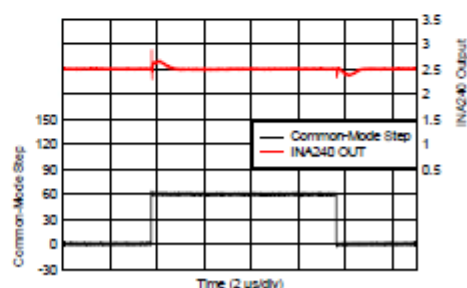
PART NUMBER	PACKAGE	BODY SIZE (NOM)
INA240-Q1	TSSOP (8)	3.00 mm \times 4.40 mm
	SOIC (8)	4.00 mm \times 3.91 mm

(1) For all available packages, see the package option addendum at the end of the data sheet.

Typical Application



Enhanced PWM Rejection



LMV7275-Q1 Automotive Single 1.8-V Low Power Comparator With Rail-to-Rail Input

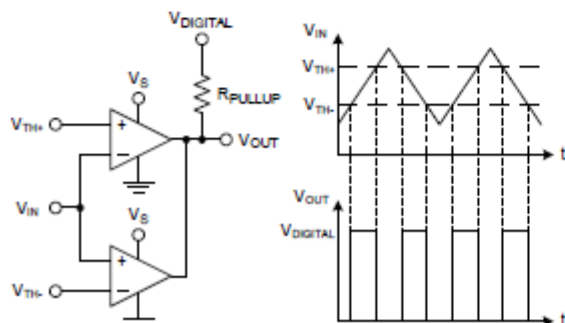
1 Features

- Qualified for Automotive Applications
- AEC-Q100 Qualified With the Following Results:
 - Device Temperature Grade 3: -40°C to 85°C Ambient Operating Temperature Range
 - Device HBM ESD Classification Level 2
 - Device CDM ESD Classification Level C6
- ($V_S = 1.8\text{ V}$, $T_A = 25^\circ\text{C}$, Typical Values Unless Specified).
- Single or Dual Supplies
- Open Drain Output
- Ultra Low Supply Current 9 μA Per Channel
- Low Input Bias Current 10 nA
- Low Input Offset Current 200 pA
- Low Ensured V_{OS} 4 mV
- Propagation Delay 880 ns (20-mV Overdrive)
- Input Common Mode Voltage Range 0.1 V Beyond Rails

2 Applications

- Wearable Devices
- Mobile Phones and Tablets
- Battery-Powered Electronics
- General Purpose Low Voltage Applications

LMV7275-Q1 as a Window Comparator



3 Description

The LMV7275-Q1 is a single rail-to-rail input low power comparator, characterized at supply voltages of 1.8 V, 2.7 V, and 5 V. It consumes as little as 9- μA supply current per channel while achieving a 800-ns propagation delay.

The LMV7275-Q1 is available in a SC-70 package. With these tiny packages, the PCB area can be significantly reduced. They are ideal for low voltage, low power, and space-critical designs.

The LMV7275-Q1 features an open-drain output stage that allows for wired-OR configurations. The open-drain output also offers the advantage of allowing the output to be pulled to any voltage up to 5.5 V, regardless of the supply voltage of the LMV7275-Q1, which is useful for level-shifting applications.

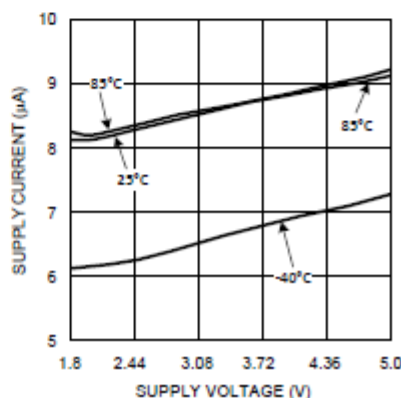
The LMV7275-Q1 is built with Texas Instruments' advance submicron silicon-gate BiCMOS process. It has bipolar inputs for improved noise performance, and CMOS outputs for lowest negative output swing.

Device Information⁽¹⁾

PART NUMBER	PACKAGE	BODY SIZE (NOM)
LMV7275-Q1	SC70 (5)	1.25 mm x 2.00 mm

(1) For all available packages, see the orderable addendum at the end of the data sheet.

Low Supply Current



TLVx316-Q1

10-MHz, Rail-to-Rail Input/Output, Low-Voltage, 1.8-V CMOS Operational Amplifiers

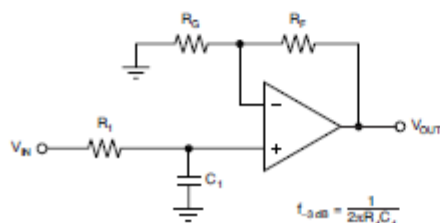
1 Features

- Qualified for Automotive Applications
- AEC-Q100 With the Following Results:
 - Device Temperature Grade 1: -40°C to $+125^{\circ}\text{C}$ Ambient Operating Temperature Range
 - Device HBM ESD Classification Level 3A
 - Device CDM ESD Classification Level C5
- Unity-Gain Bandwidth: **10 MHz**
- Low I_Q : 400 $\mu\text{A}/\text{ch}$
 - Excellent Power-to-Bandwidth Ratio
 - Stable I_Q Over Temperature and Supply Range
- Wide Supply Range: **1.8 V to 5.5 V**
- Low Noise: 12 $\text{nV}/\sqrt{\text{Hz}}$ at 1 kHz
- Low Input Bias Current: ± 10 pA
- Offset Voltage: ± 0.75 mV
- Unity-Gain Stable
- Internal RFI and EMI Filter
- Number of Channels:
 - TLV316-Q1: 1
 - TLV2316-Q1: 2
 - TLV4316-Q1: 4
- Extended Temperature Range: **-40°C to $+125^{\circ}\text{C}$**

2 Applications

- Automotive Applications:
 - ADAS
 - Body Electronics and Lighting
 - Current Sensing
 - Battery Management Systems

Single-Pole, Low-Pass Filter



$$\frac{V_{OUT}}{V_{IN}} = \left(1 + \frac{R_F}{R_2}\right) \left(\frac{1}{1 + sR_1C_1}\right)$$

3 Description

The TLV316-Q1 (single), TLV2316-Q1 (dual), and TLV4316-Q1 (quad) devices comprise a family of general-purpose, low-power operational amplifiers. Features such as rail-to-rail input and output swings, low quiescent current (400 $\mu\text{A}/\text{ch}$ typical) combined with a wide bandwidth of 10 MHz, and very-low noise (12 $\text{nV}/\sqrt{\text{Hz}}$ at 1 kHz) make this family suitable for a circuits requiring a good speed and power ratio. The low input bias current supports operational amplifiers that are used in applications with megaohm source impedances. The low-input bias current of the TLVx316-Q1 yields a very-low current noise to make the family attractive for high impedance sensor interfaces.

The robust design of the TLVx316-Q1 provides ease-of-use to the circuit designer: a unity-gain stable, integrated RFI and EMI rejection filter, no phase reversal in overdrive condition, and high electrostatic discharge (ESD) protection (4-kV HBM).

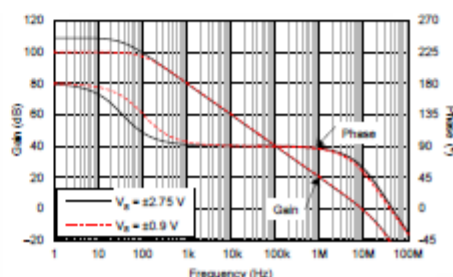
These devices are optimized for low-voltage operation as low as 1.8 V (± 0.9 V) and up to 5.5 V (± 2.75 V). This latest addition of low-voltage CMOS operational amplifiers to the portfolio, in conjunction with the TLVx313-Q1 and TLVx314-Q1 series, offer a family of bandwidth, noise, and power options to meet the needs of a wide variety of applications.

Device Information⁽¹⁾

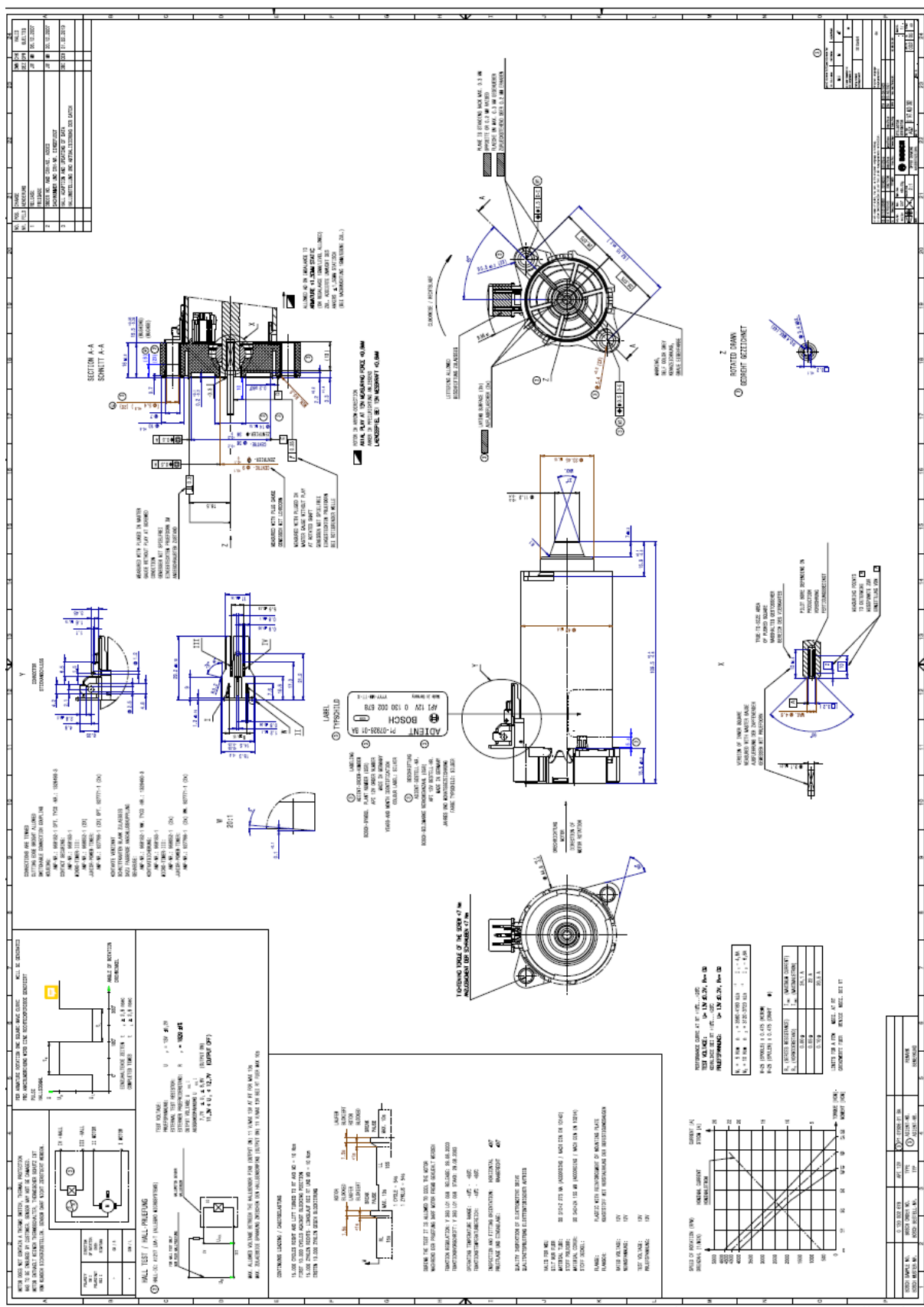
PART NUMBER	PACKAGE	BODY SIZE (NOM)
TLV316-Q1	SOT-23 (5)	1.60 mm × 2.90 mm
TLV2316-Q1	VSSOP (8)	3.00 mm × 3.00 mm
TLV4316-Q1	TSSOP (14)	4.40 mm × 5.00 mm

(1) For all available packages, see the orderable addendum at the end of the data sheet.

Low Supply Current (400 $\mu\text{A}/\text{Ch}$) for 10-MHz Bandwidth



Brushed DC Motor



7.2 Final Schematics

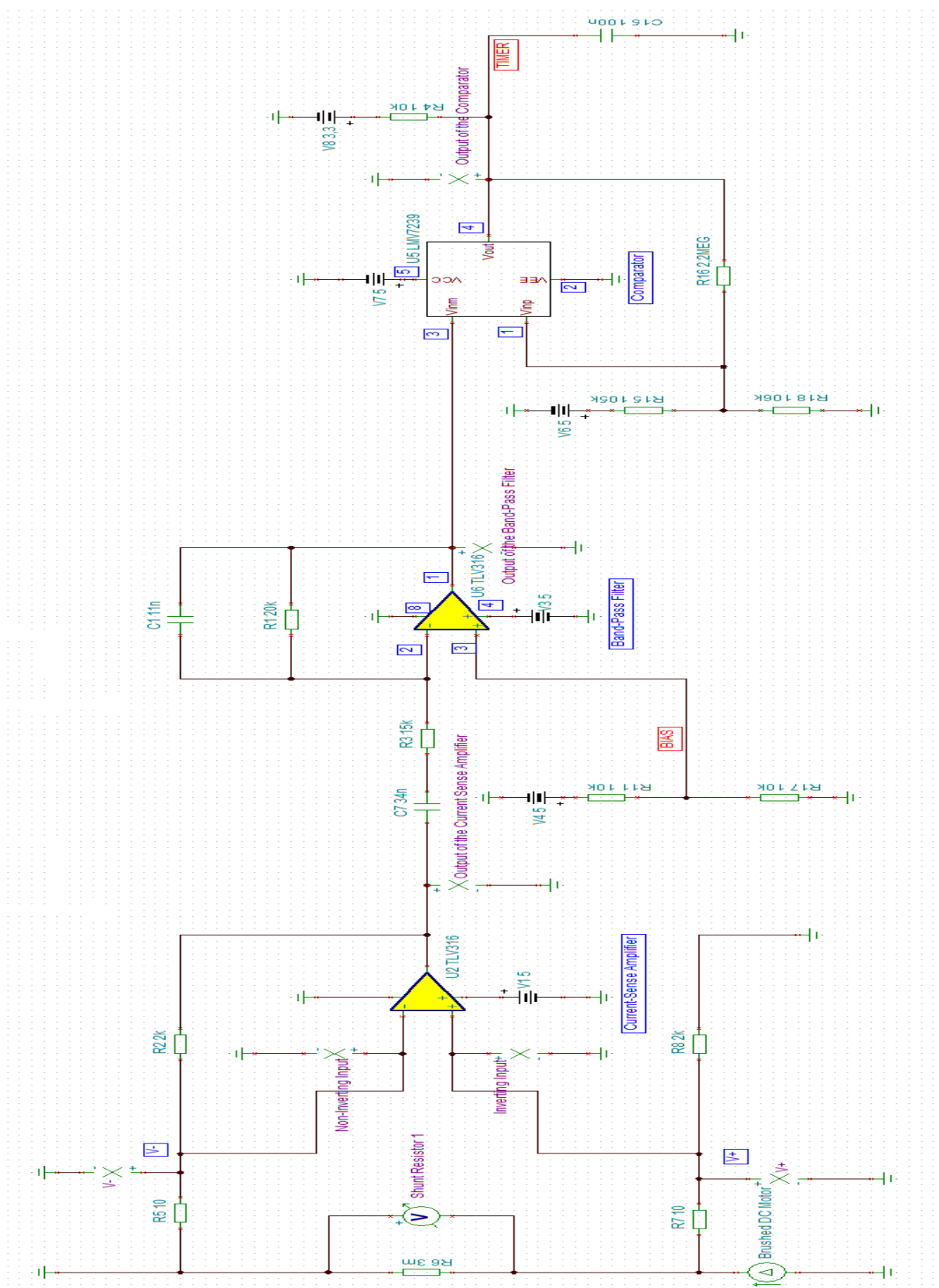


Figure 103: Final Electrical Schematic of System

References

[1] Automotive Brushed-Motor Ripple Counter Reference Design for Sensorless Position Measurement -Texas Instruments Incorporated, 2017, revised 2018

[2] Automotive Power Seat Reference Design- Texas Instruments Incorporated, 2018

[3] Brushed DC Motor Fundamentals- Microchip Technology Incorporated, 2006

[4] Condit R. 2004, Brushed DC Motor Fundamentals- Microchip Technology Incorporated

[5] The seat remembers: Brushed DC motor ripple counting drives innovation in full-featured memory seats (2019, 10 October)

https://e2e.ti.com/blogs_/b/behind_the_wheel/archive/2017/08/16/the-seat-remembers-brushed-dc-motor-ripple-counting-drives-innovation-in-full-featured-memory-seats#

[6] Brush DC Motor Guide (2019, 5 September)

<https://www.anaheimautomation.com/manuals/forms/brush-dc-motor-guide.php>

[7] How Brushed Motors Work (2019, 7 September)

<https://www.roboteq.com/index.php/87-products/417-how-brushed-motors-work>

[8] Brushed DC (BDC) Motor (2019, 9 September)

<https://au.element14.com/motor-control-brushed-dc-bdc-technology>

[9] Chi C.T. 2013, Communications in Information Science and Management Engineering, Chienkuo Technology University